A MACHINE LEARNING BASED APPROACH FOR QUANTIFYING MUSCLE SPASTICITY LEVEL IN NEUROLOGICAL DISORDER PATIENTS

BY

MUHAMAD ALIFF IMRAN DAUD

A dissertation submitted in fulfillment of the requirement for the degree of Master of Computer Science and Information Technology.

Kulliyyah of Information and Communication Technology
International Islamic University Malaysia

FEBRUARY 2025

ABSTRACT

Muscle spasticity is a condition that occurs in patients with neurological disorders when their muscles are stiff, tight, and resistant to stretching. The current assessment method, relying on the subjective judgment of therapists using the Modified Ashworth Scale (MAS), introduces variability that may affect the rehabilitation process. In addition, many existing computational models are not aligned with clinical standards such as MAS, limiting their practical adoption in clinical settings. They also often overlook direction-specific movement phases and fail to distinguish muscle responses across different axes and muscle groups. To address the limitations, this research aimed to develop a quantitative assessment method by muscle spasticity characteristics based on mechanomyography (MMG) signals and MAS levels, utilising machine learning techniques. A Quantitative Spasticity Assessment Technology (QSAT) platform has been developed which consists of two sensors that were tri-axial accelerometer mechanomyography (ACC-MMG) functioning in measure acceleration of biceps and triceps muscle contraction and potentiometer to measure the angular position of forearm during flexion and extension movement. A comprehensive investigation was conducted to assess muscle spasticity level by recording ACC-MMG signals from patients' forearm musculature during flexion and extension movements using QSAT platform. A total of 30 patients with neurological disorders were classified into five MAS levels (0, 1, 1+, 2, and 3), along with 10 healthy subjects serving as a baseline group. The pre-processed data comprised 48 extracted features from ACC-MMG signals along the *x*, *y*, and *z* axes for both flexion and extension movements of the biceps and triceps. These features corresponded to the longitudinal, lateral, and transverse muscle orientations. For both flexion and extension movements, machine learning models were trained using the selected subset of 25 significant features and the full set of 48 features respectively, with performance comparisons made to identify the most effective approach. Various machine learning models algorithms, including Linear Discriminant Analysis (LDA), Decision Tree (DT), Support Vector Machine (SVM), and K-Nearest Neighbour (KNN), were tested. The KNN-based classifier demonstrated the highest performance using a 90% training and 10% testing data split surpassing the performance of other classifiers. Specifically, at k = 15 using Euclidean distance, the KNN achieved an accuracy of 91.29% for flexion using the significant features, with corresponding precision, recall, and F1-score of 91.64%, 91.25%, and 91.47%, respectively. For extension, the same configuration resulted with 96.30% for extension using the full feature set, with precision, recall, and F1-score of 96.53%, 96.30%, and 96.33%, respectively. These results indicate high classification performance, with minimal false positives or false negatives, particularly in distinguishing between different MAS levels. This research suggests that the muscle characteristic model embedded in the QSAT can serve as a standardised and objective assessment tool for measuring the spasticity level of the affected limb using computational method, leading to support clinical evaluations and enabling more effective rehabilitation strategies.

ملخص البحث

التشنج العضلي هي حالة تحدث لدى المرضى الذين يعانون من اضطرابات عصبية عندما تكون عضلاتهم متصلبة، ومشدودة، ومقاومة للتمدد. تعتمد الطريقة الحالية لتقييم التشنج العضلي على ، مما يؤدي إلى تباين قد يؤثر (MAS) التقييم الذاتي للمعالجين باستخدام مقياس آشورث المعدل على عملية إعادة التأهيل. بالإضافة إلى ذلك، فإن العديد من النماذج الحاسوبية الحالية لا تتماشى ، مما يحد من إمكانية تبنيها في البيئات العلاجية. كما MAS مع المعايير السريرية مثل مقياس أنها غالبًا ما تغفل مراحل الحركة المرتبطة باتجاه معين، ولا تميز بين استجابات العضلات عبر المحاور والمجموعات العضلية المختلفة. لمعالجة هذا القيد، يهدف هذا البحث إلى تطوير طريقة تقييم كمية ومستويات (MMG) لخصائص التشنج العضلي بالاعتماد على إشارات ميكانيكية العضلات باستخدام تقنيات التعلم الآلي. تم تطوير منصة "تكنولوجيا (MAS) مقياس آشورث المعدل التي تتكون من مستشعرين: مستشعر ميكانيكي ثلاثي المحاور (QSAT) "تقييم التشنج الكمي لقياس تسارع تقلص العضلات في العضلة ذات الرأسين (البايسبس) (ACC-MMG) والعضلة ثلاثية الرؤوس (الترايسبس)، ومقياس الجهد لقياس الزاوية أثناء حركات الثني والبسط للساعد. تم إجراء تحقيق شامل لتقييم مستوى التشنج العضلي من خلال تسجيل إشارات من عضلات ساعد المرضى أثناء حركات الثني والبسط باستخدام منصة ACC-MMG شملت الدراسة 30 شخصًا مريضًا يعانون من اضطرابات عصبية، تم تصنيفهم إلى .QSAT خمس مستويات من مقياس آشورث المعدل (0، 1، 1+، 2، 3)، بالإضافة إلى 10 مشاركين أصحاء كمجموعة مرجعية. تضمنت البيانات المعالجة مسبقًا 48 ميزة مستخرجة من إشارات لكل من حركات الثني والبسط للعضلة ذات z و y و x على المحاور ACC-MMG الرأسين والعضلة ثلاثية الرؤوس. هذه الميزات تتوافق مع الاتجاهات الطولية والجانبية والعرضية

للعضلات. تم تدريب نماذج التعلم الآلي باستخدام مجموعة مختارة من 25 ميزة مهمة ومجموعة كاملة من 48 ميزة لكلا حركتي الثني والبسط على التوالي، مع إجراء مقارنات الأداء لتحديد النهج الأكثر فعالية. تم اختبار خوارزميات مختلفة لنماذج التعلم الآلي، بما في ذلك تحليل التمييز الخطي (LDA) ، وأشجار القرار(DT) ، وآلة الدعم المتجهات(SVM) ، وأقرب الجيران(KNN). أظهر المصنف المعتمد على خوارزمية أقرب الجيران (KNN) أعلى أداء باستخدام تقسيم البيانات بنسبة 90% للتدريب و10% للاختبار، متفوقًا على أداء المصنفات الأخرى. دقة بنسبة KNN وباستخدام المسافة الإقليدية، حقق k = 15 بشكل محدد، عند قيمة بلغت (precision) 91.29% لحركات الثني باستخدام الميزات المهمة، مع دقة إيجابية بنسبة 91.47%. أما F1 بنسبة 91.25%، ودرجة (recall) 91.64%، واسترجاع لحركات البسط، فقد حقق نفس التكوين دقة بنسبة 96.30% باستخدام المجموعة الكاملة من الميزات، مع دقة إيجابية بلغت 96.53%، واسترجاع بنسبة 96.30%، ودرجة F1 بنسبة 96.33%. تشير هذه النتائج إلى أداء تصنيفي عالٍ، مع الحد الأدنى من الإيجابيات أو السلبيات الكاذبة، خصوصًا في التمييز بين مستويات مقياس آشورث المعدل (MAS). يشير هذا البحث إلى أن نموذج خصائص العضلات المدمج في QSAT يمكن أن يعمل كأداة تقييم معيارية وموضوعية لقياس مستوى التشنج في الطرف المصاب باستخدام الأساليب الحاسوبية، مما يدعم استراتيجيات إعادة التأهيل بشكل أكثر فعالية.التقييمات السريرية ويعزز

APPROVAL PAGE

I certify that I have supervised and read this study and that in my opinion, it conforms to acceptable standards of scholarly presentation and is fully adequate, in scope and quality, as a dissertation for the degree of Master of Computer Science and Information Technology

…….
Asmarani Ahmad Puzi
Supervisor

…….
Shahrul Na'im Sidek
Co-Supervisor

…….
Ahmad Anwar Zainuddin
Co-Supervisor

…….
Salmah Anim Abu Hassan
Co-Supervisor

I certify that I have read this study and that in my opinion it conforms to acceptable standards of scholarly presentation and is fully adequate, in scope and quality, as a dissertation for the degree of Master of Computer Science and Information Technology

…….
Dini Oktarina Dwi Handayani
Internal Examiner

…….
Mohd Ibrahim Bin Shapiai
External Examiner

This dissertation was submitted to the Department of Computer Science and is accepted as a fulfilment of the requirement for the degree of Master of Computer Science and Information Technology

…….
Amir Aatieff Amir Hussin
Head, Department of Computer Science

This dissertation was submitted to the Kulliyyah of Information and Communication Technology and is accepted as a fulfillment of the requirement for the degree of Master of Computer Science and Information Technology

…….
Murni Mahmud Dean, Kulliyyah of Information and Communication Technology

DECLARATION

I hereby declare that this dissertation is the result of my own investigations, except where otherwise stated. I also declare that it has not been previously or concurrently submitted as a whole for any other degrees at IIUM or other institutions.

Muhamad Aliff Imran Daud

Signature…… Date…14/02/2025……

INTERNATIONAL ISLAMIC UNIVERSITY MALAYSIA

DECLARATION OF COPYRIGHT AND AFFIRMATION OF FAIR USE OF UNPUBLISHED RESEARCH

COMPUTATIONAL MODEL FOR QUANTIFYING SPASTICITY LEVEL OF NEUROLOGICAL DISORDER PATIENTS

I declare that the copyright holder of this thesis/dissertation is Name of the Student.

By signing this form, I acknowledged that I have read and understand the IIUM Intellectual Property Right and Commercialization policy.

Affirmed by Muhamad Aliff Imran Daud

…… 14/02/2025 ……..

Signature Date

ACKNOWLEDGEMENTS

All glory is due to Allah, the Almighty, whose Grace and Mercies have been with me throughout the duration of my programme. Although, it has been tasking, His Mercies and Blessings on me ease the herculean task of completing this thesis.

My utmost pleasure to dedicate this work to my parents; Daud Bin Dollah and Zaleha Binti Muhammad, for their blessings and encouragement in pursuing my master's degree. Thanks to their prayers and affection, I am able to attain my current achievements and maintain my excellence throughout this academic path. I sincerely appreciate my siblings for their support throughout my initial decision to pursue a master's degree.

I am most indebted to my supervisor, Dr. Asmarani Ahmad Puzi, whose enduring disposition, kindness, promptitude, thoroughness and friendship have facilitated the successful completion of my work. I put on record and appreciate her detailed comments, useful suggestions and inspiring queries which have considerably improved this thesis. Her brilliant grasp of the aim and content of this work led to his insightful comments, suggestions and queries which helped me a great deal. Despite her commitments, she took time to listen and attend to me whenever requested. The moral support she extended to me is no doubt a boost that helped in building and writing thedraft of this research work. Lastly, I extend my gratitude to Dr. Asmarani for accepting me as your first Master student and for the faith shown in me throughout my study.

I extend my gratitude to my co-supervisor, Prof. Dr. Shahrul Na'im Sidek, for his support and collaboration, which significantly influenced the results of this work. I also express gratefulness for the provision of a well-equipped Research Lab at the Biomechatronics Research Laboratory, Kulliyyah of Engineering (KOE) during this period of the study. I would like to acknowledge Sultan Ahmad Shah Medical Centre (SASMEC) and the National Stroke Association of Malaysia (NASAM) for granting me the opportunity to conduct my research at their facilities. Their support in facilitating data collection and their cooperation throughout the study have been invaluable. I am also grateful to the medical staff and personnel who assisted in the research process.

I express my appreciation to my lab mates, Ikmal, Azri, Hafiz, Ariff, Hariz, and Faisal, for their assistance and support at challenging times, as well as for the enjoyable experiences we shared throughout my studies. I would like to acknowledge my close friends Asyraf, Zul, Zaki, Baim, and Azim for their unwavering moral support and assistance during my hardships, as well as their attempts to accompany me during my conference and data acquisition at SASMEC and NASAM.

Once again, we glorify Allah for His endless mercy on us, one of which is enabling us to successfully round off the efforts of writing this thesis. Alhamdulillah

TABLE OF CONTENTS

LIST OF TABLES

LIST OF FIGURES

LIST OF SYMBOLS

K	Kurtosis
MAV	Mean Average Value
Max	Maximum
Min	Minimum
PTP	Peak to Peak Amplitude
RMS	Root Mean Square
S	Skewness
SD	Standard Deviation
x_b	Muscle Vibration of biceps in x axis
y_b	Muscle Vibration of biceps in y axis
z_b	Muscle Vibration of biceps in z axis
x_t	Muscle Vibration of triceps in x axis
y_t	Muscle Vibration of triceps in y axis
z_t	Muscle Vibration of triceps in z axis

LIST OF ABBREVIATIONS

ACC-MMG	Accelerometer Mechanomyography
AIS	Arterial Ischaemic Stroke
ALS	Amyotrophic Lateral Sclerosis
CNS	Central Nervous System
CP	Cerebral Palsy
IREC	International Islamic University Malaysia Research Ethics Committee
KNN	K-Nearest Neighbors
MANOVA	Multivariate Analysis of Variance
MAS	Modified Ashworth Scale
MATLAB	Matrix Laboratory
MMG	Mechanomyography
MS	Multiple sclerosis
NASAM	National Stroke Association of Malaysia
QSAT	Quantitative Spasticity Assessment Technology
ROM	Range of Motion
SASMEC	Sultan Ahmad Shah Medical Centre
SCI	Spinal Sord Injury
TBI	Traumatic Brain Injury
UMNS	Upper Motor Neuron Syndrome

CHAPTER ONE

INTRODUCTION

1.1 BACKGROUND

Muscles are a vital part of the human body and are susceptible to damage from various sources, including accidents, exhaustion, inflammation, illnesses, infections, and the adverse effects of harmful substances (El-Tallawy et al., 2021). At the same time, muscles may be impacted by diverse disorders and ailments, leading to weakness, discomfort, reduced mobility, or even paralysis, which may exaggerate muscle spasticity (None Felix Siaw-Debrah et al., 2024). Among the various muscle disorders, spasticity stands out as a significant manifestation of upper motor neuron syndrome, a neurological condition associated with disorders such as amyotrophic lateral sclerosis (ALS), traumatic brain injury (TBI), cerebral palsy (CP), stroke, and spinal cord injury (SCI) (Shaikh et al., 2024; Spieker et al., 2024). Spasticity frequently occurs in the upper extremities, with a higher prevalence in the forearm (79%), wrist (66%), and shoulder (58%) (Bavikatte et al., 2021). Stroke patients commonly experience spasticity, affecting between 4% to 42.6% of cases (Zeng et al., 2021). Furthermore, throughout the course of multiple sclerosis (MS), spasticity affects anywhere from 66% to 84% of patients, making it the leading cause of disability for this population (Ellerbusch et al., 2023). Approximately 795,000 people worldwide suffer a new or recurrent stroke each year, making it the third most common cause of death worldwide.

In 1980, Lance became the first person to define spasticity, describing it as a motor disorder characterised by a velocity-dependent increase in tonic stretch reflexes (muscle tone), with exaggerated tendon jerks, as one component of the upper motor neuron syndrome (Lance, 1980; Whitten et al., 2024). The condition is characterised by increased

muscle tone and pronounced tendon reflexes, influenced by movement velocity and resulting from excessive stretch reflex activation (Takeuchi et al., 2024). Spasticity arises from altered rheological muscle properties, such as rigidity, fibrosis, and atrophy, as well as impaired reflex function. Spasticity is among the positive signs following lesions in the descending corticospinal system, which also include spastic dystonia, spastic co-contraction, extensor or flexor spasms, clonus, and exaggerated deep tendon reflexes. Negative symptoms include muscle weakness, loss of dexterity, and fatigue. Spasticity can manifest in both sexes at any age and can be caused by conditions such as cerebral palsy, traumatic brain injury, spinal cord injury (SCI), multiple sclerosis (MS), or stroke (Ellerbusch et al., 2023). The severity of spasticity varies widely among patients, with some exhibiting mild spasticity characterised by muscular stiffness and reduced movement, while others may endure severe, uncontrollable spasms accompanied by contractures and frozen joint positions, rendering movement impossible (Enslin et al., 2020). Severe spasticity significantly impacts quality of life, limiting functional abilities and social aspirations while causing discomfort and pain (Billington et al. 2022). A comprehensive and accurate assessment of spasticity is critical, as it forms the foundation for identifying the most appropriate interventions to manage symptoms and promote functional recovery. Given the variability in spasticity severity and its impact on patients' daily lives, reliable and standardised clinical assessment tools are essential for evaluating muscle tone abnormalities and guiding rehabilitation strategies.

To address the need for standardised clinical assessments, various scales have been developed, with the Modified Ashworth Scale (MAS) and the Australian Spasticity Assessment Scale (ASAS) being among the most widely used tools in clinical practice (Wang et al., 2022; Yu et al., 2020). The MAS commonly be used as the measurement technique for determining spasticity in stroke rehabilitation. The assessment generally involves therapists conducting passive movements to determine the level of muscle resistance during passive stretching and subsequently giving spasticity grades (Fujimura et al., 2022). The scale, assessing the joint's resistance and spasticity (also known as catch) when the patient is not actively moving, allows therapists to rate the resistance on the

Modified Ashworth Scale from 0 to 5 (Haas et al., 1996; Lee et al., 1989). The scale is comparable to the neurological examination's tone assessment; however, MAS level only rates muscle tone as normal or increased, whereas the neurological examination grades muscle tone as decreased or increased (Hugos & Cameron, 2019). Even though experts might favour MAS awareness of its drawbacks is essential due to factors such as hyperexcitability, antagonist muscle co-contraction during voluntary movement, spasms, or limb dystonia, which can impose increased muscular endurance. The MAS also permits differences in interrater outcomes, affecting assessment consistency. Other clinical tools used to assess spasticity in addition to the MAS and ASAS include the Penn Spasm Frequency Scale (PSFS), the Modified Tardieu Scale (MTS), the Fugl-Meyer Assessment (FMA), and the Spinal Cord Assessment Tool for Spastic Reflexes (SCATS) (Billington et al., 2022; Luo et al., 2019). The tools provide therapists with various approaches to evaluate spasticity severity and its impact on motor function, ultimately aiding in the development of more targeted and effective treatment strategies.

Despite the widespread use of the clinical scales, they remain inherently subjective and prone to interrater variability. To overcome the limitations, researchers have explored sensor-based technologies for quantitative spasticity assessment. Utilising various types of sensors in measuring muscle spasticity serves as a quantitative assessment approach that overcomes some of the limitations associated with subjective clinical scales. Surface electromyography (sEMG), near-infrared spectroscopy (NIRS), and mechanomyography (MMG) are widely used techniques for assessing muscle fatigue. Each method measures different physiological aspects, including metabolic responses, electrical signals, and mechanical properties of contracting muscles, to estimate performance and fatigue levels. Muscle responses recorded by sensors exhibit distinct characteristics during both non-fatigue and fatigued contractions, highlighting the unique insights provided by each technique. Among sensor technologies, the family of MMG-based devices introduced a relatively novel muscle-contraction sensor (MC) in 2011, offering a new approach to capturing muscle activity. The MC sensor operates by measuring skin-surface tension when a muscle is activated. The tip, which is affixed to the skin surface directly over the muscle

belly, applies a compression force to the skin, the underlying tissue, and the muscle itself, allowing for detailed observation of muscle contractions (Mohamad et al., 2017).

The proposed research concentrates on developing a model delineating muscle spasticity characteristic derived from MMG signals through the application of machine learning techniques. The model serves as a quantitative evaluative tool, employing the MAS, to determine the severity of spasticity in the affected upper limb. Quantitative Spasticity Assessment Technology (QSAT) platform has been devised, comprising of a pair of sensors, specifically the tri-axial accelerometer mechanomyography (ACC-MMG). The sensors are utilised to gauge the acceleration of both the biceps and triceps muscle movements. Additionally, a potentiometer is employed to ascertain the angular position of the upper limb movement. The purpose of employing the sensors is to gather signal characterisations from patients with various MAS clinical assessment scores. The platform's residual component consists of an arm holder and a data logging running Python IDE (Thonny), which is linked to a data acquisition (Raspberry Pi Pico). Figure 1.1 shows the QSAT system used for the research work. Moreover, time domain feature for upper limb will be model and mapping the patients' spasticity muscle characteristics with the MAS tool.

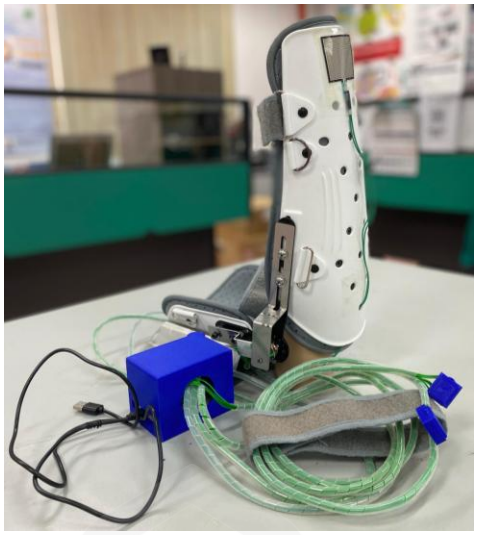

Figure 1.1: QSAT system

1.2 PROBLEM STATEMENT

Individuals suffering from neurological conditions often experience affected limbs function due to spasticity, which significantly affects their ability to perform daily activities. Accurate assessment of muscle spasticity is crucial in determining appropriate rehabilitation strategies. However, therapists face significant challenges in ensuring the effectiveness of rehabilitation training due to limitations in current practices. Muscle spasticity is characterised by rigid, tight muscles that resist stretching, complicating rehabilitation efforts. Currently, therapists rely on subjective assessments, such as MAS, to evaluate spasticity (Erden et al., 2020).

While MAS has been widely used in practice due to its simplicity and ease of implementation, it relies heavily on the subjective judgment of therapists during passive movement assessments. This subjectivity leads to variability in scoring across different therapists, which undermines the consistency and reliability of spasticity evaluation.

Moreover, current methods fail to provide a clear and quantitative description of spasticity severity, which is crucial for designing effective rehabilitation plans. Although some progress has been made in quantifying clinical assessments, existing approaches often overlook the composition of measured signals, resulting in inaccurate identification of spasticity characteristics.

Previous studies have demonstrated that conventional assessment tools like MAS and the MTS, although widely accepted, are susceptible to inter- and intra-rater inconsistencies and limited sensitivity, especially in distinguishing mild variations in spasticity levels. Additionally, these tools capture only passive resistance and often overlook the biomechanical or neuromuscular characteristics underlying spasticity, which are essential for a holistic understanding of muscle tone abnormalities. In response to these limitations, recent research has focused on sensor-based and computational approaches to improve the objectivity and precision of spasticity assessment. Techniques involving sEMG, isokinetic dynamometry, and ACC-MMG have been explored for their ability to quantify muscle responses during controlled movements. These methods, when combined with machine learning algorithms, have demonstrated promising results in capturing complex patterns in muscle behaviour and in classifying spasticity severity with greater accuracy. However, existing computational models often lack integration with clinical standards like MAS, limiting their clinical adoption. Moreover, many models do not account for direction-specific movement phases (flexion and extension) or fail to differentiate muscle responses across multiple axes and muscle groups.

To address the limitations mentioned above, the research proposes a computational method by integrating the machine learning model to quantitatively characterise spasticity levels based on the MAS tool which captured through MMG signals during passive movements. By leveraging advanced analytical techniques, the proposed approach aims to provide consistent and reproducible assessments of muscle spasticity. Consistent assessment is essential for developing personalised rehabilitation plans, which can significantly improve patient outcomes by targeting specific levels of spasticity.

Ultimately, the research has the potential to revolutionize rehabilitation practices by equipping therapists with a reliable tool to assess spasticity, leading to more effective and tailored treatment strategies for patients with neurological disorders.

1.3 RESEARCH OBJECTIVES

The research main objective is to develop a muscle spasticity characteristics model obtained through mechanomyography (MMG) signals based on Modified Ashworth Scale (MAS) scores within the forearm musculature by employing machine learning techniques. The main objectives can be divided into 3 sub objectives as follows:

1. To identify significant features in time domain from the MMG signal of the forearm musculature.
2. To develop a muscle spasticity model of neurological disorders patients using machine learning.
3. To evaluate the performance of the muscle spasticity model for neurological disorder patients.

1.4 RESEARCH METHODOLOGY

The research will start with literature review of scientific papers and securing ethical clearance. The proposal is divided into 6 phases that comprise of literature review of technical and scientific papers, research design on muscle spasticity assessment system, data acquisition of the neurological disorder patients, data analysis on the gathered clinical data, development of muscle spasticity model and performance evaluation of muscle spasticity model. The following is a synopsis, which can be found in the flowchart shown in Figure 1.2:

1. Phase 1: Literature review of scientific papers and securing ethical clearance

   Starting to design the spasticity muscle characteristics model involves careful planning. Technical and scientific literature was conducted to get important information for designing systems that match with the research goals. Understanding the unique features of the muscles under research and the rehabilitation platform supporting individuals with neurological disorders in their upper limbs was focused upon. In order to conduct research, an Ethical clearance was obtained from IIUM Research Ethics Committee (IREC). Moreover, a meeting with the physiotherapists from Sultan Ahmad Shah Medical Centre (SASMEC) and National Stroke Association of Malaysia (NASAM) were conducted to recruit a proper set of patients.

2. Phase 2: Research design on forearm musculature muscle spasticity assessment system

   The subsequent phase of the research highlighted the research design. The research employed quantitative design procedures, collecting all data in numerical form and analysing it with statistical tools. The experiment for the assessment involved the development of a muscle spasticity assessment system, namely Quantitative Spasticity Assessment Technology (QSAT) to acquire data. QSAT consists of two sensors that were tri-axial accelerometer mechanomyography (ACC-MMG) functioning in measuring the muscle vibration (acceleration) of biceps and triceps muscle movement and potentiometer for assessing the angular position of upper limb movements. The data were subsequently employed to classify muscle spasticity levels based on the Modified Ashworth Scale (MAS).

3. Phase 3: Data Acquisition

   A total of thirty (30) patients with neurological disorders and ten (10) healthy patients were selected for data acquisition utilising the proposed QSAT, particularly developed to assess the spasticity levels of the forearm musculature. The health of the research participants was meticulously assessed, ensuring that the prescribed criteria were adequately fulfilled.

4. Phase 4: Data Analysis

   In this segment of the research, the gathered clinical data was meticulously analysed, and an appropriate set of features was identified and evaluated to ascertain the optimal independent features by a statistical methodology. The significant features were recognised as independent variables by one-way MANOVA, while the MAS level was classified as the dependent variable, varying in relation to the extracted features. Additionally, the relationship between features with muscle spasticity levels were identified using linear regression and Pearson correlation. To make sure the data was reliable, the data evaluated both clinical and measurement information. This helps to figure out which properties of the features are important for understanding spasticity. Following the analysis, development efforts were focused on developing a model that uses the Modified Ashworth Scale (MAS) tool to map the characteristics of spasticity muscles. This model was important because it can improve the comprehension and assessment of spasticity in the muscles that are being studied.

5. Phase 5: Development of a Muscle Spasticity Model Using Machine Learning Techniques

   Following comprehensive analysis, concerted efforts were dedicated to the development of a model employing machine learning techniques. The model utilised the MAS tool to systematically map the intricate characteristics of spasticity within the musculature under scrutiny, encompassing both flexion and extension movements. The conceptualisation and implementation of this model proved paramount, augmenting the comprehensibility and precision in the assessment of spasticity exhibited by the targeted muscles. Following the development, the model underwent rigorous testing with a patient afflicted by a neurological condition. This pivotal stage ensures both the refinement and validation of the developed platform's efficacy and its suitability for application in neurological conditions.

6. Phase 6: Performance Evaluation of Muscle Spasticity Model

   Based on the comprehensive analysis results, the classifier exhibiting the greatest accuracy was chosen for additional analysis to improve its performance. The best algorithm underwent k-fold cross-validation, being trained and evaluated with k

values of 5, 10, and 15 with using different measure distance that are Euclidean, Cosine and Correlation. The efficacy of the machine learning algorithms was assessed using confusion matrices, accuracy metrics, training duration, and distance measures, facilitating a thorough investigation of the classifier models across various muscle motions.

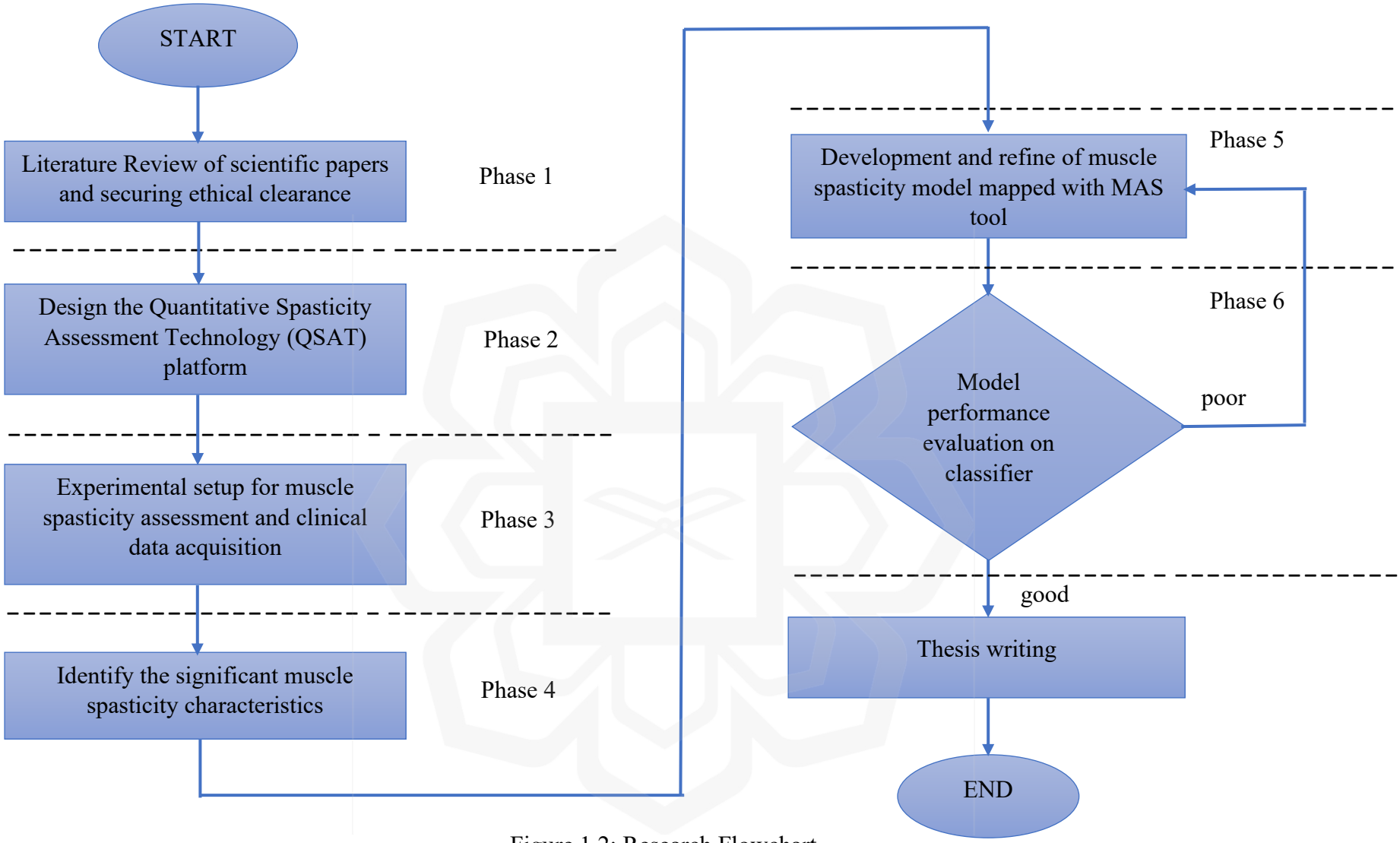

Figure 1.2: Research Flowchart

1.5 RESEARCH SCOPE

The research is conducted to develop muscle spasticity characteristics model obtained through MMG signals based on standard clinical tool namely, MAS scores. The primary biomechanical signals that the system is intended to capture are the angular position and mechanical vibration of the injured elbow joint during contraction and elongation for both flexion and extension movements. Machine learning techniques were utilised to model muscle recovery characteristics depending on MAS levels, employing the quantifiable features of biomechanical data. Machine learning models were utilised for both flexion and extension motions, enabling thorough research of the MMG signals during distinct movement phases and enhancing the precision of muscle spasticity predictions across diverse movement types. This dual movement strategy enabled the models to encompass the entire range of muscle behaviour, enhancing the robustness and generalisation of spasticity classification level.

The quantitative muscle spasticity assessment system was designed to address the needs of individuals experiencing upper limb impairment resulting from neurological disorders. In adherence to safety protocols, the research obtained ethical clearance, and all system components were meticulously selected to meet established medical-grade standards. The participants that have been recruited for this research were selected from MAS level 0, 1, 1+, 2 and 3. MAS level 4 was excluded as it does not show any rigid movement of flexion and extension during the assessment. The anatomical focus of this research pertained to the musculature of the forearm, encompassing both the left and right sides.

The research involved the recruitment of 30 participants diagnosed with diverse neurological disorders which 29 being post-stroke patients and one diagnosed with cerebral palsy, following a comprehensive clinical assessment conducted by therapists affiliated with the Sultan Ahmad Shah Medical Centre (SASMEC) and National Stroke Association

of Malaysia (NASAM) in Kuantan, Pahang. Additionally, a baseline group consisting of 10 healthy patients was included to provide a comparison between healthy and non-healthy individuals. This baseline group allowed for a more comprehensive understanding of the differences in muscle spasticity levels and MMG signal characteristics between healthy controls and individuals affected by neurological disorders. The measurement and data acquisition adhered rigorously to the specified procedures outlined in the ethical clearance document, approved by the International Islamic University Malaysia Research Ethics Committee (IREC) under the identification number IREC 2023-025. All measurements were acquired using the Raspberry Pi Pico, orchestrated by Python IDE software (Thonny) that saved data in CSV file, employing non-invasive methodologies in accordance with the obtained informed consent.

1.6 THESIS ORGANIZATION

The **Chapter One** of the current work provides an overview of the research foundations and concepts, problem statement, objectives, scope, and methodology involved. **Chapter Two** deliberates on the literature review of clinical tools that have been employed to measure muscle spasticity and the quantitative evaluation of spasticity severity using differences sensors that are mapped to clinical tools. Additionally, the chapter identifies and emphasizes gaps in existing research. In **Chapter Three**, the methodology employed throughout the investigation is briefly described. Explicitly describing the design and development of the QSAT Platform, this section encompasses the implementation of software and hardware systems for spasticity assessment as well as the biomechanical parameters extracted as features from the data signals, which were subsequently utilised to develop a machine learning model for both flexion and extension movements. The experiment procedures that were implemented for data acquisition are then briefly described. Prior to that, IREC provides ethical authorisation to authorise consent for the experimentation on patients with neurological disorders. In **Chapter Four**, the results and

discussion of the statistical test, data analysis, and model accuracy and performance are presented. The research's development and outcomes are reported in **Chapter Five**, which concludes the research. In addition, the chapter provides information regarding the research's limitations and prospective future research that could be expanded upon.

CHAPTER TWO

LITERATURE REVIEW

2.1 INTRODUCTION

The chapter begins by discussing the phenomenon of spasticity in individuals with neurological disorders, followed by an exploration of various types of neurological disorders that contribute to the development of muscle tone abnormalities. The discussion then delves into the conventional methods of assessing spasticity levels, particularly Passive Range of Motion (PROM) techniques involving passive stretching. The chapter continues with an in-depth analysis of clinical assessment tools used to evaluate the severity of limb spasticity. Among the most frequently employed measures for assessing spasticity levels are the Fugl-Meyer Assessment (FMA), the Modified Tardieu Scale (MTS), the Australian Spasticity Assessment Scale (ASAS) and the Modified Ashworth Scale (MAS). The benefits, limitations, and reliability of various neurological assessment tools, as reported in previous studies, are thoroughly examined. Subsequent sections provide a detailed explanation of the characteristics and advantages of mechanomyography (MMG) in measuring muscle spasticity, followed by a comprehensive review of past and ongoing studies utilising MMG alongside alternative approaches in neurological assessment. Both MMG and alternative assessment methods are examined not only for effectiveness in measuring spasticity but also for broader applicability in evaluating other forms of muscle impairment, ensuring a thorough exploration of quantitative measurement techniques. The chapter also identifies the latest advancements in objectively determining spasticity levels using machine learning. In line with the review, a critical analysis of existing research is presented to identify prevailing methodological limitations and inconsistencies in current approaches. The analysis highlights the gaps that the present study seeks to address, particularly the need for objective, reliable, and clinically adaptable tools for assessing spasticity. Ultimately, the chapter concludes with a summary of key insights that will serve

as the foundation for designing robust, quantitative spasticity evaluation framework tailored for the QSAT platform, specifically targeting the human upper limb.

2.2 SPASTICITY

Spasticity, a common symptom of upper motor neuron lesions, is characterised by increased muscle stiffness, rigidity, and reflex hyperexcitability, often leading to involuntary muscle contractions or sudden movements (Otman et al., 2016). While there is no universally agreed-upon definition of spasticity, it is widely recorgnised as a positive feature of upper motor neuron syndrome (UMNS), manifesting as resistance to passive muscle stretching (Gill et al., 2024). In cases where spasticity is confined to a single muscle or a small group of muscles, it is referred to as 'focal' or 'multi-focal' spasticity, highlighting its localized nature (Williams et al., 2022). The varying levels of spasticity severity can have a significant influence on everyday tasks, movement, and speech, potentially resulting in discomfort or pain (Cha & Arami, 2020).

Upper motor neuron lesions present as positive symptoms, including increased muscle tone, enhanced stretch reflexes, clonus, and spasms, as well as negative symptoms such as incoordination, fatigue, weakness, and compromised motor control, all of which negatively impact the patient's quality of life and impose financial burdens on families (He et al., 2023). Both symptoms can lead to various secondary functional impairments, such as deficits in walking, static or dynamic postural stability, reduced hand dexterity, challenges with swallowing, and speech which complication may arise over time (Dressler et al., 2018).

Stroke is recognised as the second greatest cause of death and the primary source of impairment globally, rendering it the third highest contribution to both mortality and

disability worldwide (Feigin et al., 2022; J. H. Kim et al., 2021; Starosta et al., 2024). The "Global Burden of Diseases, Injuries, and Risk Factors Study" (GBD) indicates that between 1990 to 2019, the global incidence of stroke rose by 70%, the number of cases of stroke rose by 85%, and stroke-related fatalities escalated by 43% (Sheng et al., 2024), as illustrated in Figure 2.1. Additionally, spasticity characterised by high muscle tone affects antigravity muscle groups particularly in the arms, legs, hips, knees, and ankles (Nair & Marsden, 2014). Muscle tone, which refers to the tension in a relaxed muscle or the resistance felt during passive joint stretching, plays a critical role in understanding spasticity (Ganguly et al., 2021). Notably, muscle tone comprises two distinct components: active tone, driven by neural activity, and passive tone, resulting from the muscle's intrinsic properties (Swaiman & Phillips, 2018). Excessive flexion of fingers and thumb adduction results in a clenched fist, while high tone in flexors and adductors of the hips, knees, and ankles leads to hyperextension of the big toe and difficulty in footwear use.

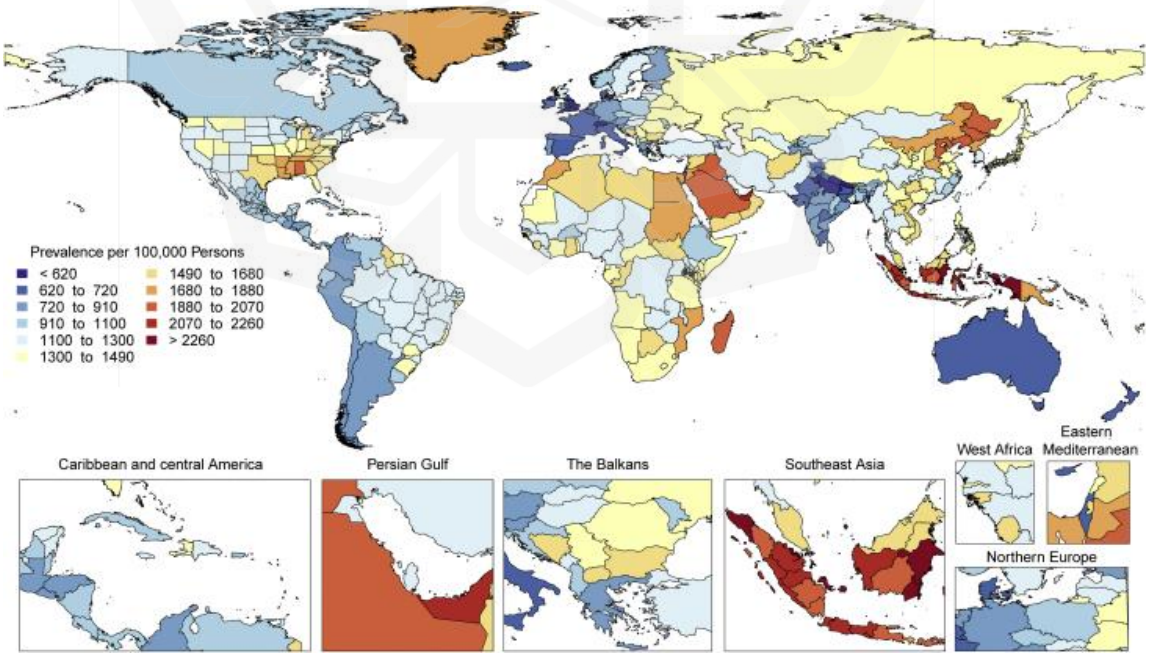

Figure 2.1 Global Distribution of Stroke Survivor in 2019 (Roth et al., 2020)

Spasticity, which is a commonly observed symptom subsequent to a stroke, affects roughly 30% of patients and typically becomes apparent during the initial few days or weeks following the stroke. Conversely, the initiation of spasticity displays a considerable amount of variability, occurring either shortly, moderately, or significantly after a stroke. Symptoms manifest most frequently in the lower and upper extremities, with the elbow (69%), wrist (66%), and ankle (66%) being the most commonly affected (Doussoulin et al., 2020). In the upper limbs, typical patterns of spasticity include shoulder adduction and internal rotation, elbow flexion, wrist and finger flexion, and forearm pronation, while in the lower limbs, extensor synergy is commonly observed, involving hip adduction, hip and knee extension, and equinovarus foot (Kuo & Hu, 2018), as illustrated in Figure 2.2. Post-stroke spasticity has been observed in 4% to 27% of patients during the acute phase (1 to 4 weeks post-stroke), 19% to 26.7% in the subacute phase (1 to 3 months post-stroke), and 17% to 42.6% in the chronic phase (beyond 3 months post-stroke) (Falcone et al., 2024).

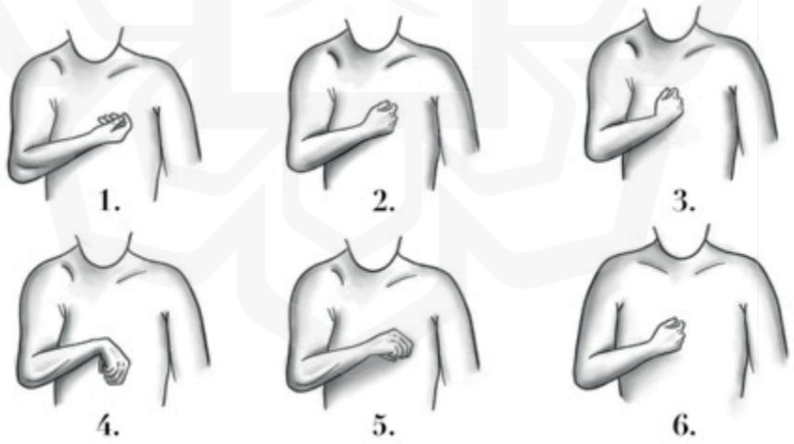

a)

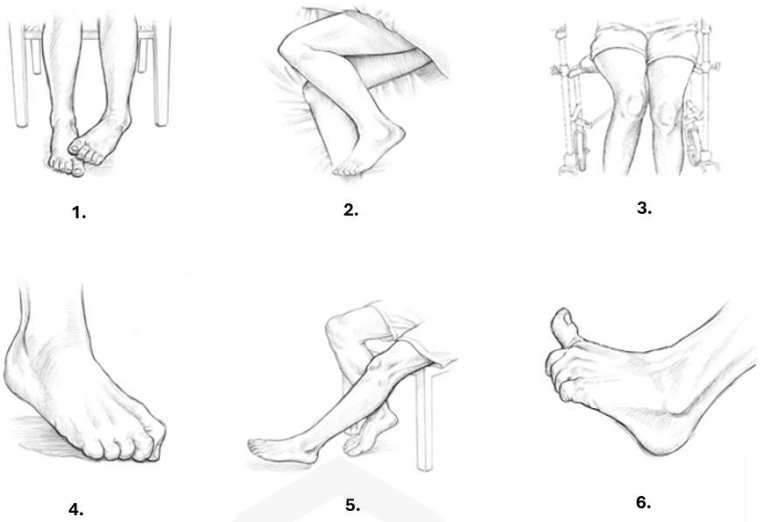

b)

Figure 2.2 Spasticity patterns for: a) upper limbs and b) lower limbs (Esquenazi et al., 2017; Filippetti et al., 2024)

Considering the significance of spasticity assessment and its correlation with motor dysfunction and rehabilitation, together with the acknowledged limits of current clinical scales, several efforts have been undertaken to provide efficient and reliable technological solutions for this evaluation (Guo et al., 2022). Since the late 1980s, two primary categories of systems have emerged (Katz et al., 1992; Powers et al., 1988): passive instruments designed to precisely measure resistance force and/or muscle activity at a specific joint manually stretched by a therapist, and active (i.e., robotic) devices that generate controlled movement of a particular joint at various velocities while simultaneously measuring resistance force or muscle activity. Over the past 30 years, various scales for assessing spasticity, particularly in adults and older children, have become widely available, with the Ashworth Scale (AS) and the Modified Ashworth Scale (MAS) being the most referenced, followed by the MTS and other clinical tools (Ayala et al., 2021). Besides that, Neurophysiological and biomechanical techniques, including isokinetic dynamometers and electrophysiological assessments like the Hoffmann reflex and F-wave, have been

employed to measure spasticity; however, their limitations such as restricted mobility, absence of standardised protocols, and neglect of biomechanical variability impede their regular application in clinical settings (Hong et al., 2018).

2.2.1 Types of Neurological Disorder

Spasticity is a prevalent neuromuscular impairment arising from damage to the central nervous system (CNS), leading to exaggerated muscle stiffness, involuntary contractions, and impaired movement control. This condition is frequently observed in individuals with neurological disorders, where disruptions in the motor pathways affect the regulation of muscle tone. The severity of spasticity varies based on the underlying neurological condition, the extent of neural damage, and the affected muscle groups. Gaining a deeper understanding of neurological disorders associated with spasticity is essential, as such medical conditions contribute to the development and progression of abnormal muscle tone.

Neurological disorders comprise a multitude of conditions that impact the central nervous system (CNS) and the peripheral nervous system (PNS), constituting a comprehensive category (Brandt, 2003). The nervous system comprises the central nervous system (CNS), encompassing the brain and spinal cord, and the peripheral nervous system (PNS), a network of nerves that facilitates communication between the brain and various body organs (Hoffman, 2015; Jakob et al., 2021). Neurological disorders can arise from genetic factors, congenital abnormalities, infections, autoimmune reactions, traumatic injuries, or degenerative processes (Paterson et al., 2020). Each contributing factor plays a significant role in the development of pathophysiological conditions in the nervous system, resulting in various neurological diseases characterised by abnormal structure and function of the central nervous system (CNS) (Su et al., 2020). Conditions such as stroke, cerebral palsy, traumatic brain injury, spinal cord injury, multiple sclerosis, and various

neuromuscular disorders present with diverse manifestations, affecting sensory, motor, or cognitive functions.

Cerebral palsy (CP), the most prevalent motor disability in childhood, is a nonprogressive brain injury that damages the brain region responsible for body coordination, hindering musculoskeletal function and leading to spasticity (Kaya Keles & Ates, 2022), the primary motor impairment affecting 78% to 88% of individuals with the condition (Hägglund et al., 2021). In individuals with CP, upper motor neurone lesions arise from a nonprogressive brain damage in the developing foetal or infant brain, resulting in a cluster of persistent abnormalities that impair movement, posture, and activity (Roldan et al., 2022). CP is also associated with sensory, perceptual, cognitive, communicative, and behavioral disturbances, along with epilepsy and musculoskeletal complications (Patel et al., 2020).

Traumatic brain injury (TBI) is a leading cause of global morbidity and mortality, resulting from mechanical or penetrating head trauma that induces cellular, structural, and vascular damage, ranging from mild to severe (Rezaei et al., 2023). It can cause loss of consciousness, amnesia, muscle weakness, impaired balance, vision changes, and cognitive deficits such as confusion or disorientation (Ardila et al., 2019). In the United States alone, over 1.7 million people sustain TBI annually, with more than 50,000 deaths and long-term disabilities affecting one-third of survivors (Chakraborty et al., 2017).

Spinal cord injury (SCI) occurs due to trauma or disease affecting the spinal cord, resulting in sensory, motor, and autonomic dysfunction, which may be temporary or permanent (Ahuja et al., 2017; Hashimoto et al., 2024). It is often associated with paralysis and can lead to dysfunction in multiple organ systems (Wulf & Tom, 2023). Moreover, neurotrauma affecting the brain and spine is recognized as the leading cause of disability worldwide from a public health perspective (Alvi et al., 2024). SCI affects approximately 250,000 to 500,000 individuals annually, with 2 to 3 million people living with SCI-related

disabilities worldwide (Quadri et al., 2020). Older adults over 60 years experience poorer outcomes due to age-related skeletal abnormalities, with falls being the primary cause of SCI in this population (Hachem et al., 2017).

Multiple sclerosis (MS) represents a multifaceted inflammatory and demyelinating disorder affecting the central nervous system (CNS), initially presenting as intermittent and subsequently evolving into progressively deteriorating neurological impairment (Houtchens & Khoury, 2013). MS typically begins with intermittent neurological symptoms and progresses into a state of continuous deterioration, affecting around 2.5 million people worldwide, with women being affected at roughly twice the rate of men (Norbye et al., 2020). As the most prevalent chronic neurological condition in young adults, MS leads to the development of focal demyelinating lesions, widespread neuroinflammation, and neuronal loss in both the brain and spinal cord (Andelova et al., 2022). Spasticity, one of the most debilitating symptoms, affects the majority of MS patients, significantly impairing mobility and quality of life (Milinis et al., 2016).

A stroke, defined as a neurological deficit caused by localized injury to the central nervous system affecting the brain, retina, or spinal cord due to a vascular source (Campbell & Khatri, 2020), is a leading cause of death and the third most common cause of long-term disability among adults in developed countries (Gupta et al., 2019). The prevalence of upper limb spasticity following a stroke varies between 17% and 42%, markedly exceeding that of lower limb spasticity, with severity increasing over time, reaching its peak at 18 months post-stroke (Y. Wang et al., 2025). Ischemic stroke, which accounts for approximately 80% of all strokes, is predominantly caused by large-artery ischemia in 60% of cases, while the rarer venous infarction results from cerebral vein or venous sinus obstruction (Man Lau et al., 2016). As the condition progresses over time following an acute stroke, the effects of ischemia become more pronounced, further complicating the recovery process (Puig et al., 2020). On the other hand, intracerebral hemorrhages (ICH), responsible for 10% to 15% of all acute strokes, represent the most severe subtype, carrying

a significant risk of mortality, long-term disability, epilepsy, and dementia, making ICH a critical public health concern (Mendiola et al., 2023).

2.2.2 Passive Range of Motion (PROM) in Spasticity Assessment

The International Federation of Orthopaedic Manipulative Physical Therapists (IFOMPT) has been a benchmark for global excellence in Orthopaedic Manual Physical Therapy (OMPT) since its establishment in 1974 (Lonnemann et al., 2021). Orthopaedic Manual Physical Therapists (OMPTs), distinguished for their proficiency beyond musculoskeletal care, employ specific therapy modalities, encompassing manual techniques and therapeutic exercises. One such method methods involves evaluating spasticity using passive range of motion (PROM), during which the therapist manually performs slow and fast joint movements to assess the resistance encountered (Kristinsdóttir et al., 2023). The process engages the muscle through controlled contraction and elongation, providing valuable insights into the muscle's tone, stiffness, and response to stretching. By varying the speed of joint movement, PROM helps differentiate between normal and abnormal muscle behavior, such as heightened resistance during faster movements—a hallmark of spasticity. As a widely used clinical assessment tool, PROM offers critical information for diagnosing spasticity severity and informing individualized therapeutic interventions. However, the subjective nature highlights the need for complementary objective assessment methods to enhance diagnostic accuracy.

Furthermore, PROM itself involves stretching and contraction of the muscle, and one of the most common therapeutic approaches to managing spasticity is stretching. Stretching helps improve flexibility, reduce discomfort, and normalize muscle tone (Gomez-Cuaresma et al., 2021). Stretching is extensively utilised as a therapeutic measure to improve the viscoelastic characteristics of muscle-tendon units, especially in stroke patients (Harvey et al., 2017). In some instances, hypertonicity, caused by heightened

muscular activity during passive stretching, presents as muscle overactivity or diminished extensibility, frequently due to secondary abnormalities such as sarcomere loss and the accumulation of fat and collagen (Currà et al., 2021; Forman et al., 2019; Lorentzen et al., 2018). Physiotherapists employ diverse stretching techniques, encompassing passive and active methods (Figure 2.3), with static stretching being the most commonly utilised where θ_c represents catch angle and θ_{max} represents the maximum flexion angle (Akkaya & Elbasan, 2021). Stretching is performed with a gradual, substantial effort until the point where further passive movement would cause pain or jeopardise joint integrity, while maintaining a minimal speed to avoid triggering the phasic stretch reflex and applying maximum force to counteract spastic dystonia in a supine patient (Pradines et al., 2018). The stretching method can be implemented through several techniques, including manual application by physiotherapists or the utilisation of splints, orthoses, and plaster casts (Salazar et al., 2019).

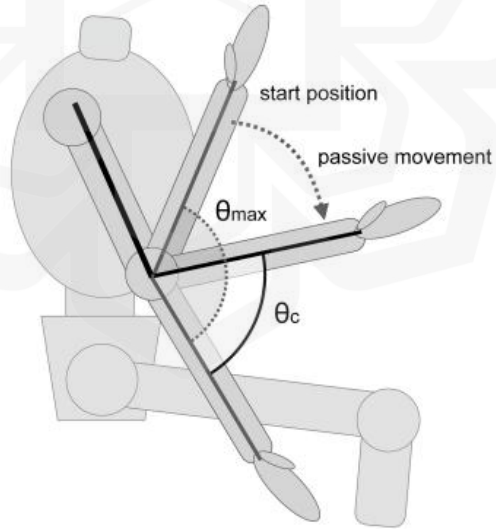

Figure 2.3 Passive range of motion in measuring spasticity (Fujimura et al., 2022)

2.3 NEUROLOGICAL ASSESSMENT TOOL

In the context of subjective clinical evaluations, the management of spasticity is imperative, emphasizing the necessity to utilize a validated assessment technique for the accurate appraisal of spasticity. Effectively addressing spasticity underscores the necessity to employ a validated assessment technique for the accurate appraisal of this condition. The predominant methodologies in conventional clinical interventions incorporate the utilization of the FMA, MTS, ASAS and MAS. The assessment tools not only provide valuable insights into the severity of spasticity but also play a pivotal role in guiding tailored interventions for optimal patient care.

2.3.1 Fugl-Meyer Assessment (FMA)

People who suffer from chronic stroke are diverse and can have a variety of motor impairments affecting their upper extremities (UE) (Woytowicz et al., 2017). Whether in a community, research, or clinical setting, stroke survivors need comprehensive assessments to help with treatment planning and progress evaluation. The FMA is extensively employed in clinical settings to quantify motor impairment and evaluate resistance to passive movement, specifically spasticity (Rech et al., 2020). Recommended by the American Physical Therapy Association—Neurology Section, the FMA serves as a key clinical outcome measure, especially for stroke patients (Goliwąs et al., 2024). The assessment has been utilised to thoroughly assess motor function in the upper extremities, and it has demonstrated strong reliability among different raters and within the same rater (S. Lee et al., 2018). Stroke severity and recovery can be measured with the help of the Fugl-Meyer Assessment, which is commonly used in the medical field (Hernández et al., 2019). The scale measures reflex activity, voluntary movements both within and outside of synergies, the ability to isolate movements, and coordination. The severity of impairment is then determined by the cumulative score, where a score of 0 reflects the most severe impairment, and a score of 100 represents the least severe (Axel R et al., 1975). The FMA assesses

hierarchical characteristics, as well as unidimensional underlying components and motor disability. This indicates that the scale can be utilised in the evaluation of the level of motor function in patients who have suffered a stroke. However, because the primary aim of the FMA is to assess motor control of a particular affected region, the instrument is insufficient for detecting spasticity, as the main function focuses on evaluating motor control.

2.3.2 Modified Tardieu Scale (MTS)

MTS, another widely used tool for quantifying spasticity, differs from the MAS by considering the velocity of passive joint movement, the angle of contraction onset, and the potential for tendon retraction (Yoo et al., 2022). The Tardieu Scale (TS) and its numerous adaptations MTS measures spasticity by assessing muscle resistance to stretching at two distinct velocities that are slow and fast extensions allowing for the detection of a noticeable 'catch' and determining the presence and severity of spasticity (Noor Ayuni Che Zakaria et al., 2015; Shu et al., 2021) which shown in Table 2.1. Therapists assess the angle of full slow passive range of motion (R2) and the angle of first resistance encountered during rapid passive movements (R1) to elucidate the physiological and neurological mechanisms influencing resistance to passive movements, respectively (Deshmukh et al., 2021).

Table 2.1 Modified Tardieu Scale for grading spasticity

Grade	Description
0	No resistance throughout the course of the passive movement
1	Slight resistance throughout the course of passive movement, no clear catch at a precise angle
2	Clear catch at a precise angle, interrupting the passive movement, followed by release
3	Fatigable clonus with less than 10 seconds when maintaining the pressure and appearing at the precise angle
4	Unfatigable clonus with more than 10 seconds when maintaining the pressure and appearing at a precise angle
5	Joint is fixed

The MTS demonstrates greater sensitivity to post-treatment changes due to its ability to evaluate both muscle resistance and the velocity at which movement triggers muscular contraction. However, the correlation between the mean scores of the MTS and other scales like MAS, is limited, as each tools measure distinct dimensions of spasticity. MTS is considered as a suitable tool for assessing muscle spasticity, particularly as it aligns with Lance's definition of spasticity (Banky et al., 2021). Its reliability has been supported by extensive studies in children with cerebral palsy and adults with cerebral-origin spasticity (Akpinar et al., 2017), although reliability coefficients indicate poor consistency for assessing both upper and lower limbs (Morris & Williams, 2018). The MTS has shown moderate reliability in evaluating spasticity in lower limb muscles, except for the quadriceps and soleus, which demonstrated poor reliability (Vattanasilp et al., 2000). While the TS and MTS can distinguish between resistance at slow and fast velocities, similar to the AS and MAS, they share notable limitations: they require substantial training and

experience, assess only passive resistance, and lack validated reliability and established applicability for populations with multiple sclerosis (Naghdi et al., 2017).

2.3.3 Australian Spasticity Assessment Scale (ASAS)

ASAS has been a newly devised instrument that was primarily designed to evaluate muscle spasticity in children with cerebral palsy (Nourizadeh et al., 2024). ASAS examines the velocity-dependent characteristics of TS and MTS and employs a scoring methodology analogous to the MAS for clinical adherence (Calame & Singer, 2015). It focuses on two primary aspects: the existence or location of the "catch" and the level of resistance subsequent to the capture (Love et al., 2016). The ASAS, like the MTS, incorporates R1 and R2 measurements, which, although not explicitly included in the final ASAS score, serve as the foundational data for its calculation and are visually estimated in clinical practice (Gracies et al., 2000; Haugh et al., 2006). ASAS is not only efficient and easy to perform but also follows a well-defined testing protocol and utilizes a clear 5-grade rating system, as shown in Table 2.2.

Table 2.2 Australian Spasticity Scale for grading spasticity

Grade	Description
0	No catch on rapid passive movement (RPM)
1	Catch occurs on RPM followed by release. There is no resistance to RPM throughout rest of range
2	Catch occurs in second half of available range (after halfway point) during PRM and is followed by resistance throughout remaining range

Table 2.2 Australian Spasticity Scale for grading spasticity (cont.)

Grade	Description
3	Catch occurs in first half of available range (up to and including halfway point) during RPM and is followed by resistance throughout the remaining range
4	When attempting RPM, the body part appears fixed but moves on slow passive movement

The ASAS incorporates movements performed "as rapidly as possible" to maximise the likelihood of detecting spasticity, if present. During ASAS testing, three rapid passive motions are executed at maximum speed, ensuring consistency in identifying the catch angle and eliminating voluntary resistance. A final rapid passive motion applies sufficient force to move the muscle or muscle group through the catch to the end of its range, allowing for subjective assessment of resistance between the catch point and the end range. Notably, the ASAS demonstrates superior inter-rater reliability compared to other clinical scales used in children with cerebral palsy, owing to its explicit and standardized testing procedure (Bayram et al., 2022).

2.3.4 Modified Ashworth Scale (MAS)

The MAS, an adaptation of the original AS with an added category (1+) shown in Table 2.3, is a widely used measurement in clinical practice to assess the perceived level of resistance (tone) during passive limb movement, and its use is endorsed by the National Institute of Neurological Disorders and Stroke Common Data Element (Baunsgaard et al.,

2016; Sarathy et al., 2019). The MAS is favoured by physiotherapists due to its ease of use in clinical environments, lack of necessity for specialised equipment, and safety when performed by the same evaluator (Blackburn et al., 2002). Recognising limitations on the original scale, Bohannon & Smith (1987) observed that many patients with hemiplegia displayed spasticity levels at the lower end of the Ashworth Scale, where the grade 1 lacked sufficient distinction. To improve its precision, they introduced grade 1+ and refined the definitions (Ansari et al., 2022). A score of 1+ is established when the observer experiences a marginal resistance throughout the remaining range of motion, accompanied by a slight increase in muscle tone visible in a catch (below 90 degrees) (Bohannon & Smith, 1987). While the MAS provides a straightforward and efficient means of evaluating spasticity, it differs from Lance's definition of spasticity as it is not influenced by movement speed. The MAS is a 6-point rating system that evaluates muscular tone by clinically documenting the resistance to passive movements while manually manipulating the joint through its available range of motion (Trompetto et al., 2023).

Table 2.3 Modified Ashworth Scale for grading spasticity

Grade	Description
0	No increase in muscle tone
1	Slight increase in muscle tone, manifested by a catch and release or by minimal resistance at the end of the range of motion when the affected part(s) is moved in flexion or extension
1+	Slight increase in muscle tone, manifested by a catch, followed by minimal resistance throughout the remainder (less than half) of the Range of Motion (ROM)
2	More marked increase in muscle tone through most of the ROM, but affected part(s) easily moved

Table 2.3 Modified Ashworth Scale for grading spasticity (cont.)

Grade	Description
3	Considerable increases in muscle tone, passive movement difficult
4	Affected part(s) rigid in flexion or extension

During the assessment, the therapist must quickly move the tested limb through the full range of motion and evaluate the perceived resistance (Zurawski et al., 2019). Spastic limbs, characterised by increased resistance to joint movement, exhibit this resistance more prominently with greater deflection angles and higher speeds (Annaswamy et al., 2007). The resistance, quantified as torque, arises from both reflex activity and the passive properties of tissues, serving as a reliable quantitative indicator of spasticity that correlates with MAS level (Zakaria et al., 2014). Although the MAS is widely used and extensively studied, its reliability has primarily been validated for assessing spasticity in the elbow and wrist (Gregson et al., 1999). Despite its widespread use and extensive research, the MAS has limitations, as it only captures passive resistance during stretching, reflecting a single aspect of spasticity namely, increased muscle tone at rest (Lackritz et al., 2021).

2.4 MECHANOMYOGRAPHY (MMG) SIGNALS: CHARACTERISTICS AND ADVANTAGES IN SPASTICITY ASSESSMENT

The application of electromyography (EMG) in standard therapeutic practices signifies a modern and innovative method for neurorehabilitation in stroke recovery patients (Lewandowska-Sroka et al., 2021). While EMG has long been employed to capture electrical muscle activity, its use has primarily been confined to therapeutic purposes (Brambilla et al., 2021). However, EMG is particularly vulnerable to interference from noise and fluctuations in resistance, which compromises its reliability in various

environments or during extended data acquisition, such as when the patient begins to perspire (Correa et al., 2023). In contrast, MMG emerges as a valuable alternative by measuring muscle vibrations or mechanical activity produced by muscle contractions, using sensors like microphones or accelerometers (Esposito et al., 2018; Meagher et al., 2020; Santos et al., 2024). The mechanical vibrations, referred to as MMG, are generated by the contraction of muscle fibers, which occurs due to the release of calcium ions from the sarcoplasmic reticulum in response to an action potential (Fang et al., 2023). The development of piezoelectric microphones and accelerometers facilitated the effective detection of mechanical signals from skeletal muscle surfaces at low frequencies, referred to as MMG signals, which frequently get disrupted by electrical noise (Hazem et al., 2023; Uwamahoro et al., 2021).

MMG offers a distinct advantage in detecting and quantifying vibrations produced by muscular contractions and stretching (E. L. Santos et al., 2016), with highly sensitive transducers operating within the 2 Hz to 100 Hz range. The transducers are not only biocompatible and easy to attach but also cost-effective and less prone to noise interference (Ibitoye et al., 2014). Numerous studies have validated the significance of MMG signal parameters in skeletal muscle research and their potential for clinical applications. MMG, beyond its general utility in measuring muscle dynamics, has demonstrated the ability to identify specific muscle or hand movement patterns with an accuracy of 89.7% when combined with linear discriminant analysis (LDA) classifiers, underscoring its potential for precise muscle activity monitoring and neuromuscular assessments (Asheghabadi et al., 2021). From a biomechanical perspective, MMG signals represent low-frequency lateral vibrations produced by skeletal muscle fibers after muscle contraction, reflecting the mechanical representation of the underlying electrical activity in the motor units (Z. Wu et al., 2021). Motor units (MU), fundamental elements of the neuromuscular system, have been shown to correlate with MMG amplitude, while MMG frequency characteristics reflect the global firing rates of active MU. By analyzing the temporal and spectral features of MMG signals, researchers can gain insights into motor control strategies that modulate force generation in both voluntary and involuntary muscle activities.

MMG, also referred to various names such as acousticmyography, soundmyography, phonomyography, vibromyography, and acceleromyography, offers several advantages over EMG, including simplified equipment handling, lower costs, and closer alignment with muscle mechanics (Islam et al., 2013). Unlike EMG, MMG presents several advantages such as resistance to skin impedance variations, an enhanced signal-to-noise ratio, and reduced sensitivity to sensor positioning on the target muscle; however, the absence of standardised sensors and issues with acoustic or vibrational interference have impeded its widespread adoption (Woodward et al., 2019). MMG has been shown to be useful for evaluating spasticity in clinical settings, while the mechanomyogram (MMG-derived signal) provides a mechanical representation of the musculature's overall dynamics (Turnsek & Paravlic, 2024). Despite its benefits, MMG is a relatively new technique that requires further exploration in terms of equipment refinement, sensor improvements, and expanded applications to better understand intricate muscle movements (Talib et al., 2018). Nevertheless, the use of advanced transducers, including accelerometers, piezoelectric contact sensors, and laser distance sensors, has established MMG as a reliable and durable method for assessing muscle contraction dynamics (Li et al., 2024).

Among the various sensor modalities employed in MMG acquisition, accelerometers are particularly favored due to their compact size, low cost, high sensitivity to low-frequency vibrations, and ease of integration into wearable systems. These features make them highly suitable for real-time, non-invasive monitoring in clinical environments. Accelerometers are capable of capturing three-dimensional mechanical oscillations, which is essential when analyzing complex muscle dynamics such as those involved in spasticity assessments. However, despite their advantages, previous studies have reported certain limitations in the application of accelerometers for MMG. These include susceptibility to motion artifacts, difficulty in isolating muscle-specific signals in multi-muscle groups, and challenges related to optimal sensor placement, which can affect the accuracy and repeatability of the measurements. Furthermore, variations in muscle geometry and subcutaneous fat can influence the quality of the recorded signals. Highlighting these limitations helps underscore the necessity for methodological improvements in sensor

placement, signal processing, and standardization, as addressed in the present study's design.

MMG offers a biomechanical approach by detecting mechanical vibrations during muscle contraction and elongation using sensors affixed to the skin's surface (E. Santos et al., 2017) which shown in Figure 2.4. In this setup, the accelerometer is strategically placed on the biceps muscle belly, aligned with the muscle fibers to accurately capture mechanical vibrations along the x, y, and z axes. Proper anatomical placement is essential, as it ensures consistent and high-quality signal acquisition across different assessment sessions. These mechanical vibrations, which result from both passive stretching and active contraction of the muscle, are transmitted through the surrounding tissue and detected at the skin's surface (E. L. Santos et al., 2016).

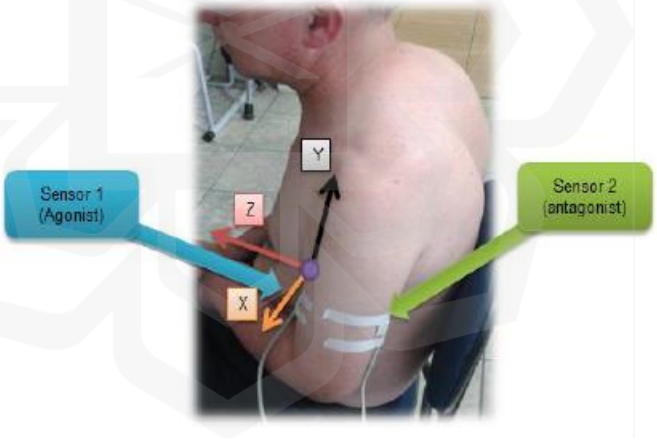

Figure 2.4 Sensor placement for acquiring MMG signals (E. Santos et al., 2017)

MMG signals reflect the mechanical oscillation produced by the spatiotemporal summation of individual muscle fibers (H. Wu et al., 2018). Furthermore, MMG is independent of its muscular position, whereas the normalised amplitude is contingent upon it, and the centroid shifts with increased force (Fang et al., 2023). This suggests that muscle activation can potentially be transformed into mechanical motion, a concept that has

recently evolved into a broader sensor technology known as a soft sensor (Chen et al., 2017; Tony et al., 2021). Three primary mechanisms govern muscle activation, contributing to MMG: (i) extensive lateral movements of the muscle, as it approaches or recedes from its tension line during both the contraction and relaxation phases; (ii) the resonant frequency inducing slight lateral vibrations in the muscle; and (iii) modifications in the dimensions of active muscle fibers.

In order to improve the categorization of different muscular activities, the useful characteristics are extracted by converting the temporal waveforms of the MMG signals into the time-frequency domain (Wołczowski & Zdunek, 2017). The typical method used for this conversion is the short-time Fourier transform (STFT), although other options such as the discrete wavelet transform (DWT) can also be utilised. In MMG research, the root mean square (RMS) analysis is frequently employed. The method uses the intensity quadratic mean value as an indicator of the range of muscle displacement represented by its acceleration (RMSa) and it is one of the most frequently used statistical methods in MMG research (Krueger et al., 2014). The analysis of MMG can also be conducted in the frequency domain by calculating the mean frequency (MPF or MF) and/or the median frequency (MNF) of the power spectrum density distribution (Cè et al., 2015). This approach yields valuable insights into the underlying physiological and biomechanical characteristics of the muscles under scrutiny (Uwamahoro et al., 2021). Notwithstanding, MMG possesses a broad spectrum of prospective applications, encompassing the control of prosthetic devices, recognition of gestures in human-machine interfaces (HMIs), and the investigation of fundamental physiological mechanisms within the neuromuscular system in the realm of scientific research (Szumilas et al., 2021).

2.5 QUANTITATIVE MEASUREMENT OF MUSCLE IMPAIRMENT IN NEUROLOGICAL DISORDERS

2.5.1 Sensor-Clinical Tool Correlation in Measuring Muscle Impairments

Although muscle dysfunction is a well-recognised condition, its measurement and evaluation continue to present significant challenges. Numerous methods for assessing muscle impairment have been devised, categorized into clinical evaluation methods and quantitative evaluation methods (Petek Balci, 2018). Despite reports of low inter-rater reliability, the MAS is the most prevalent tool in clinical practice due to its simplicity (Park et al., 2019). Inter-rater reliability can be improved in two ways. First, quantitative and objective measurement can replace or supplement the subjective instrument currently in use. Additionally, standardised training based on quantitative and statistical analysis can improve inter-rater reliability without modifying the simplest protocol. The section provides an overview of prior research papers that have explicitly investigated the evaluation of muscle dysfunction using sensor-based technologies. These studies explored muscle conditions such as fatigue, rigidity, and weaknesses across various muscle groups. Table 2.4 summarizes the findings related to muscle function assessment in the specified muscle groups, highlighting key aspects such as the types of sensors utilised, signal analysis techniques employed, and the outcomes achieved.

One notable research by Tsuji et al., 2021 employed portable MMG and EMG devices to objectively assess the patellar tendon reflex hyperreflexia. Three sensors were carefully positioned on the quadriceps muscle area while the patients were seated upright with their knees at 70° and their hips at 80°. The EMG/MMG devices were taped to the thigh with great care. In the rectus femoris (RF), vastus medialis (VM), and vastus lateralis (VL) muscles, the obtained results showed significantly increased root mean square (RMS) amplitudes and reduced mean power frequency (MPF), as observed in both EMG and MMG signals during both maximal and constant force contractions. Particularly

noteworthy were the results in patients with cervical and thoracic myelopathy, where the receiver operating characteristic (ROC) curve analysis showed moderate to very high areas under the curve (AUC) for all EMG-RMS, EMG-MPF, MMG-RMS, and MMG-MPF values, indicating the diagnostic potential of these measures for determining patellar tendon hyperreflexia. Future therapeutic applications and the ability to aid in the identification of various neurological illnesses are both made possible by the use of EMG and MMG as objective techniques for measuring the patellar tendon reflex.

Building upon the use of sensor-based assessments, De POL et al., 2021 explored the effects of punctual mechanical oscillation (PO) on biceps brachii (BB) muscle spasticity in children with cerebral palsy (CP), with the primary objective of examining its impact. Two interventions were administered to all patients (7 children with CP) at intervals of 7 to 15 days to evaluate two distinct approaches for applying oscillation: Intervention 1 targeted the tendon of the spastic muscle, while Intervention 2 focused on the muscle belly of the spastic antagonist muscle. The effects of the interventions were evaluated using the MAS, and concurrent data on MMG signals were recorded. Data acquisition occurred before the interventions and at various time intervals thereafter. The results demonstrated that both intervention protocols resulted in a statistically significant reduction in MAS values following the interventions. However, the MMG values, analysed in both temporal and spectral domains, did not exhibit a consistent pattern. Furthermore, no significant differences were observed between the two protocols in terms of their effects on MAS, MMG mean frequency (MMG_{MF}), and MMG root mean square (MMG_{RMS}). Collectively, the research suggests that punctual mechanical oscillation (PO) holds potential as a valuable therapeutic modality for modulating spasticity in children diagnosed with cerebral palsy. However, further research is needed to gain a deeper understanding of the underlying mechanisms and optimize the application of PO in clinical practice.

Further expanding on MMG applications, Cruz et al., 2020 performed a comparative analysis of muscle MMG signals collected from the flexor and extensor muscles in two groups: six athletes experiencing spasticity and six without impairments.

Two MMG sensors were strategically placed on the participant's skin. Sensor 1 was attached to the motor point of the wrist flexors, while Sensor 2 was positioned on the motor point of the wrist extensors. MMG signals were recorded and stored for subsequent examination. In the cerebral palsy (CP) group, the mean MMG_{RMS} voltage values were 0.4058 mV for the left wrist flexor muscles and 0.4258 mV for the left wrist extensor muscles. For the right wrist flexor and extensor muscles, the values measured were 0.4215 mV and 0.4529 mV, respectively. In comparison, the non-impaired (NI) group displayed mean MMG_{RMS} values of 0.3694 mV for the left wrist flexors, 0.3945 mV for the left wrist extensors, 0.3503 mV for the right wrist flexors, and 0.3728 mV for the right wrist extensors. Additionally, the mean MMG_{RMS} 3D module was observed to be higher in the CP group than in the NI group. The results highlight MMG's potential to identify vibrational differences in muscle activity, enabling clear distinctions between individuals with spasticity and without spasticity.

While previous studies explored MMG diagnostic potential, Pan et al., 2020 proposed a novel approach by developing MMG sensors using PVDF piezoelectric electrospinning specifically for lower limb rehabilitation exoskeletons. The research introduces an innovative MMG sensor fabricated through near field electrospinning technology and applies it to detect human body motion in the context of a lower limb exoskeleton robot (LLRE). The MMG sensors demonstrated exceptional sensitivity, enabling the direct capture of muscle movement signals, even during subtle motion intentions. The main objective of the research was to develop a motor control technology integrated with a highly sensitive physiological signal sensor to accurately capture physiological signals. Through the integration of the newly developed MMG sensor signals with motor control, the utilization of the LLRE aims to enhance the efficiency of patient movement. In the comparative analysis, commercial electromyography (EMG) sensors were included alongside the as-made MMG sensors. The maximum signal amplitude recorded by the commercial EMG sensor was approximately 0.2 V, whereas the MMG sensor achieved an amplitude of around 2.8 V. Furthermore, the signal-to-noise ratio (SNR) of the EMG sensor was approximately 4, whereas the MMG sensor demonstrated an SNR

of approximately 25. This novel sensor technology effectively improved sensitivity in driving the LLRE by capturing physiological signals using the MMG sensor during human walking with the LLRE system.

Beyond MMG and EMG-based assessments, Moreta et al., 2020 conducted research to assess the reliability and validity of the Modified Heckmatt Scale for evaluating muscle changes in spasticity using ultrasound. The research included 50 patients, of which 45 undertook Botulinum Toxin (BoNT) treatment for upper or lower limb spasticity. Additionally, five healthy subjects served as a control group, providing normal reference images for comparison with the spasticity-affected images. Clinical spasticity was defined as a score of 2 or higher on the MAS. Among patients, the average MAS level for the upper extremity joints (elbow, wrist, and fingers) ranged between 1.39 and 1.89, while the scores for the lower extremity joints (hip, knee, and ankle) ranged between 1.71 and 2.20. Each of the four raters evaluated between 3 and 27 images per muscle, including five images for the flexor carpi radialis, ten for the flexor digitorum superficialis, seven for the flexor digitorum profundus, three for the pronator teres, fourteen for the biceps brachii, ten for the brachialis, twenty-seven for the gastrocnemius, twelve for the soleus, and twelve for the rectus femoris. The findings indicated that experienced clinicians demonstrated moderate intra-rater reliability and substantial inter-rater reliability. In contrast, novice ultrasonographers exhibited fair to poor inter-rater reliability. Interestingly, the research revealed no significant differences in reliability based on physician experience, suggesting that the Modified Heckmatt Scale could be beneficial for clinicians regardless of their expertise level. By incorporating assessments of additional muscles across both the upper and lower limbs, the research also improved the generalizability of the scale.

Apart from that, Park et al., 2019 employed an AI-based method to analyze how human experts determine MAS levels by evaluating the contributions of various characteristic features quantified by biomechanical parameters. The study included 34 subjects with hemiplegia, scores for joint motion, resistance, and MAS simultaneously collected from 848 trials conducted by multiple therapists. The AI-based analysis could be

used to characterise the standard perception of each MAS rating for consistent training, ultimately improving inter-rater reliability, or to facilitate the transition of MAS to new quantitative instruments systematically. Conventional methods such as correlation and regression analyses often lead to uncertainty in clinical score prediction. In the study, joint motion and resistance of a joint were measured using nine biomechanical parameters, which were then used to train an AI algorithm to predict MAS levels. The algorithm effectively learned MAS ratings, achieving an average percentage agreement of 82.2% and a Cohen's kappa of 0.743 (95% CI: [0.735, 0.751]). The respective agreement percentages for MAS 0 to 3 were 76.7%, 80.4%, 85.0%, 84.9%, and 88.4%. The AI predictions were highly correlated with human ratings, with a correlation coefficient of Z: 0.825. Each parameter and its significance were analyzed across experiments with the same MAS level.

Hong et al., 2018 compared findings with MAS and MTS tools after evaluating post-stroke spasticity using sEMG and ultrasonic imaging. Eight post-stroke patients and eight healthy controls comprised the study. MAS and MTS were used to assess clinical spasticity. Sonoelastographic data were gathered for comparison while surface EMG readings followed the Brain Motor Control Assessment (BMCA) technique. From the medial gastrocnemius muscle (GCM), the sonoelastographic calculated muscle architecture and elasticity index on both affected and unaffected sides. Multiple regression analysis and Spearman correlation coefficient let one evaluate the relationship between ultrasonic parameters and clinical assessment instruments. With sEMG activity, MAS and MTS shown notable association. Whereas the elasticity index was much raised on the unaffected side, the medial GCM on the hemiplegic side displayed reduced fascicle length and pennation angle. The MTS X and R2-R1 values showed a strong correlation with the elasticity index in the hemiplegic GCM, therefore suggesting a link between BMCA and sonoelastography and clinical evaluation instruments. Results showed MTS had more variations than MAS in identifying spasticity. Multiple regression analysis, however, revealed no statistically significant linear link between BMCA or sonoelastography data and clinical evaluation instruments (MAS and MTS).

Besides that, Jun et al., 2018 investigated the use of MMG to assess spasticity in patients with brain lesions, focusing on its correlation with the MAS for low spasticity levels. The study included 10 patients with brain lesions, with MMG sensors were placed on the vastus lateralis (VL) and semitendinosus (ST) muscles. Passive stretch reflexes were evaluated by three therapists to confirm the presence of spasticity in all patients. The research found that the coefficient of concordance among the therapists was mostly non-significant. However, a significant difference was identified in the normalized hull area ratio between spastic and normal muscles as measured by MMG and EMG ($p = 0.01$, $p = 0.02$). A "less than one point" result suggested that antagonist muscle activity exceeded that of the agonist, signaling spasticity. Furthermore, a significant correlation was observed between the normalized hull area ratio and the mean MAS level provided by the examiners ($r = 0.69$, $p = 0.01$), while the correlation between EMG data and MAS level was not significant ($r = -0.09$, $p = 0.71$). The relationship between the normalized hull area ratio and MAS was influenced by spasticity severity. Specifically, normalized hull areas were found to be 0.28 for the lowest passive contraction and 0.32 and 0.33 for the highest passive contractions of the antagonist and agonist muscles, respectively. The findings suggest MMG as a promising objective tool for clinical spasticity assessment, particularly in low spasticity cases.

Krueger et al., 2018 contributed to the development of a wearable device designed to monitor muscle fatigue through MMG, specifically in the context of motor neural prosthetics. The research primarily aimed to establish a method for detecting fatigue in muscles stimulated by surface functional electrical stimulation (sFES). The research involved six patients with spinal cord injuries (SCI), who engaged in quasi-isometric contractions prompted by electrical stimulation of three distinct quadriceps muscles: the rectus femoris (RF), vastus lateralis (VL), and vastus medialis. To facilitate movement of the knee joint in the sagittal plane, the system employed voltage-controlled monophasic square pulses. The stimulation protocol pulses operated at a frequency of 1 kHz with a 50% duty cycle and at 50 Hz with a 15% duty cycle. The findings of the research indicated that MMG could serve as a reliable biomarker for monitoring real-time muscle fatigue during

isometric quadriceps contractions induced by functional electrical stimulation (FES). Furthermore, MMG demonstrated its potential in detecting fatigue within closed-loop control frameworks.

Besides using EMG and MMG in muscle spasticity measurement, dynamometer is also one of the methods that can be used in measuring muscle spasticity. In previous research, Yamaguchi et al., 2018 evaluated the accuracy and reproducibility of a clinically applicable method for assessing muscle-tendon stiffness using a dynamometer. The method combined force measurement, joint movement, and reflex-mediated muscle activity to quantify passive and reflex-mediated stiffness in the triceps surae muscle-tendon complex. The research included 8 healthy individuals (mean age: 39.3 years), 9 patients with spastic cerebral palsy (CP, mean age: 39.8 years), and 8 patients with multiple sclerosis (MS, mean age: 49.9 years). Slow and rapid ankle joint dorsiflexion strains were performed to assess passive stiffness, reflex-mediated stiffness, and range of motion (ROM). The results showed that patients with CP and MS had significantly higher passive stiffness and reduced ROM compared to healthy subjects, while reflex-mediated stiffness did not differ significantly between groups. The method demonstrated good to excellent inter- and intra-rater reliability for both passive and reflex-mediated stiffness measurements, with intra-class correlation coefficients (ICC) ranging from 0.62 to 0.91. The research highlights the utility of a valid and reproducible approach for measuring passive ankle stiffness and reflex-mediated stiffness, revealing increased stiffness in individuals with cerebral palsy and multiple sclerosis.

Table 2.4 Correlation Between Sensor-Based Features and Standardised Clinical Scales

Author/year	Instruments	Muscle	Subjects	Research	Used Parameters
Tsuji et al., 2021	Force transducers, accelerometers, and motion analysis	Quadriceps and tendon	12 healthy volunteers	Use portable MMG and EMG devices to objectively assess hyperreflexia in the patellar tendon reflex	RMS, MPF
De POL et al., 2021	Triaxial-accelerometer MMG and MAS tool	Spastic antagonist muscle	7 children with CP	Study different protocols for applying punctual mechanical oscillation (PO) and assess their respective effects	RMS, MPF
Cruz et al., 2020	Triaxial accelerometer MMG	Flexors and extensors muscles	6 athletes with spasticity and 6 non-impaired.	Compare muscle MMG signals from flexor and extensor muscles	RMS
Pan et al., 2020	Piezoelectric Sensor for MMG	Thigh muscles	Not stated	Create advanced motor control technology with a highly sensitive physiological signal sensor to capture signals with exceptional sensitivity	MMG amplitude and Signal-to-Noise Ratio (SNR)
Moreta et al., 2020	US image acquisition and MAS tool	Upper extremity (elbow, wrist, and fingers)	50 patients, 5 healthy subjects	Investigation into the reliability and validity of the Modified Heckmatt Scale for assessing muscle changes using ultrasound in spasticity	Ultrasound Image

Table 2.4 Correlation Between Sensor-Based Features and Standardised Clinical Scales (cont.)

Author/year	Instruments	Muscle	Subjects	Research	Used Parameters
Park et al., 2019	Biomechanical data (joint motion and resistance), MAS and AI algorithm or artificial neural network	Joint	34 patients with hemiplegia	Utilises an AI-based method to understand how human experts determine MAS levels by evaluating biomechanical parameters' contributions to characteristic features	Biomechanical Parameters (motion and resistance of a joint)
Hong et al., 2018	Ultrasonography, sEMG, MAS tool and MTS tool	Upper Limb	8 patients with stroke and 8 healthy subjects	Quantitatively assess post-stroke spasticity using sEMG and ultrasonography, establishing their correlation with clinical spasticity	Sonoelastography, Spearman Correlation Coefficient and Multiple Regression Analysis
Jun et al., 2018	Triaxial-accelerometer MMG and MAS tool	Vastus lateralis muscle (agonist) and semitendinosus muscle (antagonist)	10 patients with brain lesions	Establish the correlation between muscle MMG and MAS in patients with low spasticity levels	Signal Vector Magnitude (SVM) and Spearman Correlation
Krueger et al., 2018	Triaxial-accelerometer MMG	Quadriceps (rectus femoris), vastus lateralis and vastus medialis muscles	6 patients with SCI	Develop a method using MMG sensors on the quadriceps to detect muscle fatigue from sFES	Cauchy Wavelet Transform (CaW), Wilcoxon Signed Rank

Table 2.4 Correlation Between Sensor-Based Features and Standardised Clinical Scales (cont.)

Author/year	Instruments	Muscle	Subjects	Research	Used Parameters
Yamaguchi et al., 2018	Hand-held dynamometer	Triceps surae muscle tendon	8 healthy subjects, 9 patients with CP and 8 patients with MS	Examined the precision and consistency of a practical clinical approach utilizing a dynamometer	ICC

2.5.2 Machine Learning Approaches in Sensor-Based Assessment of Muscle Spasticity

Machine-learning classifiers were utilised to automatically infer a prediction function from labelled data derived from inertial signals obtained during passive stretching. In this context, therapist provided MAS ratings to annotate these inertial signals, thus structuring the task as a supervised learning problem. Most offline approaches rely on supervised Machine Learning (ML) models for activity recognition, such as Support Vector Machine (SVM), Decision Tree (DT), K-Nearest Neighbors (KNN) and Linear Discriminant Analysis (LDA) (J. Y. Kim et al., 2020; Martins et al., 2022). The key advantage of supervised machine learning algorithms compared to unsupervised methods is their capacity to provide suitable labels to training data according to established categories. This functionality eliminates the need for constructing "artificial" categories, hence improving the model's accuracy and relevance (Zhang & Ma, 2019).

In the context of rehabilitation, Khairuddin et al., 2021 investigated the use of EMG signals to detect user intentions for motion commands in a robot-assisted upper limb rehabilitation platform. The system included a PC workstation, DAQ system, and sensors (torque sensor, potentiometer, EMG electrode). By recording EMG signals from the biceps of ten healthy participants during voluntary elbow flexion and extension, the study extracted features such as Waveform Length (WL), Mean Absolute Value (MAV), Root Mean Square (RMS), Standard Deviation (SD), minimum (MIN), and maximum (MAX). The research evaluated multiple classifiers, including Linear Discriminant Analysis (LDA), Logistic Regression (LR), Decision Tree (DT), Support Vector Machine (SVM), and K Nearest Neighbour (KNN), for their performance in classifying pre-intention and intention states. Feature selection was carried out using the Extremely Randomized Tree technique, which identified MIN and MAX as the most significant features. Among the evaluated classifiers—LDA, Logistic Regression (LR), DT, SVM, and KNN—the Decision Tree (DT) achieved the highest accuracy (100%, 99%, and 99% on training, testing, and

validation datasets, respectively), highlighting its potential for enabling adaptive rehabilitation systems that encourage active patient participation.

Similarly, Liu et al., 2020 focused on muscle spasticity assessment by analysing wrist flexor and extensor muscles using temporal signals and wavelet packet decomposition (WPD) coefficients. Both temporal signals and coefficients produced using wavelet packet decomposition (WPD) were used in the research to extract features. Sequential forward selection (SFS) was employed to identify the most relevant features, improving model accuracy and processing speed. The research compared the performance of K Nearest Neighbours (KNN), Support Vector Machines (SVM), Linear Discriminant Analysis (LDA), and Deep Neural Networks (DNN). A 3D-printed watch casing with an embedded 3-axis accelerometer was used to capture MMG signals, ensuring consistent skin contact. At the base of the watch case, a 1 mm thick PLA (Polylactic Acid) plate was used to help transmit the MMG signal. The posterior ulna, which offered a flat surface and served as the case's stable mounting point, allowed for constant skin contact with the watch case. The research included the evaluation of eight distinctive and unusual movements, including clapping, flicking the index finger, snapping the finger, flipping a coin, shooting, extending the wrist, flexing the wrist, and making a fist. KNN with 7 nearest neighbours achieved the highest model accuracy of 94.56% for the eight gestures among the four methods used (SVM, LDA, and DNN).

Expanding on the use of inertial sensors, Kim et al., 2020 investigated machine learning-based assessment for elbow spasticity in 47 patients with cerebrovascular accidents (CVA) and one with spinal cord injury (SCI). Similar to the MAS score, the acceleration and rotation attributes collected from affected patients' elbows were analysed to classify the degree of spastic movement. Machine learning classifiers were used to predict categories based on labelled data processed from passive stretching inertial signals. It was a supervised learning problem because the signals were labelled with MAS level rated by therapists. There were two feature sets used: FS1 for common statistical features and FS2 for additional features to improve the model performance. Root mean square,

mean, standard deviation, energy, spectral energy, absolute difference, variance, signal magnitude area, and SV were all included in FS2. Median accuracy of 75.7% came from the classification performance utilising dataset FS1. Although this change was not statistically significant ($Z = -0.944$, $p = 0.345$), the accuracy improved to 81.9% for FS2 when further features were included. Especially, the segmentation method with a 50% overlap greatly improved classification accuracy, so improving performance by DS2 by 7.4%. Random Forest (RF) obtained the best accuracy among the investigated classifiers—almost 95.4%; Support Vector Machines (SVMs) were the least successful. Though it had difficulty differentiating between lesser grades of spasticity, the RF classifier showed great accuracy and recall, especially for greater MAS level. The results generally show the promise of inertial sensors and machine learning in efficiently evaluating elbow spasticity.

Further advancing the field, Puzi et al., 2020 applied a classifier to quantitatively evaluate spasticity levels using clinical data from the affected upper limb, aiming to address the subjectivity and inconsistency of traditional methods reliant on therapist expertise. The research, involving 25 patients with varying spasticity levels, demonstrated that the Support Vector Machine (SVM) classifier outperformed the Adaptive Neuro-Fuzzy Inference System (ANFIS), achieving an accuracy of 88.0%. Gaussian membership functions (MF) yielded lower root mean square error (RMSE) compared to triangle MF, with smaller RMSE values correlating with an increased number of MFs. However, more MFs led to higher training costs due to longer convergence times. Similarly, Puzi et al., 2019 explored machine learning techniques using torque and angle signals from arm muscles to classify spasticity levels based on the MAS. Extracting seven features from 25 subjects, the research found that a Linear SVM classifier with four selected features achieved the highest accuracy of 84%. Key features such as Three-Way Decision (TWD) for region halves, catch position, and post-catch stiffness showed strong correlations with MAS levels. Together, the studies highlight the potential of machine learning classifiers, particularly SVM, in providing systematic and objective quantification of muscle spasticity.

Other than that, Zhang et al., 2019 developed a regression-based framework for quantitative muscle spasticity assessment using a wearable system with surface electromyography (sEMG) and inertial sensors. The study involved 16 spasticity patients and 8 healthy controls, employing a custom multi-channel system with 16 sEMG channels and 9-axis inertial measurement units (IMUs). Each sEMG sensor consisted of two parallel bar electrodes (1 mm wide, 10 mm long, spaced 10 mm apart), forming a single-differential recording channel. During the tests, participants were instructed to fully extend their elbows to 180 degrees with palms facing upward. The experimenter then passively flexed the elbow to 40–60 degrees (stretching across a 120–140-degree range), paused for 2 seconds, and passively extended the elbow back to 180 degrees. Both lambda model and kinematic model were built from the collected data in the suggested framework; biomarkers were extracted correspondingly from the two models to explain the neurogenic component and biomechanical component of the muscle spasticity, respectively. Then three assessment techniques employing single-/multi-variable linear regression and support vector regression (SVR) were used to calibrate biomarkers from every single model or combination of two models into evaluation scores using supervised machine learning algorithms. With the same significance and clinical interpretation, every one of these evaluation scores can be considered as a forecast of the MAS grade for spasticity assessment. With low mean square error (MSE, 0.14 and 0.47) between the resulting assessment score and the MAS, both approaches with each individual model attained good performance. On the other hand, by contrast with the lowest MSE at 0.059, the approach combining SVR to merge biomarkers from both models beat other two techniques. Appropriate for clinical, community, and home-based rehabilitation, the trial results revealed the usefulness and practicality of the suggested framework and offer an objective, quantitative, and practical approach for spasticity assessment.

Based on the previous studies, feature selection plays a pivotal role in improving the accuracy, robustness, and generalizability of machine learning models used in spasticity assessment. It reduces dimensionality, enhances interpretability, and eliminates redundant or irrelevant data that may lead to overfitting. Techniques such as Sequential Forward

Selection (SFS) and Extremely Randomized Trees were frequently applied to identify critical features (e.g., MIN, MAX, RMS, signal variance), which not only reduced computational burden but also improved classification performance in several studies (Khairuddin et al., 2021; Liu et al., 2020). The importance of feature selection is further highlighted by studies showing significant accuracy gains after incorporating optimized feature sets, such as FS2 in Kim et al. (2020), which led to an 81.9% accuracy compared to 75.7% using a basic feature set. From a methodological standpoint, several machine learning classifiers have been widely adopted in this domain, each offering specific strengths. DT and RF are often preferred for their interpretability and ability to handle nonlinear relationships and feature interactions effectively. For instance, Khairuddin et al. (2021) reported near-perfect accuracy with a DT model, while Kim et al. (2020) demonstrated RF's superiority in capturing complex spasticity patterns. SVM, although popular for their robustness in high-dimensional spaces, often struggled with multiclass classification problems and imbalanced datasets in spasticity-related research, as observed in Kim et al. (2020), where SVM underperformed relative to RF.

KNN has also been explored, particularly for its simplicity and non-parametric nature, but its performance is heavily dependent on data scaling and the choice of k, with Liu et al. (2020) finding KNN to outperform more complex models in gesture recognition tasks. LDA and LR are valued for their speed and efficiency in linearly separable cases, yet they may fall short in modeling more complex or nonlinear spasticity patterns. DNNs, though capable of automatically learning hierarchical features, require large datasets and high computational resources, which may limit their practical applicability in smaller clinical studies. Ultimately, the choice of machine learning algorithm is highly context-dependent and influenced by factors such as dataset size, noise levels, type of features, and clinical interpretability requirements. Supervised learning remains the most dominant approach due to the availability of therapist-annotated MAS scores, allowing for robust mapping between input signals and clinical outcomes. The evidence suggests that while ensemble methods like RF offer superior accuracy, simpler models such as DT or LDA

may still be preferred in clinical settings where transparency, computational speed, and interpretability are crucial for real-time decision-making and therapist trust.

Table 2.5 Overview of Machine Learning Models Used in Sensor-Based Muscle Spasticity Assessment

Author/year	Instrument	Muscle	Subjects	Research Objective	Used Parameters
Khairuddin et al., 2021	Arm robotic platform of robotic rehabilitation system with EMG	Biceps muscles	10 healthy subjects	Identify the user's intentions and generate motion commands for a robot-assisted upper limb rehabilitation platform by using EMG signals	Time domain parameters and machine learning accuracy
Liu et al., 2020	Triaxial accelerometer MMG	Wrist Flexors or Extensors	35 subjects	Identify key features for enhanced model accuracy and faster processing	Time-frequency features, KNN, SVM, LDA, and DNN
Kim et al., 2020	Three axes of accelerometer, gyroscope, magnetometer and MAS tool	Upper Limb (Elbow)	47 patients with CVA and 1 patient with SCI	To assess elbow spasticity severity by analyzing acceleration and rotation data from the affected elbow and using machine learning to classify spastic movement, similar to assigning an MAS level.	RF, SVM, LDA, and multilayer perceptrons
Zhang et al., 2019	Wearable IMU sensors, EMG, MAS tool and MTS tool	Elbow	16 patients with spasticity and 8 healthy controls	Introducing a new method for evaluating muscle spasticity using a wearable system with surface EMG and inertial sensors	MSE
Puzi et al., 2020, 2019	AMSAS and MAS tool	Biceps muscles	25 patients with spasticity	To assess the muscle spasticity, especially highlighting the application of machine learning techniques and develop a classifier using the MAS in combination with a one-way ANOVA test to assess degrees of muscular spasticity	SVM, ANFIS

2.6 CRITICAL REVIEW OF EXISTING STUDIES AND RESEARCH LIMITATIONS

Although numerous studies have been conducted to assess muscle spasticity in individuals with neurological disorders, existing approaches—both clinical and technological—still present notable limitations that hinder objective, consistent, and reproducible evaluations. This section critically examines the limitations of previous studies based on the literature discussed in earlier subsections and aligns these gaps with the problem statement highlighted in Chapter 1.

The most widely used clinical tools for evaluating muscle spasticity, including the MAS, MTS, and ASAS, are inherently subjective. These assessments depend on the therapist's perception of resistance during passive limb movement, resulting in variability in scoring due to inter-rater and intra-rater inconsistencies. While MAS is commonly applied in stroke rehabilitation due to its simplicity and accessibility, its inability to account for the velocity-dependent nature of spasticity and subtle changes in muscle tone reduces its diagnostic precision. Additionally, PROM-based assessments, though widely practiced, lack objective measurement criteria and cannot quantify the extent of resistance or muscle activity, limiting their ability to support data-driven clinical decisions.

To overcome the limitations of clinical scales, various sensor-based systems have been introduced, including sEMG, NIRS, and force sensors. However, these approaches often focus on electrical or metabolic activity without capturing the mechanical properties of muscle behavior. MMG, although showing promise in quantifying muscle vibrations and mechanical responses, has not been extensively integrated with angular measurement tools in a unified platform. Furthermore, most existing studies utilize single-axis data or isolated sensor modalities, which fail to represent the full complexity of muscular response during passive range of motion. Machine learning techniques have been applied in spasticity-related research to enhance classification accuracy and automate evaluation. Nevertheless,

many existing models are developed using small, homogeneous datasets with limited representation across MAS levels. The absence of real patient data across multiple spasticity grades reduces generalizability. Additionally, these studies often rely solely on time-domain features without performing rigorous statistical selection processes to identify clinically significant variables. Moreover, limited validation procedures, such as lack of k-fold cross-validation or appropriate testing partitions, reduce the reliability of reported classification results.

Additionally, previous studies rarely simulate clinical conditions during data collection, such as controlled passive flexion and extension typically conducted by physiotherapists. The lack of standardization in data acquisition, as well as the absence of synchronized joint angle and MMG signal recording, restricts the clinical applicability of many existing systems. Given the outlined limitations, a significant research gap remains in developing a clinically integrated, objective, and multimodal system for quantifying spasticity severity. No previous study has combined tri-axial mechanomyography (ACC-MMG) data with joint angular measurements captured during passive upper limb movement, while mapping these measurements to MAS scores using both statistical and machine learning approaches. The proposed study addresses this gap by introducing the Quantitative Spasticity Assessment Technology (QSAT), a portable platform designed to capture synchronized biomechanical data—specifically muscle vibration and joint angles—during flexion and extension. By integrating validated statistical techniques such as MANOVA, Pearson correlation, and regression analysis with machine learning classifiers, this research delivers a robust and reproducible method to objectively quantify spasticity across multiple MAS levels. The novelty of this approach lies not only in the development of the QSAT platform but also in its end-to-end methodology—from feature extraction to model validation—offering a standardized, scalable solution for clinical spasticity assessment. In doing so, this study advances current knowledge and provides practical support for more effective, data-driven rehabilitation strategies.

2.7 SUMMARY

The concept of spasticity and its defining criteria have been explained, followed by an exploration of various types of neurological disorders that contribute to the development of muscle tone abnormalities. A detailed overview of the manual assessment methods, such as passive range of motion, commonly used with neurological assessment tools, has also been provided. The precision, reliability, and effectiveness of various neurological assessment tools in measuring muscle spasticity have been compared. Among the available tools, the MAS stands out due to its widespread clinical use, ease of application, and efficiency in practice. Furthermore, the integration of MAS with sensor-based approaches has been explored to enhance spasticity assessment. This research leverages MMG signals to provide an objective measurement of spasticity levels in accordance with the MAS framework. The unique characteristics of MMG signals allow for the identification of spasticity during assessments, and the correlation between MMG data and MAS levels helps in differentiating various degrees of muscle spasticity. Additionally, machine learning techniques have been recognised as the most effective method for classifying spasticity severity by analysing biomechanical parameters derived from MMG signals, complementing the traditionally subjective nature of manual assessment methods.

CHAPTER THREE

RESEARCH METHODOLOGY

3.1 INTRODUCTION

The chapter provides a detailed exposition of the research methodology, as outlined in Figure 1.2, covering the development of the experimental research design, the hardware components of the Quantitative Spasticity Assessment Technology (QSAT) platform, the procedures for both conventional and system-based data acquisition methods, the analysis of biomechanical features, the machine learning models employed, and the evaluation of model performance. The research commenced with an experimental research design that structured the research framework, detailing the required sample size and patient recruitment criteria. The sample size was determined using G*Power analysis to ensure sufficient statistical power, while the recruitment criteria focused on including patients diagnosed with neurological disorders exhibiting various levels of spasticity based on the Modified Ashworth Scale (MAS). The design ensured the research's objectives were met while maintaining the validity and reliability of the findings. The QSAT platform was meticulously designed with input from physiotherapists, ensuring that both medical perspectives and the comfort and safety of patients were prioritised. The main component of the platform, mechanomyography (MMG), has been analysed against several transducers and chosen to provide an optimal measuring suite for muscular spasticity. In the assessment protocol, patients diagnosed with neurological disorders were first evaluated using the conventional method to measure the muscle spasticity level, followed by data acquisition using the QSAT platform. The QSAT platform, equipped with acceleration mechanomyography (ACC-MMG) and potentiometer components, was used to collect detailed data on muscle activity. The MAS level scores, and related criteria obtained from the conventional assessment were instrumental in evaluating the system's response and adaptability. Subsequently, the dataset collected through the QSAT platform

underwent statistical analysis to extract biomechanical features, which were identified as key characteristics of muscle spasticity. The features formed the foundation for developing a machine learning model aligned with MAS. A critical baseline comparison was conducted between healthy patients and stroke patients classified with no muscle tone (MAS 0) to evaluate whether subtle differences exist between both groups. Building upon this analysis, a machine learning model was developed to systematically map the intricate characteristics of spasticity in the musculature under examination, covering both flexion and extension movements. The model's performance was evaluated using the extracted features, and the classifier with the highest accuracy was selected for further refinement and optimization to enhance its predictive capability. Following model selection, inter- and intra-rater reliability assessments were conducted to support the clinical reliability of the proposed system. This analysis involved comparing the consistency of spasticity ratings obtained through the QSAT platform with those determined by the conventional MAS. These assessments were crucial in validating the repeatability and objectivity of the QSAT measurements across different raters and repeated trials.

3.2 RESEARCH DESIGN

The goal of the research is to classify muscle spasticity level based on MAS tool for the patient using QSAT platform. A quantitative approach is utilised to establish the relationships between biomechanical features of the affected muscles and the corresponding MAS level. The biomechanical features, defined as measurable properties of the signals extracted from the muscles, primarily focus on muscle vibration. Serving as key indicators of spasticity, the features represent the characteristics of muscle spasticity and act as valuable markers for assessing its severity.

The sample size was determined using G*Power Analysis Software to ensure that the research had a sufficient number of patients recruited in order to achieve a reliable level of generalization in the results (Prajapati et al., 2010.). Based on the G*Power analysis shown in Table 3.1, the sufficient sample size required for this research was determined to be 32 patients. This calculation was based on a one-tailed test with an effect size of 0.90, an error probability (α) of 0.05, and a power (1–β) of 0.80, as informed by previous research that was conducted on MMG (Mohamad, 2019). The selected parameters ensured that the research could detect meaningful differences between the two groups while minimising the risk of Type I and Type II errors. A Type I error (false positive) occurs when a difference is detected when none exists, while a Type II error (false negative) occurs when a real difference is not detected. To further strengthen statistical reliability and improve generalization, 10 additional healthy participants were recruited as a baseline group, ensuring that the study meets or exceeds the required sample size threshold of 32. Expanding the participant pool further strengthens statistical accuracy and supports the robustness of the findings.

Table 3.1 G*power Test Analysis Output

t tests – Means:	Difference between two independent means (two groups)
Analysis:	A priori: Compute required sample size
Input:	
Tail(s)	= One
Effect size d	= 0.90
err prob	= 0.05

Table 3.1 G*power Test Analysis Output (cont.)

Power (1 – err prob)	= 0.80
Allocation ratio N2/N1	
Output: Noncentrality parameter	= 2.5455844
Critical t	= 1.6972609
Df	= 30
Sample size group 1	= 16
Sample size group 2	= 16
Total sample size	= 32
Actual power	= 0.8002866

The research sample for this investigation consisted of individuals who had been diagnosed with neurological disorders and who exhibited a variety of scores and conditions on the MAS. The inclusion criteria included individuals who were 16 years of age or older, as well as those under 16 years of age who had obtained consent from their guardian (22 males, 8 females; mean age, M = 59.33, standard deviation, SD = 12.41). Recruitment took place in hospital and rehabilitation center settings, with the requirement that participants had previously undergone assessments and interventions by experienced therapists for a specified period of time. Detailed information regarding patient demographics and clinical characteristics is provided in Table 3.2, which includes variables such as age, gender, specific neurological disorders, and the affected limb.

Table 3.2 Demographic of Neurological Disorder Patients (*N*=30)

Age (years)	59.33 ± 12.41
Male	22
Female	08
Affected side:	
Right	16
Left	14
Both	0
Types of neurological disorder:	
Strokes	29
Cerebral Palsy	1

To maintain patient confidentiality throughout the research, all data was carefully anonymized and identified only by unique numerical codes. The research involved the active participation of two experienced physiotherapists who possess specialised knowledge in the field of physical rehabilitation. Physiotherapists provided valuable insights and recommendations from a medical perspective. Simultaneously, the researchers sought and obtained ethical clearance from the International Islamic University Malaysia Research Ethics Committee (IREC) with reference number IREC 2023-025 for ensuring the ethical integrity of research involving human participants conducted at the university and community.

Sultan Ahmad Shah Medical Centre (SASMEC) and National Stroke Association of Malaysia (NASAM) provided the cohort of people with neurological disorders. Patients with motor control abnormalities and hemiparesis conditions affecting their upper extremities were specifically targeted for recruitment. Prior to the start of data acquisition,

the recruited patients were given a thorough explanation of the experimental procedures and associated safety concerns. In accordance with ethical protocols, participation in the experiment, which involved the collection of clinical data, required explicit consent from either the patients or their guardians. Clinical measurements were meticulously carried out within the hospital and rehabilitation center facilities, specifically within a controlled environment characterised by a closed room in which the ambient temperature was kept at the standardized level of 32°C.

To ascertain the clinical eligibility of a patient for participation in the research, it is imperative that their health is subjected to a thorough evaluation, in addition to satisfying the subsequent criteria:

1. The individual afflicted with a neurological ailment is classified as follows:
    a. Stroke
    b. Traumatic Brain Injury (TBI)
    c. Cerebral Palsy (CB)
    d. Spinal Cord Injury (SCI)
    e. Multiple sclerosis (MS)
2. The individual in question has undergone and continues to undergo a thorough assessment while operating within the parameters of the MAS system, ranging from level 0, 1, 1+, 2 and 3, with an age range spanning from 16 to 80 years.
3. The patients with MAS level 4 were excluded as it does not show any rigid movement of flexion and extension during the assessment.
4. The patient, who is 16 years old, has willingly agreed to participate in this research or has provided consent if they are 18 years or older, with the affected upper limb being included in the study.

The investigation focused on the comprehensive assessment of muscle spasticity to achieve the research objectives, necessitating the development of a specialised system tailored to meet specific criteria. During the experimental setup's development phase,

components and materials were carefully selected and manufactured, considering the constraints imposed by the limited mobility of patients' upper limbs. Using a quantitative approach for the assessment protocol, the resulting system, known as QSAT, actively engaged subjects in collaboration with physiotherapists to collect significant data muscular conditions. Improving the machine learning model is crucial for accurately measuring upper limb muscle spasticity. At this stage, selecting the most significant biomechanical features from the measured data is essential to ensure that relevant parameters serve as input for the machine learning model, enabling precise prediction of the MAS level.

To accomplish the quantitative assessment of muscle spasticity in the affected upper limb using computational method, predicated on the MAS level, a structured four-stage methodology was implemented. The initial stage encompassed the development of specialised hardware tailored for the precise measurements envisaged. Clinical data were then carefuly gathered from the patients who participated in the research. The third stage entailed the meticulous analysis of the acquired data, facilitating the extraction of significant features, notably biomechanical features inherent in the clinical dataset. Following this, a machine learning model was systematically developed to prognosticate the level of muscle spasticity utilising the MAS tool. The resulting predictions were then employed to categorise the severity of impairment in the upper limb muscle attributable to neurological disorders.

3.3 QSAT PLATFORM DEVELOPMENT

The section outlines the development process of QSAT platform, focusing on the selection and integration of key components to develop a functional system for spasticity data acquisition. The development is divided into two main sub-sections: the selection of the MMG transducer and the assembly of the system hardware. The components play a crucial

role in ensuring accurate data acquisition, system functionality, and the effectiveness of subsequent data analysis.

3.3.1 Selection of Mechanomyography Transducer

MMG employs various transducers to capture muscle activity by detecting the mechanical vibrations generated by muscle fibres during contraction. Selecting the appropriate transducer is essential for guaranteeing the precision and dependability of the muscle measurements. The accessible MMG transducers comprise piezoelectric touch sensors, condenser microphones, laser distance sensors, and accelerometers which shown in Figure 3.1. Each type offers distinctive characteristics that render them appropriate for various experimental configurations.

Figure 3.1: Mechanomyography Transducer: a) Piezoelectric contact sensors b) Laser distance sensors c) Condenser microphones d) Accelerometers (N. Li et al., 2024).

Piezoelectric contact sensors identify mechanical tension and transmute it into electrical impulses. Despite remarkable sensitivity to small vibrations, piezoelectric sensors

are susceptible to interference from ambient noise and fluctuations in skin contact, leading to compromised signal quality. Condenser microphones, although non-intrusive and simple to position, exhibit considerable sensitivity to ambient acoustic noise, rendering them less appropriate for loud clinical settings. Conversely, laser distance sensors quantify the displacement of the skin surface resulting from muscle contractions. Despite providing non-contact measurements with excellent spatial resolution, laser-based systems are costly and may complicate clinical applications, especially due to susceptibility to movement artefacts. Among these alternatives, accelerometers offer some significant advantages. The acceleration of muscle vibrations is measured in multiple axes (x, y, and z), offering a thorough perspective on muscle activity.

In contrast to piezoelectric sensors, accelerometers exhibit reduced sensitivity to variations in skin contact, and unlike condenser microphones, they are resistant to external noise, rendering them especially appropriate for clinical settings. Their capacity to conduct dynamic, multi-directional measurements facilitates comprehensive monitoring of muscle activity during static and dynamic motions. Moreover, accelerometers fulfil essential requirements for practical application, encompassing an uncomplicated installation procedure, a lightweight construction, and an outstanding degree of reliability in signal acquisition. These characteristics establish accelerometers as the most reliable transducer for detecting MMG signals during voluntary and induced muscle contractions. The robustness of accelerometers, along with the capability to acquire high-quality data across multiple dimensions, resistance to interference, and suitability for dynamic evaluations, makes accelerometers ideal for assessing muscle spasticity during controlled passive movements. The preference for accelerometers is further supported by literature that highlights the reliability and accuracy of accelerometer-based assessments in various clinical and research settings.

To justify the selection of the accelerometer for this research, various transducer types were compared based on key characteristics such as sensitivity, frequency response, dynamic range, and noise level. Table 3.3 provides a detailed comparison of the transducers

that were considered: accelerometers, microphones, and laser distance sensors which derived from a review of current literature and reputable online databases, focusing on studies that examined the performance characteristics of various transducer types in the context of mechanomyography.

Table 3.3 Details of MMG transducers

Types of transducers	Accelerometer	Microphone	Laser Distance Sensor
Sensitivity	High sensitivity (mV/g) to capture subtle muscle vibrations	High sensitivity to detect weak acoustic signals produced by muscle contractions	High accuracy for measuring small displacements on the skin's surface caused by muscle contractions
Frequency Response	Wide frequency range, typically covering the range of muscle vibrations (10 Hz to several hundred Hz)	Adequate frequency response to capture muscle vibrations (typically in the range of 20 Hz to 2 kHz)	Adequate frequency response to cover the range of muscle vibrations (10 Hz to 1 kHz)
Dynamic Range	Sufficient dynamic range to capture variations in muscle contractions	Range from around 80 dB to 140 dB	Exceeding 100 meters
Noise Level	Range from decibels relative to 1 g (dB(g)).	Range from a few decibels to around 30 dB or lower	Range from a fraction of a millimetre to a few millimetres

The accelerometer was deemed the most appropriate transducer for recording MMG signals in this research. This selection was predicated on the advantages it presents in comparison to the alternatives. Table 3.3 demonstrates that accelerometers possess significant sensitivity (measured in mV/g) to detect even minor muscle vibrations, which is crucial for identifying muscle activity during passive stretching and regulated movements. Their extensive frequency response, generally spanning from 10 Hz to several hundred Hz, corresponds effectively with the frequency range of muscle vibrations noted during spasticity evaluations. Furthermore, accelerometers have an adequate dynamic range to detect fluctuations in muscle contractions, rendering them suitable for both static and dynamic muscle assessments.

In contrast, whereas microphones provide excellent sensitivity to faint signals, they are more vulnerable to ambient acoustic noise, which can undermine data quality in clinical environments. Laser distance sensors, while exceptionally precise in quantifying skin displacements resulting from muscle contractions, are impractical for this research due to the prohibitive cost and susceptibility to movement artefacts associated with the sensors. A significant element that impacted the decision to utilise accelerometers was their minimal noise levels. In contrast to other transducers, accelerometers demonstrate noise levels proportional to 1 g, hence allowing for the recording of muscle activity with minimal disruption. The low noise levels facilitate more accurate signal capture during clinical evaluations. Moreover, the accelerometer's compact and lightweight configuration facilitates straightforward installation and manipulation throughout the testing procedure. The requirements of installation simplicity, lightweight design, and outstanding reliability in signal collecting further solidified the decision to utilise accelerometers. As a result, accelerometers were deemed the most reliable devices for detecting MMG signals during both voluntary and induced muscular contractions.

Based on the comparison between all transducers, accelerometers were specifically employed in the research to measure muscle vibrations in the biceps and triceps, with a sensitivity range of ±2 g to ±16 g. The research selected the ±2 g range to provide optimal

sensitivity in identifying small muscle vibrations. The ACC-MMG sensor delivers a 10-bit output, equating to $2^{10} = 1024$ unique levels. Considering that the output is signed, the range is symmetrically divided between positive and negative values, resulting in 256 least significant bits (LSBs) for each 1g of acceleration. The sensitivity of the ACC-MMG sensor, essential for accurate measurements, is articulated in Equation 3.1.

$$Sensitivity = \frac{2 \times 9.81\, m/s^2}{256} \tag{3.1}$$

3.3.2 Assembly of System Hardware

Upon consulting physiotherapists, comprehensive measures were considered essential to evaluate muscle spasticity. The evaluation involved examining the feedback information on resistance obtained from the elbow joint's response to the physiotherapist's manipulations during the assessment. The necessary signals for the developed system included data on muscle acceleration in the forearm, including the biceps and triceps, as well as the angular position of the elbow joint during bending and stretching. The physiotherapist recommended the supine position as the optimal posture for patients during muscle assessment. The supine position promotes muscle relaxation, which helps to minimise any worsening of muscle spasticity. The muscle spasticity assessment system was divided into two components. The first part focused on evaluating the angle of the elbow joint during flexion and extension, while the second part was dedicated to assessing muscle spasticity by measuring the acceleration of the biceps and triceps. The hardware for the platform was shown in Figure 3.2 (a) and further explained in its Computer-Aided Design (CAD) representation, depicted in Figure 3.2 (b). The final result of this development platform was represented in Figure 3.3, which shows the completed system known as the QSAT platform together with mechanical functions of each part as described in Table 3.4.

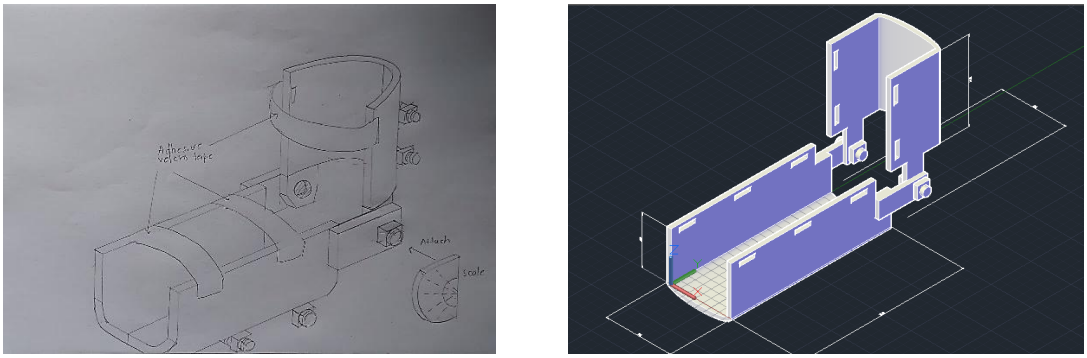

a) b)

Figure 3.2: System Design (a) Preliminary Sketch (b) Realization using CAD software

The skilled therapist will systematically manipulate and stretch the patient's forearm in a manner that aligns with established clinical protocols. At the same time, the QSAT will be utilised to identify and record both the mechanical vibration (acceleration) of the forearm muscles and the angular position data related to the elbow joint throughout the various stages of stretching and contracting. The acceleration signal, which reflects the precise movement of the joint at a specific angle, will be measured, while the potentiometer will be employed to determine the angular position of the biceps and triceps during the stretching and contracting exercises. The potentiometer sensor of QSAT platform undergoes calibration to gain an accurate measurement of the angle of forearm during flexion and extension which have to match with 135 degrees as the full range of motion.

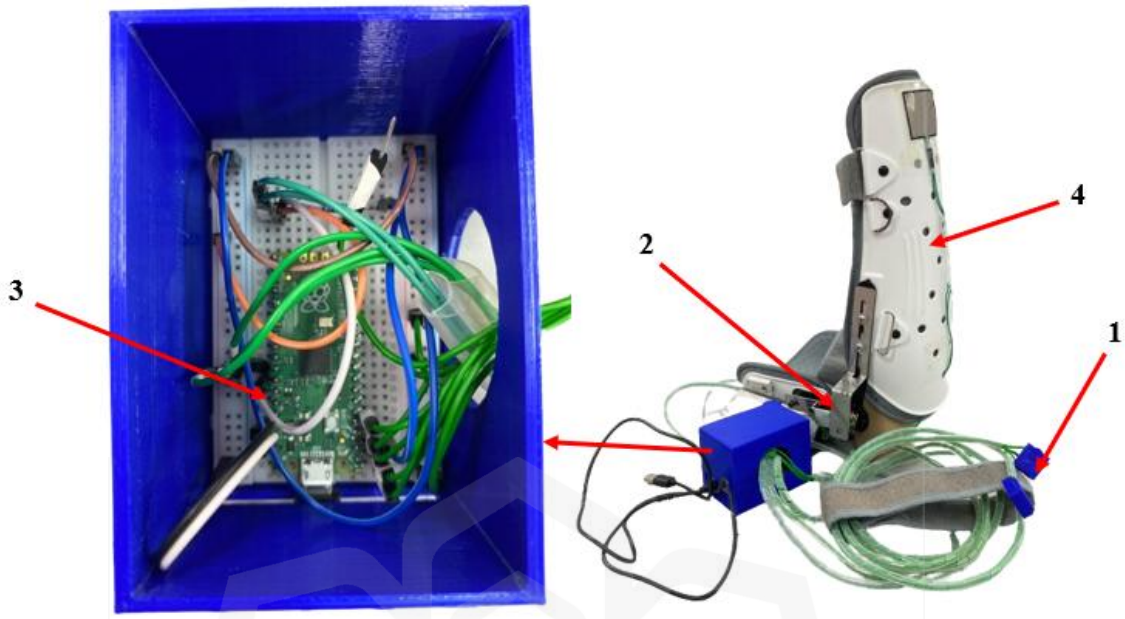

Figure 3.3: QSAT Part Description

Table 3.4 Mechanical Part Description of QSAT

Part	Description with brand
1	ACC-MMG functioning in measuring muscle vibration (acceleration) of the forearm
2	Potentiometer to measure the angle of the elbow joint during flexion and extension (angular position)
3	Electrical Box consisting of all wiring connection with the data acquisition (Raspberry Pi Pico)
4	Arm holder to place the affected forearm

The calibration procedure was delineated as follows: The output voltage of the potentiometer was measured using a 16-bit Analog-to-Digital Converter (ADC) on the microcontroller, utilising a reference voltage (V_{ref} = 5.0V) that corresponds to the ADC's full-scale output. The potentiometer did not employ the full 0-5.0V range; it generated a minimum voltage of V_{min} = 0.000V and a maximum voltage of V_{max} = 1.628 V, reflecting the mechanical constraints of the potentiometer's angular displacement. A linear calibration formula was utilised to correlate the voltage values with angular positions. The voltage V_{pot}, recorded by the ADC, was transformed into an angle θ utilising the equation 3.2:

$$\theta = \frac{V_{pot} - V_{min}}{V_{max} - V_{min}} \times (\theta_{max} - \theta_{min}) + \theta_{min} \quad (3.2)$$

where θ_{min} = 0 degree and θ_{max} = 135 degree. The linear interpolation ensured that the complete range of the potentiometer's angular displacement was precisely represented in the recorded data. As the potentiometer rotates, its voltage output is converted into a matching angular position according to the established voltage-to-angle relationship. Figure 3.4 illustrates the linear correlation between voltage and angular position. The calibration procedure was essential for obtaining precise angular readings. The 16-bit ADC, with its high resolution, delivered detailed voltage readings, facilitating accurate determinations of the potentiometer's position. Further, procedures were implemented to verify the potentiometer's performance through repeated testing, guaranteeing that the calibration remained stable and reproducible across various measurements. In addition, the precision of this mapping depended on the exact specification of the potentiometer's voltage range and the resolution of the 16-bit ADC. This method implied a linear correlation between voltage and angular position; however, certain potentiometers may demonstrate nonlinearity, necessitating a more intricate calibration process.

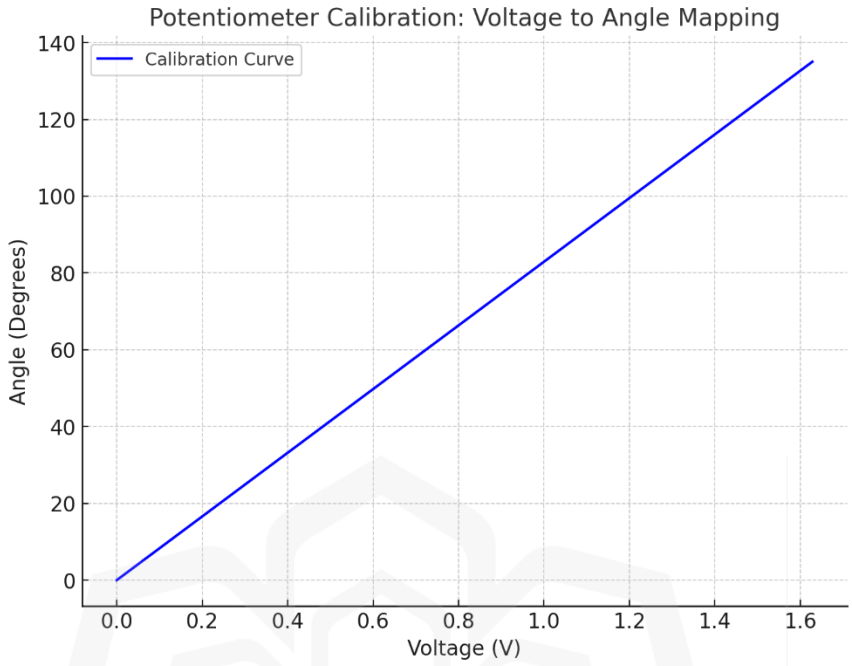

Figure 3.4: Potentiometer calibration curve

The Python program orchestrates the integration of two accelerometer and potentiometer sensors into the QSAT platform, enabling comprehensive data acquisition. Developed in the Python 3.12 environment using Thonny IDE, the program ensures synchronized operation of the sensors, with data acquisition managed by a Raspberry Pi Pico microcontroller at a high sampling rate of 166.7 Hz which is shown in Figure 3.5. This sampling rate was strategically chosen to capture the muscle vibrational frequency range of 2 Hz to 100 Hz, ensuring accurate detection of mechanomyography (MMG) signals while minimizing aliasing (Ibitoye et al. 2014). The Python program orchestrated data acquisition, ensuring efficient and synchronized operation of the sensors. The accelerometer provided muscle vibration data, while the potentiometer supplied angular position readings of the elbow joint during flexion and extension. The program timestamps each measurement, records data in real time, and allows user-defined filenames for structured CSV storage, making it adaptable for various experiments.

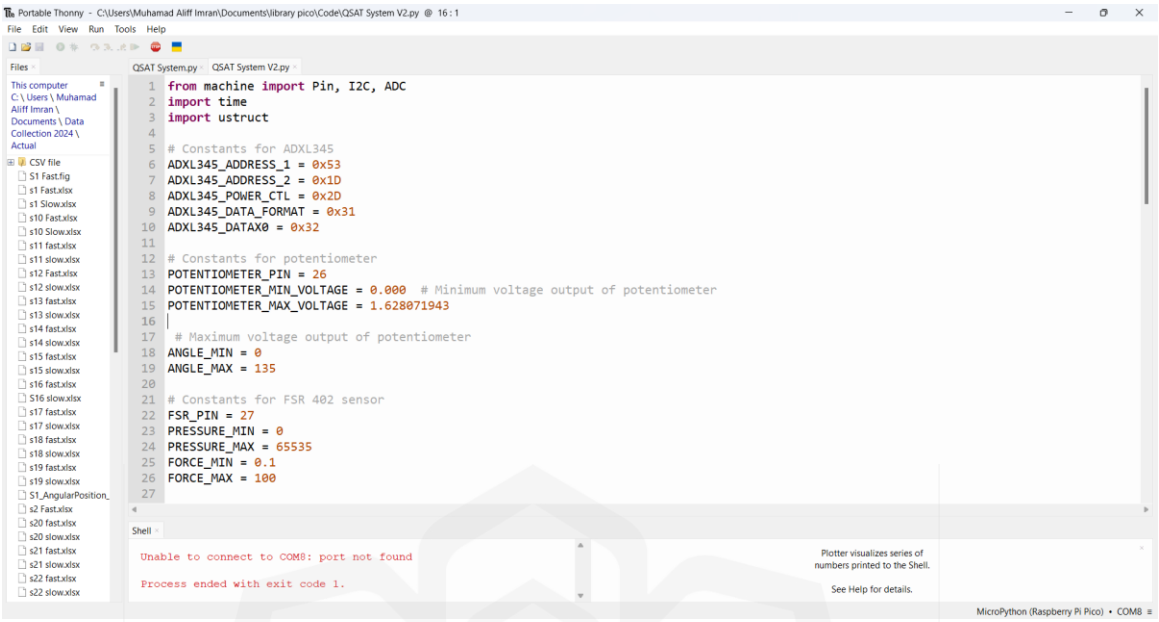

Figure 3.5: Python Program Implementation for QSAT Data Acquisition in Thonny IDE

3.4 CLINICAL DATA ACQUISITION

The acquisition of clinical data assumes utmost importance in understanding the details of spasticity characteristics and significantly contributes to the development of a model explaining muscle spasticity severity. The step-by-step explanation of this process is clearly described in Figure 3.6. The process begins with patient recruitment, where patients diagnosed with upper limb spasticity are selected based on predefined inclusion and exclusion criteria. This approach ensures that the research population is representative and aligns with the research objectives. Following this, informed consent is obtained from all patients. Patients are thoroughly briefed about the research's objectives, procedures, and potential risks or benefits, adhering to the ethical guidelines approved by the institutional ethics committee. After eligibility is confirmed and consent is provided, patients were then asked to lie down on a bed in a supine posture, with their arms positioned alongside their bodies. A qualified physiotherapist utilised the MAS tool to assess and quantify muscle

spasticity in patients diagnosed with neurological disorders, as illustrated in Figure 3.7. During the clinical assessment, the therapist performed passive movements of the upper limb, including flexion and extension, to evaluate the spasticity level. Spasticity grades were assigned based on the degree of muscle resistance encountered during passive stretching, and each movement was recorded for further analysis. To enhance the reliability of the assessment, the identical procedure was systematically administered by a second physiotherapist, as delineated in the subsequent subsection dedicated to reliability investigation.

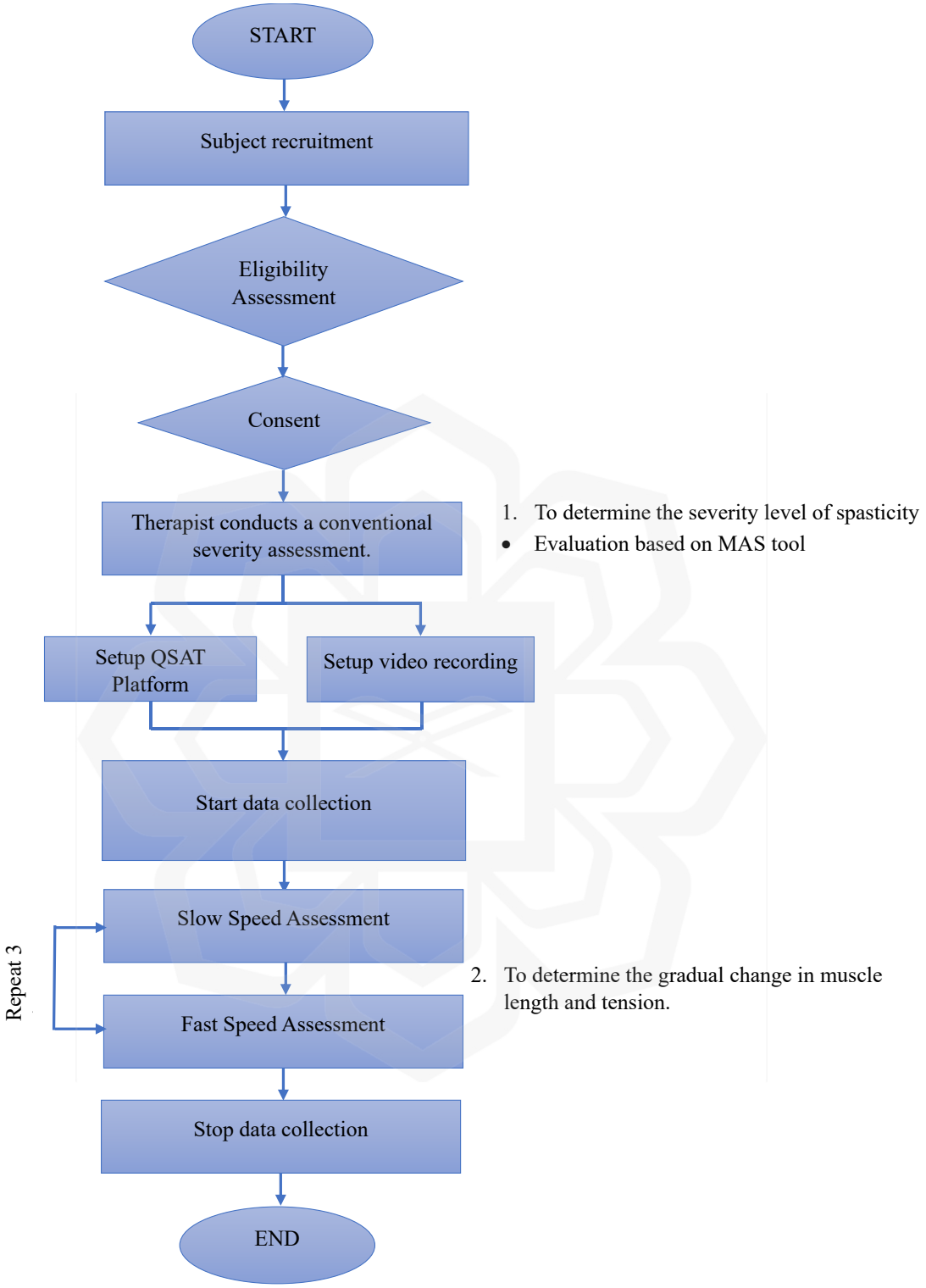

Figure 3.6: Data Acquisition Flowchart

Figure 3.7 Conventional Spasticity Assessment

After completing the conventional assessment, the QSAT platform is set up to collect MMG signals, while video recording equipment is simultaneously arranged to document the assessment process. Each patient's biceps and triceps were then fitted with a two-channel ACC-MMG sensor, securely attached to the skin using double-sided tape. The first sensor was placed on the belly of the biceps, which is located on the front of the upper arm, and the second sensor was placed on the triceps, situated on the back of the upper arm. The x-axis of the sensors was aligned with the direction of muscle fibre contraction, while the z-axis was oriented to maintain direct contact with the skin. The ACC-MMG sensors were aligned along the *x*, *y*, and *z* axes, representing the longitudinal, lateral, and transverse orientations in relation to the muscle fibres, respectively, as depicted in Figure 3.8. Subsequently, patients were directed to place their forearm on the QSAT's arm holder, ensuring precise alignment of the elbow joint with the potentiometer sensor embedded in the QSAT platform. This alignment was essential to guarantee accurate angle measurements during forearm flexion and extension, as illustrated in Figure 3.9.

a) b)

Figure 3.8 ACC-MMG Sensor placement: (a) On the Biceps and (b) On the triceps

Figure 3.9 Spasticity Data Acquisition using QSAT platform

The physiotherapist systematically used the QSAT platform to move the armrest, causing the arm to bend back and forth at both slow and fast speeds. Slow-paced movements, each lasting approximately 2 seconds, were chosen to measure passive range of motion (PROM), enabling a detailed examination of the muscle's response over an extended duration. The approach allows for a thorough analysis of the muscle's reactions to increasing tension, providing a more nuanced diagnosis of spasticity. Conversely, fast-paced motions, each lasting around 1 second, were employed to elicit more rapid changes

in muscle activity, potentially revealing different aspects of spastic dynamics. According to previous investigations, the customary range of motion for an active elbow flexion is approximately 135 degrees. This iterative procedure, involving alternating slow and fast motions, was reiterated three times for each patient to ensure a comprehensive data acquisition and to derive mean of the best-estimated model of muscle spasticity. The entire procedure, including preparation, movement execution, and data recording, required approximately 10 minutes per subject, and this duration was standardized across all MAS levels. All results have been documented and systematically arranged in an Excel spreadsheet. After completing the data acquisition process, all collected data, including MMG signals and video recordings, are securely stored for subsequent preprocessing and analysis.

3.5 BIOMECHANICAL FEATURES: MEASUREMENT AND ANALYSIS TECHNIQUES

The biomechanical features analysed in this research, specifically joint motion and resistance, were derived from the clinical data measurements of the affected upper limb. The process of extracting these biomechanical features from the recorded signals consisted of two phases: signal pre-processing and feature extraction. The raw data was initially inspected for noise contamination, which is a common issue in sensor-based data. However, due to the minimal noise observed in the recorded signals, no further filtering techniques (such as low-pass, high-pass, or band-pass filtering) were required. The minimal noise can be attributed to the selection of a sampling rate of 166.7 Hz, which effectively avoided aliasing and minimising high-frequency noise outside the MMG spectrum. As a result, the raw data was directly used for subsequent analysis, which helped preserve the authenticity and richness of the signals. The continuous data was divided into separate movement cycles by examining the angular motion of the elbow, which ranges from 0° to 135° during flexion and from 135° to 0° during extension. The motion was uninterrupted, consistently

transitioning between flexion and extension. The potentiometer data, which tracked the elbow's angular position, was employed to accurately define the limits of each cycle. Each cycle commenced and concluded at pivotal points in the potentiometer signal, signifying the moment the elbow attained the initial position of the flexion phase (0°) and the terminal position of the extension phase (135°). This method guaranteed uniform and precise segmentation of the continuous movement data. During flexion, the biceps contract, while the triceps elongate, reflect their antagonistic functions in bending the elbow joint. Conversely, during extension, the biceps elongate as the triceps contract to straighten the elbow. These contrasting muscle actions generate distinctive mechanical vibrations that are captured by the MMG signals, providing valuable insights into muscle activity and coordination during each movement. The segmentation ensured that these signal characteristics were precisely captured and analysed for both movements, enabling a comprehensive evaluation of muscle spasticity. The choice of rapid flexion and extension movements was deliberate, as faster transitions emphasise the dynamic changes in muscle activity. The rapid movements amplify the mechanical vibrations, making it easier to detect features associated with spasticity in the MMG signals. The fluctuations are essential for differentiating various degrees of spasticity, as spastic muscles typically demonstrate increased resistance during rapid movements, as indicated by the MMG signal. The increased speed of movement improves the capacity to identify spasticity-associated alterations in muscle tone, as the quick transitions between muscle contraction and relaxation boost the sensitivity of the signal. The fast-paced movement protocol was chosen for its potential to elicit a wider array of muscle responses and to yield distinct data points, crucial for precise spasticity classifying and analysis.

To facilitate the analysis, a specialised algorithm was subsequently developed to extract features from the ACC-MMG signals, conducted using MATLAB R2023a software (MathWorks Inc.). The analysed features comprised Root Mean Square (RMS), Peak to Peak Amplitude (PTP), Maximum (Max), Minimum (Min), Mean Average Value (MAV), Standard Deviation (SD), Skewness (S), and Kurtosis (K). In the feature extraction phase, time-domain features were obtained for the x_b, y_b, z_b axes (biceps) and the x_t, y_t, z_t axes

(triceps), aligned with the longitudinal, lateral, and transverse orientations relative to the muscle fibres. These time-domain features were calculated separately for both the flexion and extension phases to capture any phase-specific variations in muscle contraction. This ensured that the dataset comprehensively represented both phases, facilitating a more robust analysis of muscle performance. The collected features were subsequently organised into a dataset, enabling further statistical analysis. The formulas employed to ascertain each extracted feature are as follows:

$$RMS = \sqrt{\frac{1}{n}\sum_{i} x_i^2} \tag{3.3}$$

$$PTP = Max - Min \tag{3.4}$$

$$Max = maximum\ of\ the\ terms \tag{3.5}$$

$$Min = minimum\ of\ the\ terms \tag{3.6}$$

$$MAV = \frac{sum\ of\ the\ terms}{number\ of\ terms} \tag{3.7}$$

$$SD = \frac{\sum(x_i - MAV)^2}{n} \quad (3.8)$$

$$S = \frac{\sum_i^n (x_i - MAV)^3}{(n-1)\, SD^3} \quad (3.9)$$

$$K = \frac{n\,(n+1)}{(n-1)(n-2)(n-3)} \times \sum \left(\frac{x_i - MAV}{SD}\right)^4 - \frac{3(n-1)^2}{(n-2)(n-3)} \quad (3.10)$$

In the equations presented, xi denotes the muscle vibration data obtained from the ACC-MMG signals, which align with the accelerometric measurements of muscle vibrations. The symbol n denotes the total quantity of data points in the ACC-MMG signal, reflecting the number of samples collected during a specific period of muscle contraction.

The RMS is a statistic that quantifies signal amplitude, indicating the degree of muscle contractions or tension in the upper limbs (H. Wang et al., 2017; Xie et al., 2020). The MAV of MMG signals indicates the muscular strength and endurance of the specific muscle in issue (Rupsha Mukhopadhyay, 2015). This parameter represents the strength and energy produced by the muscle. Standard deviations were calculated for the ACC-MMG signals along the *x*, *y*, and *z* axes, offering insights into the mean muscle activity and its variability. The PTP value quantifies a signal by assessing the difference between its maximum positive peak and minimum negative peak of vibration amplitude over a designated period, thereby reflecting the magnitude spectrum of muscular oscillations or movements within the ACC-MMG signals. Furthermore, skewness and kurtosis were

computed to provide a more profound insight into the characteristics of muscle signal distributions, hence improving the understanding of muscle activity and its variability.

To clarify the structure of the dataset used in the feature extraction phase, raw ACC-MMG signal data were collected from 30 patients, each undergoing three repeated trials for both flexion and extension movements. This yielded 90 total trials per movement. For each trial, a series of time-domain features including RMS, MAV, PTP, SD, K, S, Min and Max were computed. Each feature was extracted independently and stored in a dedicated folder, resulting in a modular dataset architecture. Furthermore, because the ACC-MMG signals were acquired from both biceps and triceps muscles along three directional axes (x, y, z), every feature was calculated separately for each axis, producing six distinct datasets per feature (Biceps (x_b, y_b, z_b) and Triceps (x_t, yt, z_t)). For instance, the RMS feature produced six separate datasets (RMSx_b, RMSy_b, RMSz_b, RMSx_t, RMSy_t, RMSz_t,). This structure was then repeated identically for every other extracted feature. Thus, each time-domain feature generated six distinct vectors, each of size 90 × 1, representing one axis-direction per muscle across all trials for a single movement type. The dataset was organised such that every three consecutive rows corresponded to repeated trials for a single patient (e.g., rows 1–3 for patient 1, rows 4–6 for patient 2, and so on up to rows 88–90 for patient 30). The alignment was preserved for all features and movement types. Feature extraction was conducted separately for flexion and extension, yielding two parallel datasets with identical structure and dimensionality.

After all, MMG signal features were extracted across the six signal directions x_b, y_b, z_b (Biceps) and x_t, yt, z_t (Triceps) for each feature type, the resulting vectors were merged into a single dataset for each movement type (flexion and extension). Each extracted feature was initially calculated and stored independently, then consolidated into a unified structure to support statistical analysis. The final dataset for each movement contained 90 rows (representing 30 patients × 3 trials each), with columns representing all directional MMG features. The MAS level, which denotes the spasticity classification assigned during clinical evaluation, was appended as the final column of the dataset. The MAS level served

as the independent (categorical) variable, while all extracted MMG features were treated as dependent variables in the statistical analysis. At this stage, datasets for flexion and extension movements were kept separate, allowing for movement-specific analysis of how MMG feature patterns vary with spasticity levels.

The dataset, encompassing biomechanical features derived from clinical tests for both flexion and extension movements, was systematically analysed to investigate the relationship between MMG signal features and muscle spasticity levels as measured by the MAS. These two types of movements, flexion and extension are essential components of the passive range of motion and provide a comprehensive representation of muscle response to stretching under varying conditions of spasticity. To ensure a thorough examination, the MMG signals captured during both movements were compared to explore differences and similarities in the biomechanical parameters that influence spasticity levels. This dual analysis enabled the evaluation of whether flexion and extension movements exhibit distinct patterns in MMG signal features, offering deeper insights into the nature of muscle spasticity. Statistical methods were employed to analyse these relationships and compare the results for both movements. Linear regression and Pearson correlation were used to examine the strength and direction of the relationship between MMG features and MAS levels for each movement type while one-way MANOVA was conducted to identify significant differences in MAS levels related to the biomechanical parameters between flexion and extension movements. These analyses provided valuable information on how MMG signals varied with muscle spasticity during flexion and extension. All statistical analyses were conducted using SPSS version 27.0.1 (IBM Inc.).

Linear regression analysis was performed to explore and quantify the relationship between MMG signal characteristics, and the severity of muscular spasticity as measured by the MAS. The method allowed the identification of trends and dependencies between independent variables (MMG features) and the dependent variable (MAS level), providing a predictive framework for understanding how specific MMG traits reflect variations in spasticity severity (Maulud & Abdulazeez 2020; Set Foong et al. n.d.). The dataset included

MMG signal features were input as independent variables in the regression model, with MAS level serving as the categorical dependent variable. MMG features were selected to optimize the regression model's performance and interpretability, ensuring that only meaningful and non-redundant features were included. A combination of simple and multiple linear regression models was employed to examine the relationships between MMG features and MAS level, with key metrics such as the correlation coefficient (R), the coefficient of determination (R^2), and the F-test, were used to assess the model. The correlation coefficient quantified the strength and direction of the relationship, R^2 indicated the proportion of variance in MAS level explained by the MMG features, and the F-test evaluated the statistical significance of the overall model. Validation of the regression models was performed using cross-validation techniques to ensure generalizability across the dataset. Separate analyses were conducted for flexion and extension movements to assess movement-specific relationships, enabling the identification of MMG features that were more predictive in one movement type compared to the other.

In addition to linear regression, a Pearson correlation analysis was conducted alongside linear regression on the entire dataset to evaluate the linear association between MMG signal characteristics and MAS level. The dataset included MMG signal features extracted from both flexion and extension movements, measured across multiple axes (*x*, *y*, and *z*) for the biceps and triceps muscles. The Pearson correlation coefficient (r) was calculated for each MMG signal feature, providing a quantitative measure of the strength and direction of the linear relationship between the feature and the MAS level (Baak et al., 2020; Cui et al., 2020). This analysis facilitated the identification of MMG traits closely linked to muscular spasticity, enabling the prioritization of features for subsequent analysis. For instance, features with strong positive or negative correlations were highlighted as key indicators of spasticity, guiding further evaluation in the context of clinical relevance. To further investigate differences in MMG signal characteristics across various MAS levels, a Multivariate Analysis of Variance (MANOVA) was utilised. This analysis was necessary due to the existence of multiple continuous dependent variables (MMG features) and categorical independent variables (MAS level) (Etana et al., 2024). Unlike univariate

approaches, MANOVA considers the interrelationships among dependent variables, providing a holistic assessment of how MAS level influences MMG signal characteristics (Aliff et al., 2024).

After separately analysing the flexion and extension movements, the datasets for both were combined and analysed using the same methods to explore potential differences in MMG signal characteristics across the two movement phases. This approach aimed to determine whether there were any significant variations in the MMG features between flexion and extension movements and whether these differences influenced the relationship between MMG traits and muscle spasticity. By merging the datasets, the analysis enabled a more comprehensive comparison, helping to identify whether specific features were more strongly associated with spasticity in one movement type over the other. The results from this combined analysis provided valuable insights into how the characteristics of MMG signals might vary with movement, helping to ascertain whether analysing both phases together would lead to improved accuracy in assessing spasticity or whether separate analyses would be more effective.

3.5.1 Significance Testing Between Healthy and MAS 0 Level Patients

In this research, a baseline comparison was conducted between 10 healthy subjects and 5 stroke patients classified with no muscle tone (MAS 0) for both flexion and extension movements. Table 3.5 provides detailed demographic information about the healthy subjects, who were all male. The MAS 0 designation indicates the absence of muscle tone or resistance to passive movement, suggesting that both groups should exhibit similar muscle tone characteristics at the time of assessment. However, it is essential to recognize that stroke patients with MAS 0 had previously experienced a phase of flaccidity, which is

commonly observed following a stroke. Over time, this flaccid state can progress into spasticity, depending on the duration and recovery process.

Table 3.5 Demographic of Healthy Subjects (N=10)

Age (years)	30.60 ± 6.28
Male	10
Female	0
Hand side:	
Right	10
Left	0

The use of all-male healthy subjects can be justified as gender is unlikely to affect the results in this context (Barr et al., 2024; Clayton & Tannenbaum, 2016). The primary parameter under investigation is muscle tone in the MAS 0 category, which is characterised by a complete lack of resistance to passive movement. The absence of muscle activity is not influenced by gender, as MAS 0 reflects a physiological condition rather than gender-specific differences in muscle properties. Additionally, focusing on the MAS 0 category ensures consistency across groups, with gender having minimal impact on the observed muscle tone characteristics. Thus, the use of all-male healthy subjects does not compromise the validity of the baseline comparison.

To evaluate whether subtle differences exist between these two groups, a one-way multivariate analysis of variance (MANOVA) was performed. The test was chosen due to its ability to assess multiple dependent variables (in this case, the features extracted from

the MMG signals simultaneously, allowing for a more comprehensive understanding of potential variations. The dataset was organized into two groups: healthy individuals and stroke patients with MAS 0. Although the muscle tone for both healthy individuals and stroke patients with MAS 0 was expected to be the same at the time of measurement, the history of flaccidity in the stroke group prompted a closer examination of whether these neurological differences could manifest in the MMG data. The extracted MMG features served as the dependent variables in the MANOVA test, while the group categorisation (healthy vs. stroke with MAS 0 served as the independent variable. The test facilitated a concurrent comparison of various MMG features between the two groups, ascertaining the presence of statistically significant differences in the overall patterns of muscle activity. The inclusion of stroke patients who had previously experienced flaccidity but had not yet developed spasticity offers valuable insight into how early-stage muscle changes may differ from those in healthy individuals, potentially contributing to a better understanding of spasticity development in stroke rehabilitation.

3.6 MACHINE LEARNING ALGORITHMS FOR MAS LEVEL CLASSIFICATION

Various machine learning algorithms were examined to analyse MMG signals and predict muscle spasticity levels based on the MAS. The algorithms, including Decision Tree (DT), Linear Discriminant Analysis (LDA), Support Vector Machine (SVM) and K-Nearest Neighbours (KNN) were implemented using MATLAB, focussing on offline approaches that depend on supervised Machine Learning (ML) models for activity recognition. The machine learning models, frequently utilised across several research domains, were applied to analyse both flexion and extension movements of the upper limbs. To facilitate the development of a muscle spasticity model, two datasets were meticulously prepared and organized. The first dataset utilised all available features, while the second dataset comprised only the significant features with each dataset consisting of 90 rows,

corresponding to individual trials (30 patients × 3 trials), with columns representing the extracted MMG features and the MAS level as the target class. Each dataset was partitioned into training and testing sets with ratios of 90/10, 80/20, and 70/30. In the 90/10 split, 90% of the data (81 samples) was allocated for model training, while the remaining 10% (9 samples) was designated for testing. Similar partitioning processes were applied for the 80/20 and 70/30 splits, enabling an assessment of the models' robustness and generalization capabilities.

Following the data splits, Leave-One-Out Cross-Validation (LOOCV) was utilised to assess model performance. In LOOCV, each instance in the dataset serves as a singular test case, while the remaining instances are utilised for training purposes. The procedure continues for every data, resulting in a model that is trained and evaluated on all accessible data points. LOOCV was selected for the research because to its efficacy with limited datasets, as it optimizes the utilization of all available data for training and testing purposes. Due to the restricted sample size in the research, Leave-One-Out Cross-Validation (LOOCV) ensures that each data point assists in model validation, hence enhancing the reliability and robustness of the model outcomes. LOOCV also reduces the possibility of overfitting, as the model is evaluated on each distinct sample, yielding a more precise assessment of its performance. Furthermore, the models' performance for both flexion and extension movements were assessed to determine the algorithms' consistency and reliability across various muscle movements. The comparative research highlighted whether the prediction accuracy of the models differed between the two movement types, consequently enhancing the comprehension of the impact of movement direction on MMG signal categorisation.

The DT model was employed in the research to predict muscle spasticity levels (MAS) based on the features extracted from the mechanomyography (MMG) signals. A Decision Tree is a supervised machine learning approach that systematically divides the dataset into subsets by assessing feature values at each node (Stokic et al., 1998). The split diminishes the confusion in data classification, facilitating precise forecasts of the MAS

levels. The tree structure divides the feature space into separate regions, with each node signifying a decision rule based on a feature. The data is partitioned according to these decisions, with the objective of optimizing information gain and reducing impurity at each node, hence categorizing the data at the terminal nodes. The research involved training the DT model using the retrieved MMG features, and its performance is illustrated in Figure 3.10 which visualizes the tree structure derived during model training. The model begins at the root node to assess if the MAS feature is less than or equal to 0.5. The data is further partitioned into branches, each reflecting a further division depending on the most informative attribute. The Gini index was employed to evaluate node impurity at each node, aiming to reduce impurity for improved class differentiation, calculated as:

$$Gini(t) = 1 - \sum_{i=1}^{n} (p_i)^2 \qquad (3.11)$$

where p_i is the probability of a data point belonging to class i at node t. The DT model aimed to select features that minimized this impurity, resulting in improved classification accuracy of MAS levels.

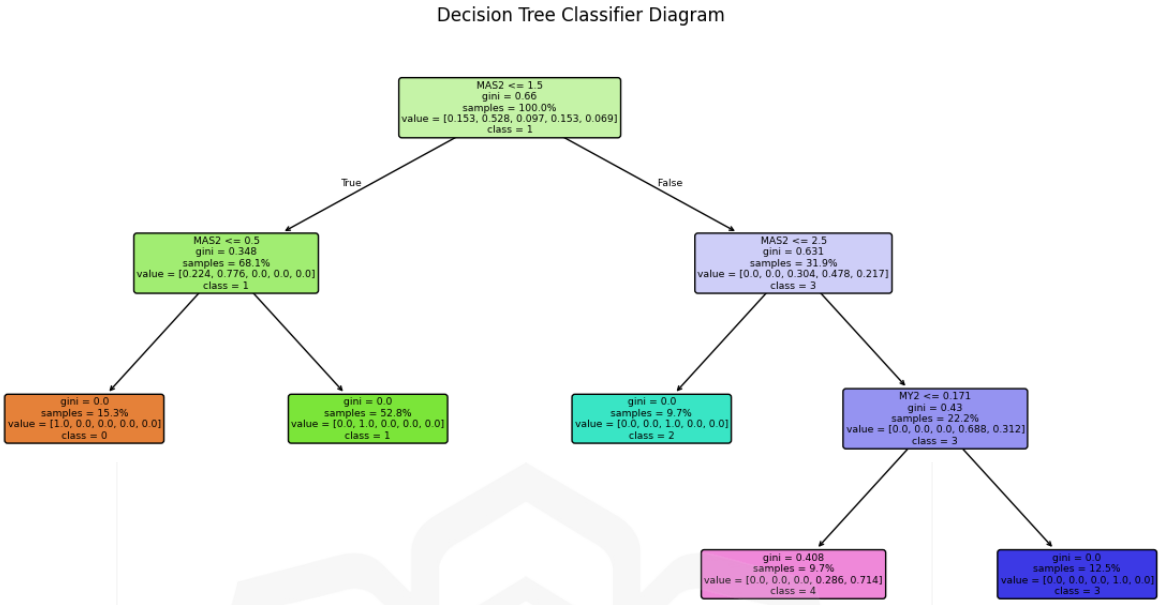

Figure 3.10 Decision Tree Classifier Visualization for MAS Level Prediction

LDA, a supervised technique for dimensionality reduction, was utilised on the retrieved MMG features to decrease the dataset's dimensionality while preserving discriminative information. LDA seeks to enhance the distinction across several classes by identifying a linear combination of features (Wen et al., 2019). The method assumes the data in each class follows a Gaussian distribution and operates by optimizing the ratio of between-class variance to within-class variance. This objective is mathematically expressed by the Fisher criterion, which LDA seeks to maximize:

$$J(w) = \frac{\mathrm{w}^T S_B \mathrm{w}}{\mathrm{w}^T S_w \mathrm{w}} \qquad (3.12)$$

where S_B is the between-class scatter matrix, S_W is the within-class scatter matrix, and w is the projection vector that transforms the feature vector x into a lower-dimensional space. The symbol W^T denotes the transpose of the vector w, used in matrix multiplication to ensure dimensional compatibility and to compute scalar projections of the variance. The feature vector x may include either all extracted features or only the significant subset selected through prior analysis. Each transformed data point is calculated as:

$$y = w^T x \tag{3.13}$$

The approach guarantees that the altered features provide optimal separation for classification. Figure 3.11 depicts the outcomes of implementing LDA, with the first and second linear discriminants (LD1 and LD2) represented on the x and y axes, respectively. Each data point signifies a sample from the dataset, distinguished by their respective MAS levels through color coding. The narrative demonstrates how LDA diminishes the feature space and enhances separability, especially between MAS 0 and MAS 3. Nonetheless, an overlap is evident among MAS levels 1, 1.5, and 2, suggesting that these levels possess analogous MMG feature properties. Nonetheless, LDA effectively streamlines the research by offering a more distinct perspective on class separability.

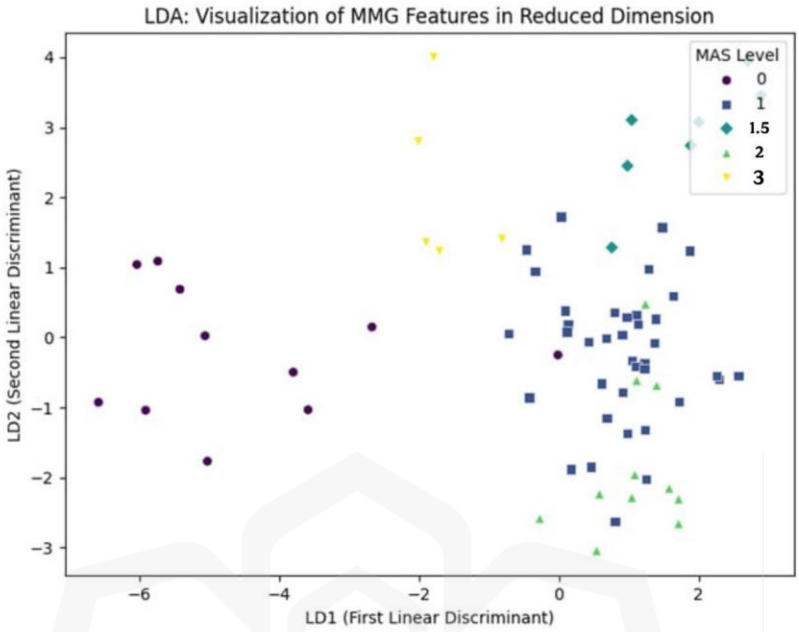

Figure 3.11 Linear Discriminant Analysis: MAS Level Visualization

Alongside LDA, a linear SVM was employed to categorise the MMG features according to MAS levels. The SVM functions as a compilation of techniques intended for classification and regression applications (Castelli et al., 2018; Vapnik, 1999). The SVM method determines a hyperplane that optimally distinguishes data points of various classes by maximizing the margin—the distance between the closest points (support vectors) of each class. For a linearly separable dataset, the SVM constructs a decision function defined as:

$$f(\mathrm{x}) = w^T \mathrm{x} + b \qquad (3.14)$$

where x represents the feature vector comprising either all extracted features or the selected significant features from the MMG signals, w is the weight vector, and b is the bias term.

The optimal hyperplane is determined by solving the following convex optimization problem:

$$\min \frac{1}{2} \|w\|^2 \text{ subject to } y_i(w^T x_i + b) \geq 1 \quad (3.15)$$

where $y_i \in \{-1,1\}$ denotes the class label of the training instance x_i. This formulation ensures that the margin between classes is maximized while correctly classifying each training point. The linear SVM model was chosen for its computational efficacy and suitability for linearly separable data. The SVM classifies data by determining the decision boundary that optimises the margin between distinct classes (Mokri et al., 2022). The research employed SVM on the MMG feature dataset, with Figure 3.12 illustrating the SVM decision border. The graph represents one of the MMG signal features processed through the SVM, showcasing how the model distinguishes between MAS levels. The SVM-generated decision boundary aims to optimize the differentiation between various MAS levels. While the SVM approach defines discrete zones for particular spasticity levels, the overlap at the decision border indicates that specific MAS levels may not be fully separable by a linear model.

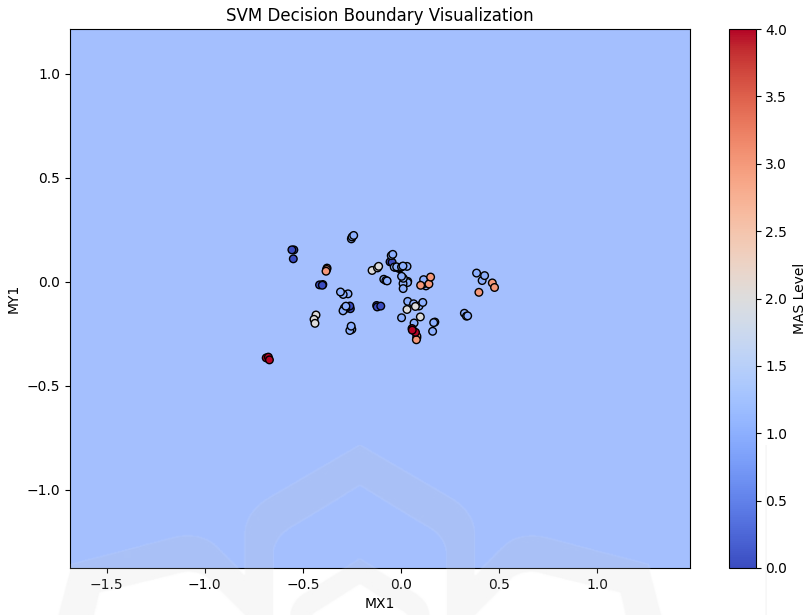

Figure 3.12 Support Vector Machine: Decision Surface for MAS Level Classification

The KNN algorithm, a non-parametric, instance-based learning technique, was also tested for research to classify muscle spasticity levels based on the extracted MMG features. KNN classifies a data point according to the predominant class of its nearest neighbors, with proximity usually determined by a distance metric like Euclidean distance (Z. Zhang, 2016). KNN is often extended to K-Nearest Neighbor Classification, where the classification of an instance is determined based on the majority class among its k nearest neighbors (Cunningham & Delany, 2021). To compute proximity, the Euclidean distance between the test feature vector x and a training sample x_i is calculated using the formula:

$$d(\mathrm{x}, \mathrm{x}_i) = \sqrt{\sum_{j=1}^{n} (x_j - x_{ij})^2} \qquad (3.16)$$

where n is the number of features used (either all features or the selected significant features), and x_j and x_{ij} represent the j^{th} feature value of the test and training samples, respectively. This distance measure was also compared against alternative metrics such as Cosine and Correlation distances to identify the most suitable configuration. The algorithm's efficacy is significantly influenced by the scaling and normalizing of the input information. To enhance KNN performance, multiple values of k (the number of neighbors) were evaluated to identify the optimal design. To support visualization, Principal Component Analysis (PCA) was employed to diminish the dimensionality of the feature set, hence facilitating the visualization of the classifier's decision boundaries. Figure 3.13 illustrates the KNN decision bordering with PCA-reduced features. The illustration illustrates how the model divides the feature space into sections that correspond to various MAS levels. The decision limits are non-linear, demonstrating KNN's capacity to identify intricate correlations among the features. The overlaid data points, tinted according to their actual class labels, provide a visual evaluation of the model's capacity to distinguish various MAS levels.

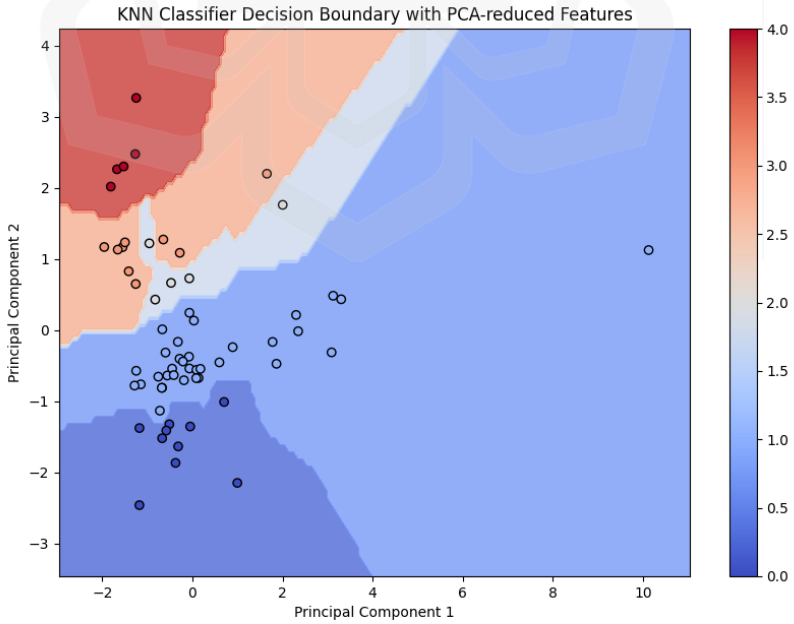

Figure 3.13 KNN Classifier Decision Boundary with PCA-Reduced Features

Following the implementation and training of the various machine learning models, the efficacy of the machine learning algorithms was assessed using accuracy metrics, training duration and confusion matrices. Accuracy serves as a key metric in evaluating model performance, defined as the ratio of correctly predicted samples to the total number of samples. Accuracy is influenced by several outcomes: True Positive (TP), where the model correctly identifies a positive class, and True Negative (TN), which refers to the accurate prediction of the negative class. Conversely, False Positives (FP) occur when the model mistakenly predicts the positive class, while False Negatives (FN) arise when the model incorrectly classifies a sample as negative. The calculation of accuracy, as shown in Equation 3.17, is based on these values of TP, TN, FP, and FN (Sarkar et al., 2023). In addition to accuracy, precision is another important measure, representing the ratio of correctly identified positive samples to the total number of samples predicted as positive, as shown in Equation 3.18. Furthermore, recall—defined as the proportion of accurately identified positive samples among all actual positive trials—can be determined using Equation 3.19. To provide a more comprehensive evaluation of the model's performance, the F1-score, which is the harmonic mean of precision and recall, is calculated as demonstrated in Equation 3.20. Together, the metrics provide a comprehensive evaluation of the model's effectiveness in predicting outcomes.

$$Accuracy = \frac{T_p + T_N}{T_p + T_N + FP + FN} \tag{3.17}$$

$$Precision = \frac{T_p}{T_p + FP} \tag{3.18}$$

$$Recall = \frac{T_p}{T_p + FN} \tag{3.19}$$

$$F1\ score = \frac{2\ \times Precision \times Recall}{Precision + \ Recall} \tag{3.20}$$

In addition to the metrics, the confusion matrix provides a comprehensive visualisation of the model's performance. A confusion matrix is a square matrix that presents the overall performance of a classification model. The rows of the matrix represent the actual instances of class labels, while the columns represent the instances of predicted class labels. The diagonal elements of the matrix indicate the number of times the predicted labels correspond to the actual labels for each trial. Thus, the confusion matrix serves as an effective tool for evaluating the model's data classification performance. Additionally, to ensure robustness and reliability, the dataset of flexion and extension movements was combined and evaluated across all algorithms using identical methods applied to the individual movements. The comprehensive investigation sought to determine if significant variations existed in the prediction accuracy of the classifiers when evaluating the movements collectively versus separately. The research examined the algorithms' ability to generalise across various muscle movements by integrating the datasets, as both flexion and extension exhibit unique biomechanical and physiological traits that could affect MMG signal patterns. The identical techniques utilised for each of the movements namely feature extraction, data partitioning, and model training and testing were also applied to the combination dataset. The approach guaranteed uniformity in the analysis and facilitated a direct comparison of performance metrics. The research sought to determine whether merging the datasets would improve the classifier models' capacity to detect spasticity levels or if it brought complexity that compromised accuracy.

3.7 PERFORMANCE EVALUATION OF MACHINE LEARNING MODELS

The machine learning model that exhibits the greatest accuracy was chosen for additional analysis to improve its performance and reliability. The selected algorithm was subjected to a k-fold cross-validation procedure with k values of 5, 10, and 15 to assess its robustness. This technique partitioned the dataset into k subsets, guaranteeing that each subset served as a validation set while the other subsets constituted the training data, so enabling the model to be assessed on various data splits. The method reduces the risk of overfitting and guarantees that the algorithm's performance remains unbiased by any particular division of the dataset. Alongside the cross-validation procedure, the model was trained and assessed utilising three separate distance metrics: Euclidean, Cosine, and Correlation. Each distance metric was utilised to evaluate its effect on the algorithm's efficacy, as these metrics affect the interpretation of feature associations during classification. Euclidean distance, favoured for its simplicity, computes the direct distance between two points, whereas Cosine distance assesses the angle between feature vectors, rendering it appropriate for datasets where directionality is paramount. Correlation distance, conversely, quantifies the statistical relationship between variables, elucidating patterns of similarity within the data. Furthermore, to support the clinical reliability of the proposed system, inter- and intra-rater reliability assessments were integrated into the evaluation process. The analysis involved comparing the consistency of spasticity ratings obtained through the QSAT platform with those determined by the conventional MAS. These assessments were crucial in validating the repeatability and objectivity of the QSAT measurements across different raters and repeated trials.

3.8 SUMMARY

The chapter outlines the research methodology, employing a quantitative approach to establish the relationship between the biomechanical features of affected muscles and their corresponding MAS levels during spasticity assessment. The sample size was determined using G*Power Analysis to ensure a sufficient number of patients for valid generalisation of results. Mechanomyography was carefully selected as the main component of the QSAT platform after evaluating several transducers, ensuring an optimal suite for measuring muscular spasticity, which guided the platform's development to achieve accurate measurements. The chapter also details the procedures for clinical data acquisition and includes a comparative analysis between healthy individuals and stroke patients with absent muscular tone (MAS 0) to identify any subtle distinctions between the groups. Additionally, it outlines the methodology for extracting biomechanical features, resulting in eight parameters per axis of the MMG signal, which were used to train the muscle spasticity machine learning model for both flexion and extension movements. The machine learning models' performance for both flexion and extension movements were assessed to determine the algorithms' consistency and reliability across various muscle movements. Furthermore, the dataset combining flexion and extension movements also underwent statistical tests for feature extraction to identify significant parameters, ensuring a comprehensive analysis. The combined dataset was then evaluated across all algorithms using the same methods applied to the individual movements, further enhancing the robustness and reliability of the machine learning models. The best algorithm underwent k-fold cross-validation, being trained and evaluated with k values of 5, 10, and 15 for both movements with using different measure distance that are Euclidean, Cosine and Correlation. To further validate the clinical applicability of the system, inter- and intra-rater reliability assessments were conducted by comparing the consistency of spasticity ratings obtained via the QSAT platform with those from the conventional MAS method. These assessments were essential in demonstrating the repeatability and objectivity of the system across different evaluators and repeated trials.

CHAPTER FOUR

RESULT AND DISCUSSION

4.1 INTRODUCTION

The chapter is divided into several distinct subsections, each focusing on the preliminary findings related to achieving the primary objectives of this research. The first subsection provides an analysis of patient participation in flexion and extension movements, including a detailed examination of the initial clinical data patterns obtained from trials involving impaired limbs across varying Modified Ashworth Scale (MAS) levels. The analysis considers angular positions during both passive flexion and extension movements. Additionally, movement selection based on speed, categorised into fast and slow flexion and extension, is analysed to assess variability in muscle response and the influence of movement speed on the clinical data. The second subsection delves into the biomechanical features extracted from clinical tests, which were compiled into a dataset and subjected to statistical analyses. Techniques such as linear regression and Pearson correlation were used to explore the relationship between Mechanomyography (MMG) signal features and muscle spasticity levels as measured by the MAS. A one-way MANOVA test was also employed to identify statistically significant differences in MAS levels concerning biomechanical features for feature selection and then utilised as inputs in training the classifier. A comparative baseline analysis was conducted between healthy subjects and stroke patients with no muscle tone (MAS 0) using one-way MANOVA. The analysis aimed to determine any statistically significant differences between these groups and further validate the dataset. The subsequent section focuses on the development of a machine learning model to determine MAS level, as outlined in Chapter Two (Table 2.2). The methodology detailed in Chapter Three guided the evaluation of flexion, extension, and combined movements, ensuring that statistical findings and extracted features informed the classifier's training process. The clinical database played a crucial role in quantifying

the characteristics of spasticity across all movements, leading to the development of robust predictive models. The machine learning models were systematically evaluated for accuracy, with the model demonstrating the highest performance selected for further refinement and optimization to enhance its predictive capability. Following this, inter- and intra-rater reliability assessments were conducted to evaluate the clinical reliability of the QSAT system. These assessments involved comparing the consistency of spasticity ratings generated by the QSAT platform with those obtained through conventional MAS evaluations. This step was essential in demonstrating the repeatability and objectivity of the QSAT system across different raters and repeated assessment sessions, thereby strengthening the clinical validity and potential for real-world implementation.

4.2 CLINICAL DATA ACQUISITION AND MEASUREMENT

4.2.1 Pre-Processing and Movement Selection for Analysis

The resulting distributions of MAS level for the flexion and extension movements of the biceps and triceps muscles are illustrated in Figures 4.1 and 4.2, respectively, providing valuable insights into the diverse characteristics of muscle spasticity across the research population. The distributions not only capture the range of spasticity levels observed but also reveal the inherent variability in individual measurements. Such variability highlights the distinct responses of each patient's muscles to passive stretching movements, emphasizing the influence of factors such as the severity of neurological impairment, muscle condition, and overall physical variability.

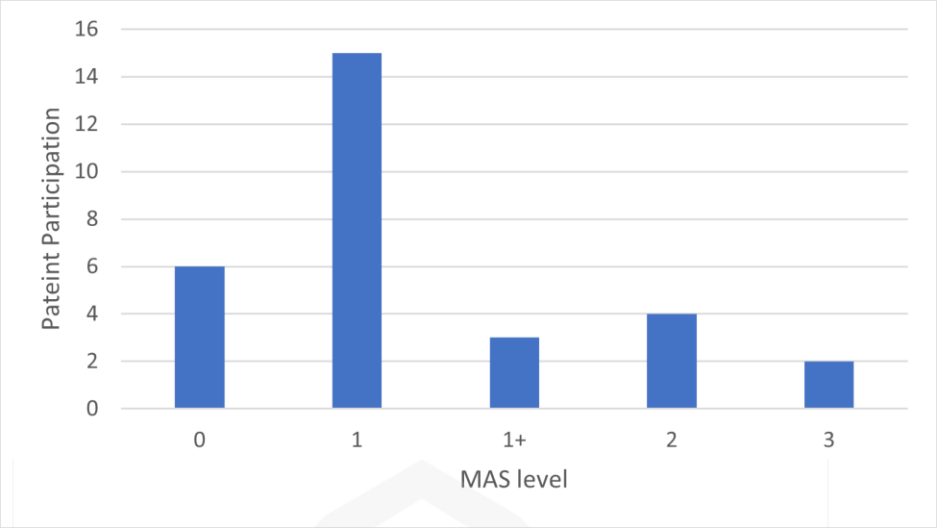

Figure 4.1 Frequency of Patient Participation for Flexion Movement according to MAS Level

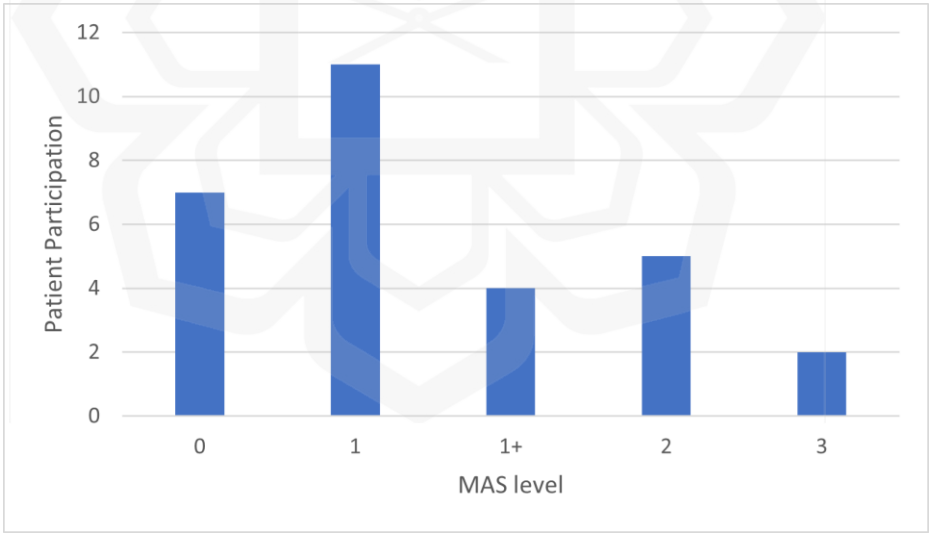

Figure 4.2 Frequency of Patient Participation for Extension Movement according to MAS Level

To ensure the quality and integrity of the collected data, signal preprocessing was conducted using MATLAB R2023a software (MathWorks Inc.). The collected ACC-MMG and potentiometer signals underwent several stages of preprocessing to enhance their precision and reliability. Given the experimental setup, the initial inspection of the raw data showed minimal noise contamination, thus eliminating the need for filtering techniques such as low-pass, high-pass, or band-pass filtering, which are typically used to remove motion artifacts or high-frequency noise from sensor signals. The observation was supported by a careful visual and statistical examination of the signal's frequency spectrum, which confirmed that the relevant frequency components for muscle activity were intact without significant interference.

To facilitate subsequent analysis, the continuous data streams were segmented into distinct epochs, with each epoch representing a single movement cycle. The cycles corresponded to the full range of elbow motion, starting from full extension at 0° to 135° during flexion and from 135° to 0° during extension. The potentiometer data, integrated within the setup, played a crucial role in this process. The potentiometer provided accurate markers for the start and end of each cycle, making it possible to synchronize the MMG signals with specific movement phases. The markers were identified through changes in voltage levels corresponding to the mechanical movement of the elbow joint. Figure 4.3 displays the corresponding muscle vibration data captured during rapid flexion movements along the x_b, y_b, and z_b axes (biceps) and the x_t, y_t, and z_t axes (triceps), as separated by the potentiometer. The graphs illustrate the acceleration data, representing muscle vibration for the biceps and triceps, along the x, y, and z axes during three consecutive flexion movements. The movements involve the contraction of the biceps and the elongation of the triceps, reflecting their roles as agonist and antagonist muscles, respectively. The agonist muscle is the primary muscle responsible for producing a specific movement through contraction, while the antagonist muscle opposes the action of the agonist by passively elongating to allow the movement to occur (Wissel & Hernandez Franco, 2024). During flexion, the biceps act as the agonist muscle by contracting to bend the elbow, whereas the triceps serve as the antagonist muscle by elongating to facilitate the movement. The data

reveal unique vibration patterns of the biceps and triceps during flexion, with signals exhibiting distinct amplitudes for each axis corresponding to the longitudinal, lateral, and transverse orientations of the muscle fibers, providing a clearer understanding of their functional roles. While the positive and negative scale of vibration in acceleration can be neglected as it merely represents the direction of movement, the overall shape and variation of the signal offer insight into the severity of muscle spasticity.

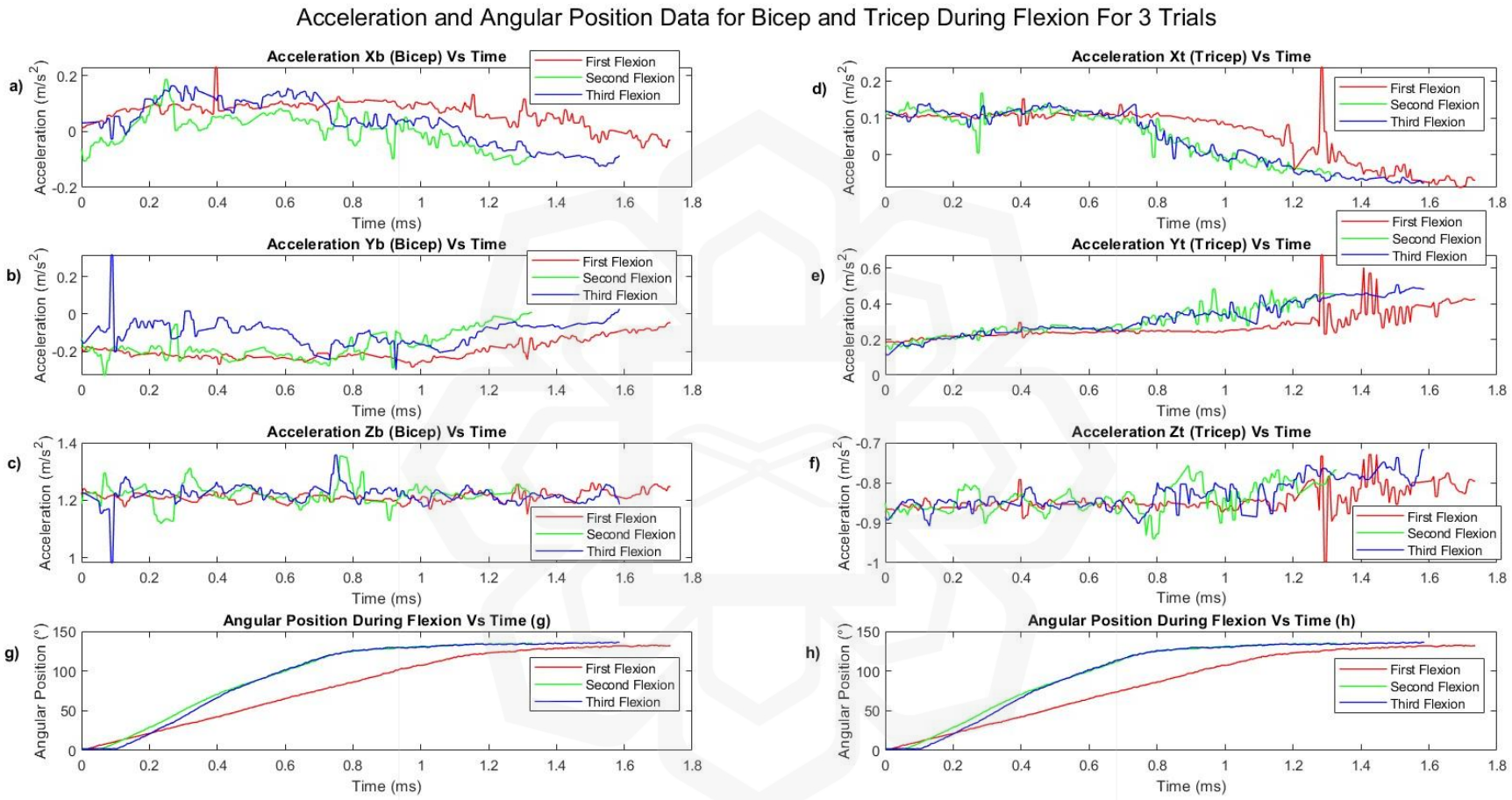

Figure 4.3 Muscle Vibration of Biceps (a, b, c) and Triceps (d, e, f) with Angular Position (g, h) During Fast Flexion Across All Trials for Patient 26 (MAS Level 3)

The vibration data for the biceps, shown in Figures 4.3 a, b, and c, reveal significant peaks and fluctuations across all three axes (x_b, y_b, z_b) during flexion. The peaks correspond to the active contraction of the biceps, which generates the force required to bend the elbow joint. The x_b axis shows the most pronounced fluctuations, indicating dominant activity along this orientation, likely aligned with the primary direction of flexion. Meanwhile, the y_b and z_b axes reveal variations that suggest multidirectional forces and vibrations generated during contraction, influenced by the anatomical structure and mechanical properties of the biceps. In contrast, the triceps vibration data, presented in Figures 4.3 d, e, and f, show more gradual and lower-amplitude acceleration patterns. The pattern reflects the passive elongation of the triceps, which act as antagonists to the contracting biceps during flexion. Along the x_t axis, the vibrations are relatively stable, with low amplitude, consistent with the triceps' elongation phase. However, the y_t and z_t axes show slight increases in activity, possibly due to the tension generated as the triceps stabilise the arm during the flexion movement. When comparing the biceps and triceps, it is evident that the biceps exhibit higher vibration amplitudes, particularly along the primary axis of motion (x_b and x_t). The observation highlights the dominant role of the biceps in flexion, with the triceps primarily playing a stabilizing role. Additionally, the consistent vibration patterns observed across the three flexion trials underscore the reliability and reproducibility of the data captured by the sensors.

Figure 4.4 presents the muscle vibration data during the extension phase of elbow movement. The graphs depict the acceleration data for muscle vibration in the biceps and triceps along the x, y, and z axes, capturing the dynamic behavior of the muscles as the biceps elongate and the triceps contract to straighten the elbow joint. In the biceps (Figures 4.4 a, b, c), the vibration patterns exhibit distinct fluctuations during extension. The x_b axis (Figure 4.4 a) shows notable peaks, suggesting significant activity in the biceps along the primary axis during elongation. However, the overall amplitude is lower compared to flexion, as expected during the elongation phase. The y_b (Figure 4.4 b) and z_b (Figure 4.4 c) axes show some variations, although these are less pronounced, reflecting the multidirectional forces involved in muscle elongation. For the triceps (Figures 4.4 d, e, f),

the acceleration data reveal more pronounced and consistent peaks, particularly in the x_t and z_t axes. The observed peaks align with the triceps' role in actively contracting during extension to straighten the elbow joint. The y_t axis (Figure 4.4 e) also shows some variations, though the overall amplitude remains lower compared to the primary axes. These findings suggest that the triceps generate significant force along specific directions (x_t and z_t), corresponding to their role in stabilising and straightening the joint.

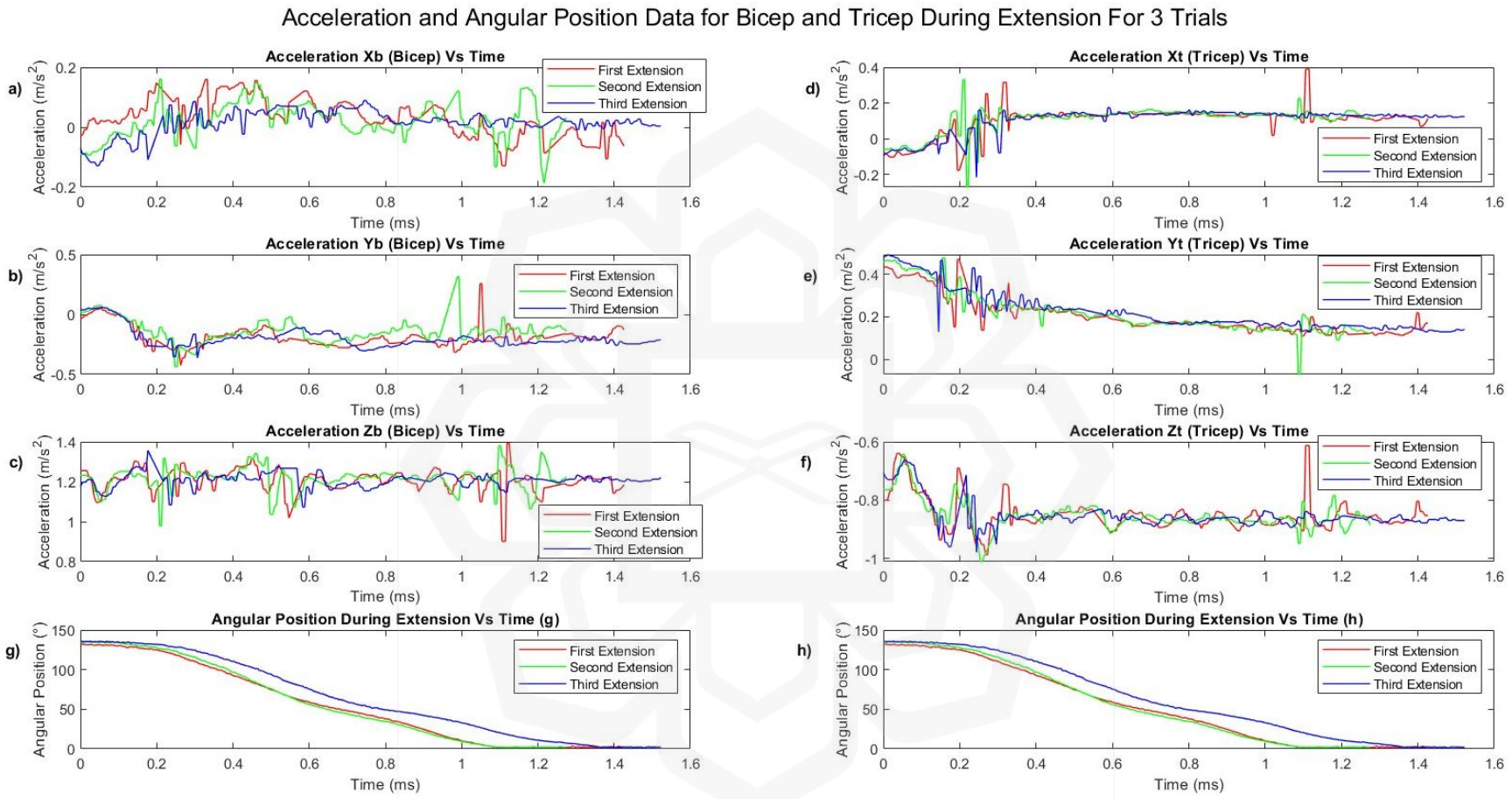

Figure 4.4 Muscle Vibration of Biceps (a, b, c) and Triceps (d, e, f) with Angular Position (g, h) During Fast Extension Across All Trials for Patient 26 (MAS Level 3)

In comparison, the biceps show lower vibration amplitudes in extension, reflecting their passive role during this phase as they elongate. In contrast, the triceps exhibit higher vibration amplitudes, indicating active contraction. The recorded differences in muscle activity highlight the relationship between the agonist and antagonist muscles during elbow extension. The triceps act as the agonist muscle, actively contracting to straighten the elbow, while the biceps serve as the antagonist muscle by passively elongating to allow the movement to occur. The consistent vibration patterns observed across the three extension trials demonstrate the reproducibility of the muscle activity data. The observed stability in recorded signals further supports the reliability of MMG as a tool for capturing muscle behaviors during dynamic joint movements such as extension.

Figure 4.5 highlights the distinct activity patterns of the biceps and triceps during slow and fast flexion movements. The biceps, acting as the agonist, contract to facilitate flexion, while the triceps elongate to accommodate the movement. The acceleration data from the x, y, and z axes, from the graph, highlights the differences in muscle activity during slow and fast flexion. The choice to include both slow and fast flexion movements in this research was deliberate, as faster transitions amplify the dynamic changes in muscle activity. During fast flexion, the biceps exhibit sharper and higher-amplitude peaks along the primary axis (x_b) in Figure 4.5a, emphasizing their capacity to generate greater force to meet the increased demands of fast motion. In contrast, slow flexion produces smoother, low-amplitude peaks, reflecting controlled, steady contractions. Similar trends are observed in the secondary axes (y_b and z_b) in Figures 4.5b and 4.5c, where fast flexion introduces greater multidirectional forces, highlighting the stabilization challenges of fast movement. Conversely, the triceps, acting as the antagonist, display subdued activity during elongation, with low-intensity vibrations during slow flexion along the x_t axis in Figure 4.5d. However, during fast flexion, there is a notable increase in acceleration peaks, as the triceps stabilize the joint against the rapid movement's forces. Multidirectional stabilization forces are also observed in the secondary axes (y_t and z_t) in Figures 4.5e and 4.5f, particularly during fast flexion.

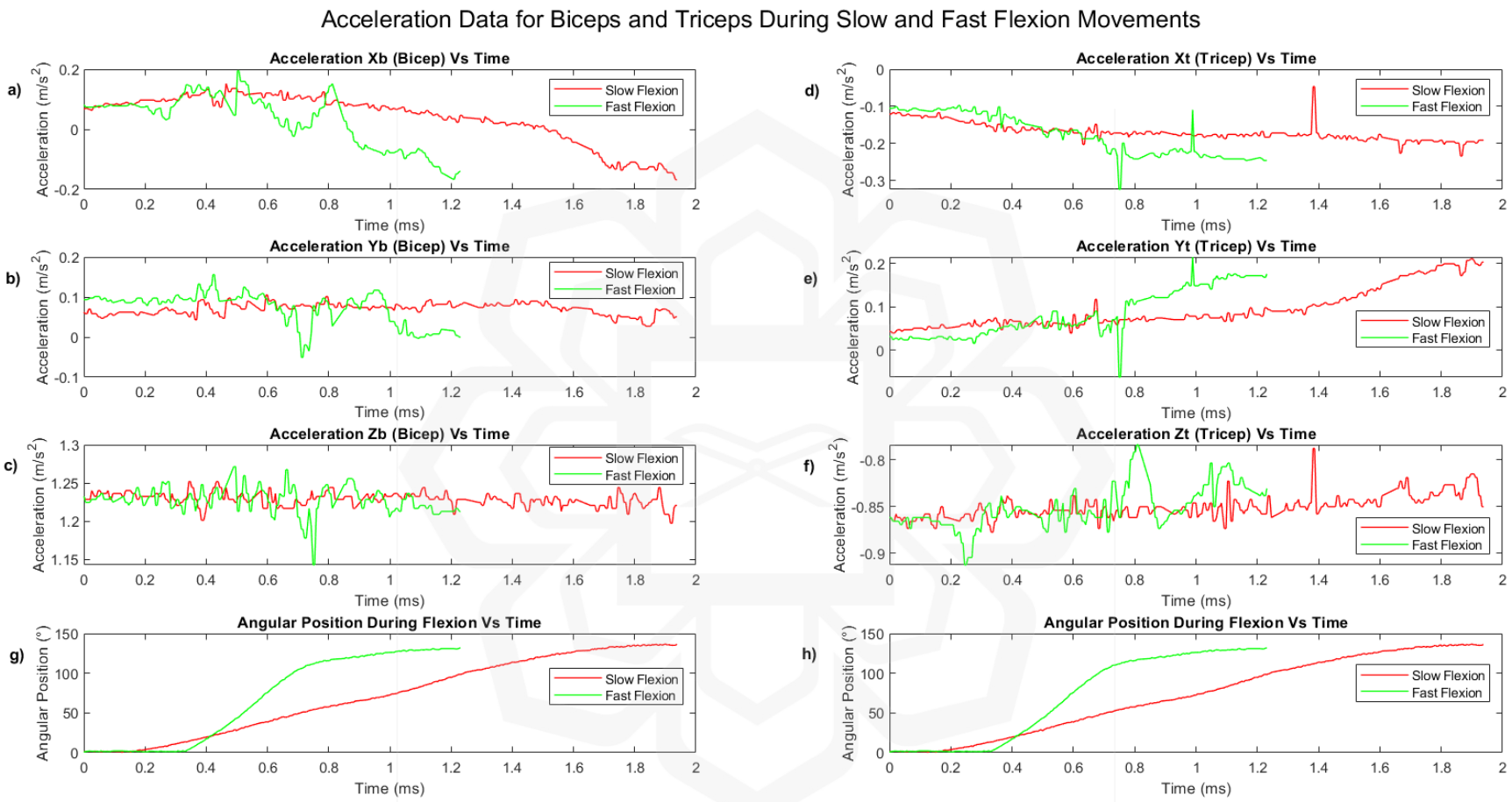

Figure 4.5 Muscle Vibrations of Biceps (a, b, c) and Triceps (d, e, f) with Angular Position (g, h) During Slow and Fast Flexion: Patient 7 (MAS Level 3)

Fast flexion movements also provoke the catch, a sudden increase in resistance and muscle activity caused by the hyperactive stretch reflex, which is a key clinical indicator of spasticity severity (van den Noort et al., 2010). This occurrence of the phenomenon is absent during slow passive stretching and in non-spastic muscles but becomes prominent during fast transitions due to the direct link with the hyperexcitability of the stretch reflex. The inclusion of fast flexion was specifically aimed at amplifying mechanical vibrations, which are critical for detecting features associated with spasticity in MMG signals. Spastic muscles, typically characterised by increased resistance during fast movements, exhibit distinct signal patterns that are more pronounced under rapid conditions. The heightened sensitivity, induced by quick transitions between contraction and relaxation, facilitates the detection of spasticity-associated alterations in muscle tone. The angular position data in Figures 4.3g and 4.3h further supports these observations, with fast flexion producing a steeper angular position curve compared to the gradual rise observed during slow flexion. A steeper curve reflects the more intense and abrupt muscle activity associated with rapid movements. Overall, the fast-paced movement protocol was chosen to elicit a broader range of muscle responses, provide a robust dataset for precise analysis of spasticity, and support the training and evaluation of the machine learning model. The pronounced fluctuations in MMG signals during rapid flexion enhance the ability to differentiate between varying degrees of spasticity, underscoring the value of fast movements in improving the sensitivity and accuracy of MMG assessments.

By emphasizing fast movements, the feature extraction process identified critical dynamics in the contraction of muscles, yielding features more appropriate for training robust machine learning models. The fast movements offered a more distinct identification of spastic activity, which is especially beneficial for analysis and predictive modelling.

4.3 STATISTICAL ANALYSIS AND FEATURES SELECTION

This subchapter presents the results of the statistical analyses conducted to examine the relationship between MMG signal features and muscle spasticity levels, as assessed using the MAS during flexion and extension movement. The datasets for both movements were combined and analysed using the same methods to explore potential differences in MMG signal characteristics across the two movement phases. The goal of the analysis was to determine the extent to which MMG signal features could serve as reliable and objective indicators of spasticity, complementing the subjective nature of traditional clinical assessments.

Several statistical methods were employed to achieve this aim. First, linear regression was applied to quantify the predictive relationship between MMG signal features and MAS levels. Pearson correlation analysis was then used to investigate the strength and direction of linear relationships between individual MMG features and spasticity levels. Finally, a one-way multivariate analysis of variance (MANOVA) was conducted to identify significant differences in feature values across different MAS levels, offering insight into the discriminative power of MMG signals in distinguishing varying degrees of spasticity.

4.3.1 Linear Regression Analysis

The results of the linear regression analysis, presented in Table 4.1, reveal key insights into the relationship between the MMG signal features and the MAS level during flexion, extension and combined movements. The analysis includes essential metrics such as the correlation coefficient (R) and the coefficient of determination (R^2). The correlation coefficient (R) quantifies both the magnitude and direction of the linear relationship between the MMG signal features and MAS levels. The coefficient of determination, R^2,

quantifies the amount of variance in the MAS level that can be explained by the MMG signal features.

Table 4.1 Linear Regression Analysis Result for Flexion, Extension and Combined Movements

Model	R	R square	Adjusted R square	*F*	df	P values
Flexion	0.881	0.777	0.586	4.076	41, 48	<0.001
Extension	0.865	0.749	0.535	3.495	41, 48	<0.001
Combined	0.673	0.453	0.290	2.786	41, 138	<0.001

During flexion movements, the correlation coefficient value of 0.881 indicates a robust positive linear association between the MMG signal features and MAS levels. The strong relationship suggests that higher MMG signal feature values correspond to higher MAS levels, reinforcing the reliability of MMG signal features as indicators of muscle spasticity. The coefficient of determination (R^2) quantifies the proportion of variance in MAS levels that can be explained by the MMG signal features. The R^2 value of 0.777 signifies that 77.7% of the variation in MAS levels can be explained by the MMG signal features incorporated in the regression model. The substantial R^2 value highlights the significant role of MMG signal characteristics in explaining variability in muscle spasticity measures. The adjusted R-squared value of 0.586, though slightly lower than the R^2 value, continues to reflect substantial explanatory power of the MMG signal features in relation to MAS levels. Furthermore, the F-test statistic of $F(41,48) = 4.076$, $p < 0.001$, confirms that the regression model is statistically significant and provides a strong fit to the data, supporting the hypothesis that MMG signal features play a significant role in predicting

MAS levels. Statistical findings reinforce the potential of MMG signal features as quantitative indicators of muscle spasticity, offering an objective alternative to subjective clinical assessments.

Similarly, during extension movements, the correlation coefficient of 0.865 indicates a robust positive linear association between MMG signal features and MAS levels, again suggesting that higher MMG signal values are associated with higher MAS levels. The coefficient of determination (R^2) of 0.749 implies that 74.9% of the variation in MAS levels can be explained by the MMG signal features. As with the flexion model, the strong R^2 value demonstrates that the MMG signal characteristics significantly explain the variability in muscle spasticity measures. The adjusted R-squared value of 0.535, although slightly lower than R^2, continues to exhibit substantial explanatory power. Additionally, the F-test statistic yielded a value of $F(41,48) = 3.495$, $p < 0.001$, indicating that the regression model is statistically significant and provides a strong fit to the data. The findings further support the hypothesis that MMG signal features serve as reliable predictors of MAS levels, reinforcing the potential application of MMG technology as an objective measure of muscle spasticity in clinical settings.

However, when the MMG signals from both flexion and extension movements were combined and analysed using linear regression, the correlation coefficient dropped to 0.673 with an R^2 value of 0.453. The reduction in correlation strength indicates that flexion and extension movements exhibit distinct characteristics, making integration into a single model unsuitable for spastic assessment. The combined model's adjusted R^2 of 0.290, along with a statistically significant F-test result ($F(41,138) = 2.786$, $p < 0.001$), underscores the need to develop separate models for flexion and extension movements for more effective spasticity assessment. Implementing distinct models for each movement phase is expected to improve accuracy and reliability, reinforcing the importance of treating flexion and extension as independent assessments rather than merging them into a unified approach.

4.3.2 Pearson Correlation Analysis

Pearson correlation analysis was conducted to evaluate the linear relationships between individual MMG signal features and MAS levels. The results of this analysis are summarized in Table 4.2 for flexion movements, Table 4.3 for extension movements, and Table 4.4 for combined movements. The Pearson correlation coefficients indicate the magnitude and direction of the linear associations across each MMG signal features and MAS levels. For flexion movement, Miny_b exhibited the most robust negative correlation with MAS levels ($r = -0.542$, $p < 0.001$), demonstrating that lower Miny_b values correspond to increased spasticity, as shown in Figure 4.6. In contrast, RMSy_b had the strongest positive correlation ($r = 0.515$, $p < 0.001$), indicating that higher RMSy_b levels are associated with greater severity of spasticity, as illustrated in Figure 4.7. Additionally, MAVy_b ($r = 0.425$, $p < 0.001$) and Maxy_t ($r = 0.395$, $p < 0.001$) also showed significant positive correlations with MAS levels. These findings highlight the importance of RMSy_b and Miny_b as crucial features for evaluating spasticity, emphasizing the significant clinical implications.

Table 4.2 Significant Pearson Correlation Coefficients Flexion Movement

Features	Pearson Correlation (r)	P values
MAVy_b	0.425**	<0.001
MAVz_b	-0.279**	0.008
SDy_b	0.405**	<0.001
PTPy_b	0.326**	0.002

Table 4.2 Significant Pearson Correlation Coefficients Flexion Movement (cont.)

Features	Pearson Correlation (r)	P values
Maxy_b	-0.301**	0.004
Miny_b	-0.542**	<0.001
Minz_b	-0.228*	0.030
Sx_b	0.263*	0.012
RMSy_b	0.515**	<0.001
RMSz_b	-0.278**	0.008
MAVy_t	0.394**	<0.001
MAVz_t	-0.288**	0.006
SDy_t	0.226*	0.032
Maxy_t	0.395**	<0.001
Maxz_t	-0.282**	0.007
Miny_t	0.342**	<0.001
Minz_t	-0.284**	0.007

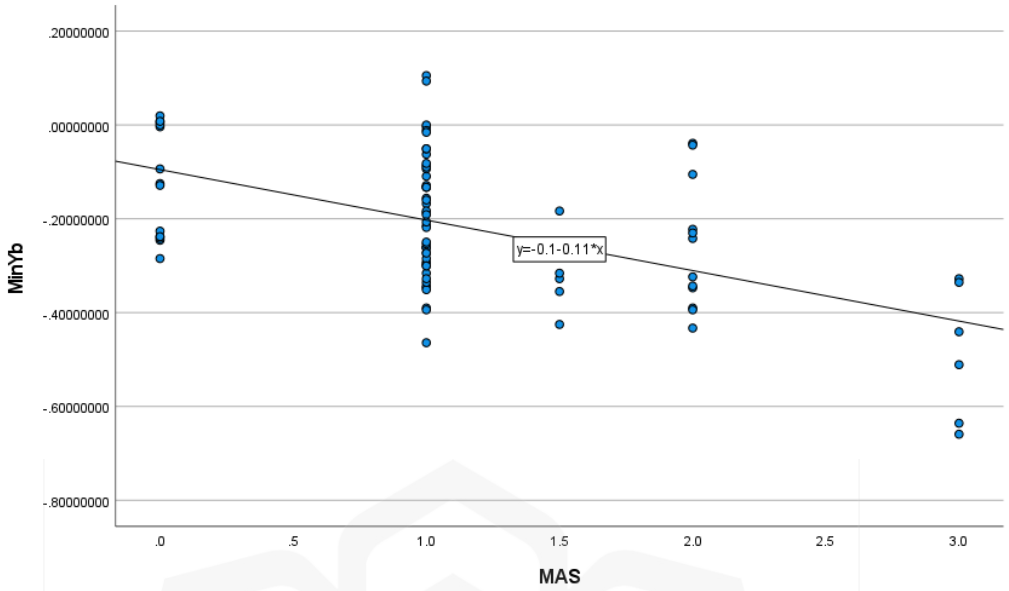

Figure 4.6 Relationship Between Miny_b and MAS Levels: Pearson Correlation Scatter Plot

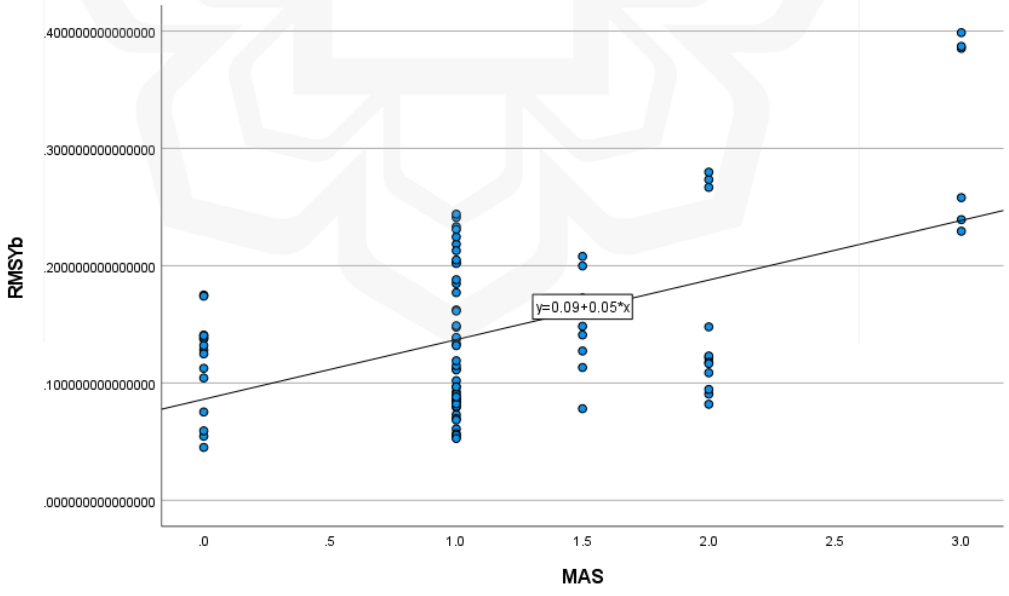

Figure 4.7 Relationship Between RMSy_b and MAS Levels: Pearson Correlation Scatter Plot

For extension movement, Maxy_b exhibited the strongest positive correlation (r = 0.455, $p < 0.001$), indicating that higher Maxy_b levels are associated with greater severity of spasticity, as shown in Figure 4.8. Furthermore, Maxz_b (r = 0.388, $p < 0.001$) also demonstrated a positive correlation with MAS levels, as illustrated in Figure 4.9. The results underscore the significance of Maxy_b and Maxz_b as key features in spasticity evaluation, reinforcing the relevance of these parameters in clinical practice.

Table 4.3 Significant Pearson Correlation Coefficients for Extension Movement

Features	Pearson Correlation (r)	P values
MAVy_b	0.375**	<0.001
MAVz_b	0.286**	0.006
SDx_b	0.345**	0.001
SDz_b	0.320**	0.002
PTPx_b	0.302**	0.004
PTPy_b	0.343**	0.001
PTPz_b	0.384**	<0.001
Maxx_b	0.289**	0.006
Maxy_b	0.455**	<0.001
Maxz_b	0.388**	<0.001
Minz_b	-0.214*	0.043
Kx_b	0.230*	0.029

Table 4.3 Significant Pearson Correlation Coefficients for Extension Movement (cont.)

Features	Pearson Correlation (r)	P values
Kz_b	0.303**	0.004
RMSy_b	-0.328**	0.002
RMSz_b	0.294**	0.005
My_t	0.237*	0.024
SDx_t	0.272**	0.009
SDz_t	0.266*	0.011
Maxy_t	0.258*	0.014
Miny_t	0.208*	0.049
Kx_t	-0.257*	0.015
RMSx_t	0.222*	0.035
RMSy_t	0.281**	0.007
RMSz_t	-0.277**	0.008

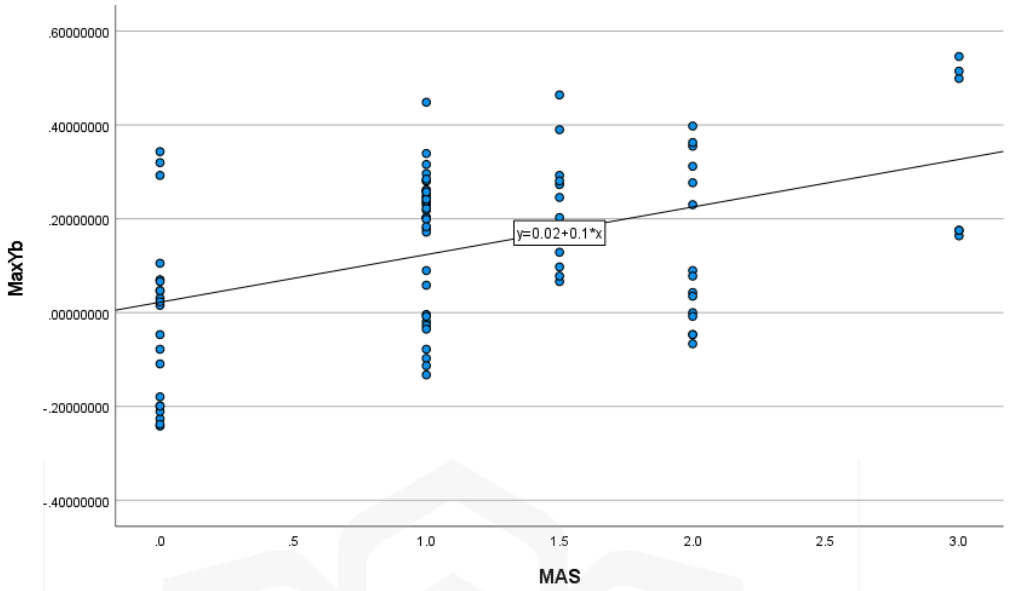

Figure 4.8 Relationship Between Maxy_b and MAS Levels: Pearson Correlation Scatter Plot

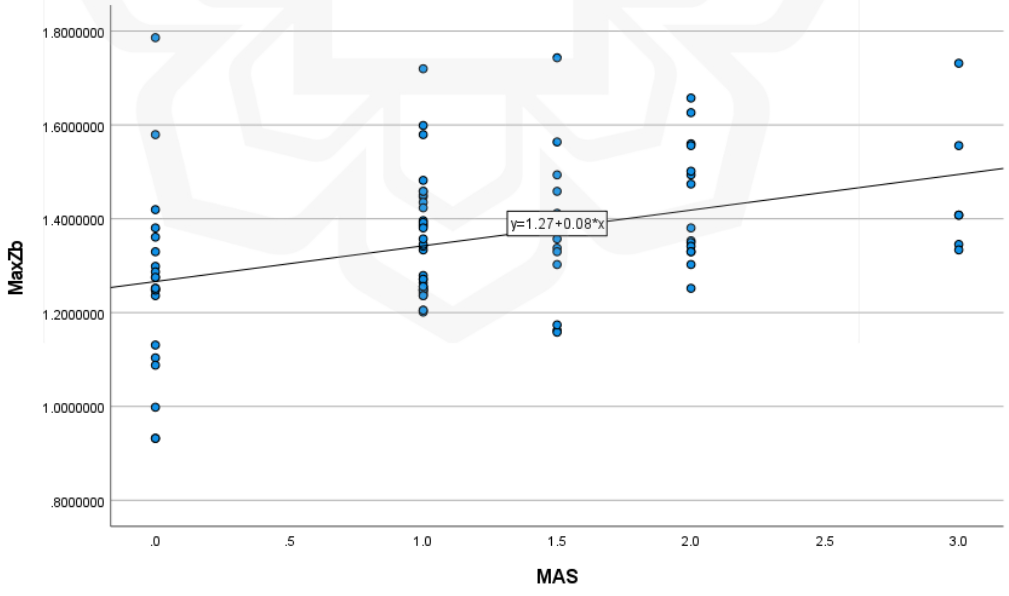

Figure 4.9 Relationship Between Maxz_b and MAS Levels: Pearson Correlation Scatter Plot

For combined movement, Maxy_t exhibited the highest positive correlation (r = 0.323, $p < 0.001$), indicating that higher Maxy_t levels are associated with greater severity of spasticity among the features, as shown in Figure 4.10. Another notable feature, MAVy_t, also showed a significant positive correlation (r = 0.311, $p < 0.001$), as depicted in Figure 4.11. The findings emphasize that specific features, such as Maxy_t and MAVy_t, are pivotal for evaluating spasticity and hold significant potential for clinical applications. However, when comparing the highest Pearson correlations for both flexion and extension movements, it becomes evident that the combination of features from these two movements results in much lower correlation values. The decrease suggests that while individual features such as Maxy_t and MAVy_t demonstrate significant associations with MAS levels, the combined effect of flexion and extension movements may provide less distinct differentiation between varying spasticity levels. The observation highlights the complexity of spasticity measurement, where movement type and feature combinations may not always produce the strongest correlations compared to isolated movements. Consequently, further exploration into the dynamic nature of spasticity and the influence of different movement patterns on the relationship with MMG signal features remains essential.

Table 4.4 Significant Pearson Correlation Coefficients for Combined Movement

Features	Pearson Correlation (r)	P values
SDx_b	0.273**	0.000
SDy_b	0.269**	0.000
SDz_b	0.227**	0.002
PTPx_b	0.238**	0.001
PTPy_b	0.305**	0.000

Table 4.4 Significant Pearson Correlation Coefficients for Combined Movement (cont.)

Features	Pearson Correlation (r)	P values
PTPz_b	0.233**	0.002
Maxx_b	0.221**	0.003
Maxz_b	0.156*	0.036
Minz_b	-0.202**	0.007
Kx_b	0.215**	0.004
MAVy_t	0.311**	0.000
SDx_t	0.189*	0.011
SDy_t	0.167*	0.025
SDz_t	0.200**	0.007
PTPy_t	0.169*	0.023
Maxy_t	0.323**	0.000
Miny_t	0.272**	0.000
RMSy_t	0.223**	0.003
RMSz_t	-0.219**	0.003

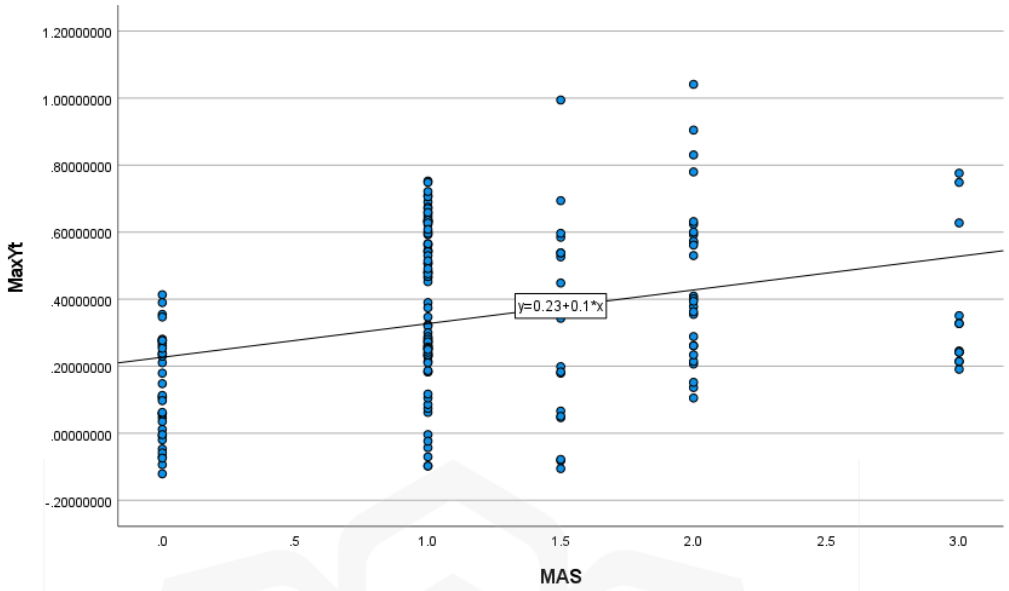

Figure 4.10 Relationship Between Maxy_t and MAS Levels: Pearson Correlation Scatter Plot

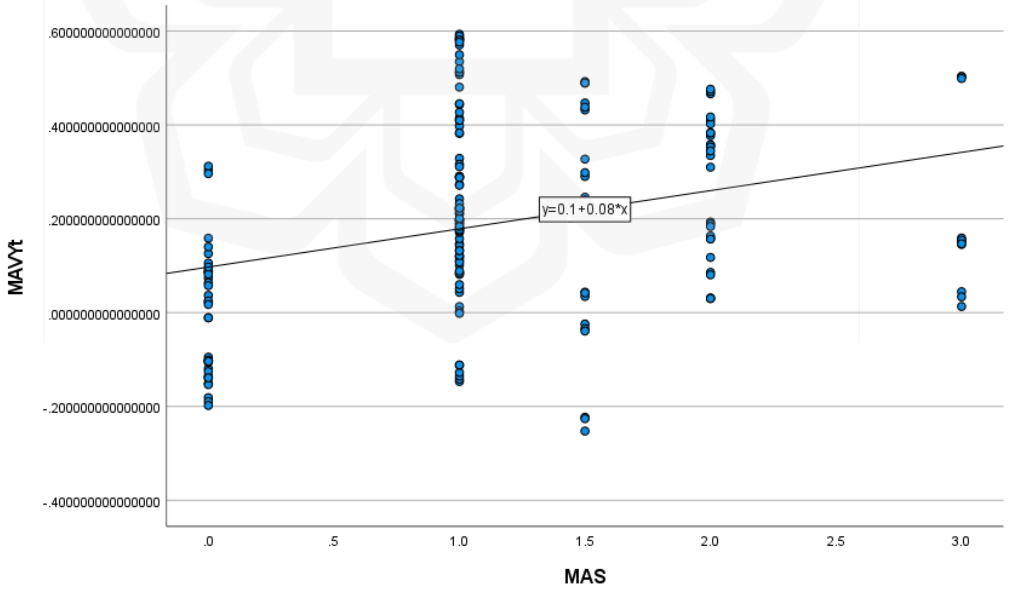

Figure 4.11 Relationship Between MAVy_t and MAS Levels: Pearson Correlation Scatter Plot

4.3.3 One-Way MANOVA Analysis

The research employed one-way MANOVA to detect and eliminate dependent and redundant features by a method of significant feature analysis. The statistical approach analysed the extracted features and identified significant differences in mean values between the groups for each axis of the biceps (x_b, y_b, and z_b) and triceps (x_t, y_t, and z_t). Table 4.5 presents the outcomes of the one-way MANOVA analysis for flexion, extension, and combined movements, emphasising the relevant factors that influence the variability in the MAS values. The findings highlight distinct MMG signal features that exhibit significant variations among different movement patterns, offering deeper insight into the relationship between spasticity and MMG signal characteristics.

Table 4.5 One-way Manova Test Result for Flexion, Extension and Combined Movement

Model	Features	P values						Significant Features Based on Axes
		Biceps			Triceps			
		x_b	y_b	z_b	x_t	y_t	z_t	
Flexion	RMS	0.004	0.000	0.000	0.909	0.000	0.002	x_b, y_b, z_b, y_t, z_t
	PTP	0.300	0.013	0.148	0.206	0.245	0.256	y_b
	MAX	0.000	0.003	0.000	0.708	0.000	0.011	x_b, y_b, z_b, y_t, z_t
	MIN	0.000	0.000	0.000	0.949	0.000	0.003	x_b, y_b, z_b, y_t, z_t
	MAV	0.000	0.000	0.000	0.896	0.000	0.006	x_b, y_b, z_b, y_t, z_t
	SD	0.583	0.001	0.157	0.335	0.282	0.042	y_b, z_t
	S	0.001	0.939	0.311	0.345	0.946	0.065	x_b
	K	0.213	0.020	0.309	0.221	0.456	0.557	y_b

Table 4.5 One-way Manova Test Result for Flexion, Extension and Combined Movement (cont.)

Model	Features	P values						Significant Features Based on Axes
		Biceps			Triceps			
		x_b	y_b	z_b	x_t	y_t	z_t	
Extension	RMS	0.166	0.000	0.007	0.107	0.004	0.049	y_b, z_b, y_t, z_t
	PTP	0.000	0.006	0.001	0.581	0.321	0.027	x_b, y_b, z_b, z_t
	Max	0.096	0.000	0.006	0.285	0.001	0.242	y_b, z_b, y_t
	Min	0.005	0.008	0.002	0.129	0.002	0.167	x_b, y_b, z_b, y_t
	MAV	0.176	0.000	0.007	0.172	0.001	0.231	y_b, z_b, y_t
	SD	0.000	0.030	0.001	0.001	0.727	0.023	x_b, y_b, z_b, x_t, z_t
	S	0.120	0.152	0.076	0.273	0.797	0.306	-
	K	0.045	0.601	0.002	0.089	0.154	0.336	x_b, z_b
Combined	RMS	0.012	0.000	0.000	0.565	0.000	0.006	x_b, y_b, z_b, y_t, z_t
	PTP	0.000	0.001	0.023	0.800	0.167	0.006	x_b, y_b, z_b, z_t
	Max	0.000	0.025	0.008	0.493	0.000	0.847	x_b, y_b, z_b, y_t
	Min	0.000	0.007	0.000	0.528	0.000	0.293	x_b, y_b, z_b, y_t
	MAV	0.000	0.012	0.000	0.552	0.000	0.543	x_b, y_b, z_b, y_t
	SD	0.000	0.000	0.002	0.006	0.236	0.006	x_b, y_b, z_b, x_t, z_t
	S	0.033	0.214	0.053	0.851	0.995	0.377	x_b, z_b
	K	0.368	0.780	0.254	0.368	0.780	0.254	-

To assess significance level, a *p*-value threshold of < 0.05 was established, allowing for the rejection of the null hypothesis, which posits no variation in the mean values between the groups. There were no variations in the mean values between the groups, according to the null hypothesis for the MANOVA test. The results for flexion movements revealed that all the *p*-values for the features, including MAVx_b, MAVy_b, MAVz_b, SDz_b,

PTPy_b, Maxx_b, Maxy_b, Maxz_b, Minx_b, Miny_b, Minz_b, Sx_b, Ky_b, RMSx_b, RMSy_b, RMSz_b, MAVy_t, MAVz_t, SDz_t, Maxy_t, Maxz_t, Miny_t, Minz_t, RMSy_t, and RMSz_t, were below 0.05 significance threshold, resulting in the rejection of the null hypothesis. Similarly, for extension movements, all p-values for features such as MAVy_b, MAVz_b, SDz_b, SDy_b, SDz_b, PTPx_b, PTPy_b, PTPz_b, Maxy_b, Maxz_b, Minx_b, Miny_b, Minz_b, Kx_b, Kz_b, RMSy_b, RMSz_b, MAVy_t, SDx_t, SDz_t, PTPz_t, Maxy_t, Miny_t, RMSy_t and RMSz_t were also below 0.05, leading to the rejection of the null hypothesis.

The analysis of combined movements further supported these findings, with all *p*-values for the features, including MAVx_b, MAVy_b, MAVz_b, SDx_b, SDy_b, SDz_b, PTPx_b, PTPy_b, PTPz_b, Maxx_b, Maxy_b, Maxz_b, Minx_b, Miny_b, Minz_b, RMSx_b, RMSy_b, RMSz_b, Sx_b, MAVy_t, SDx_t, SDz_t, PTPz_t, Maxy_t, Miny_t, RMSy_t, RMSz_t and Sz_t, falling below the significance threshold of 0.05. The statistical results led to the rejection of the null hypothesis and confirmed significant variations in these features among the groups. The strong association between these features and MAS levels underscores the pivotal role of MMG signal characteristics in characterizing muscle spasticity. Notably, compared to the number of significant features identified for both flexion and extension movements, the combined movement analysis revealed a considerably greater number of significant features, highlighting the complexity and the added value of including combined movements in the assessment of spasticity.

A comparative analysis of significant features across movement types of flexion, extension, and combination movements revealed that combination movements exhibited a higher number of significant features than flexion or extension alone. The increased number of relevant features suggests that combination movements capture a broader spectrum of MMG signal characteristics, likely to reflect the complex neuromuscular dynamics associated with spasticity. Consequently, analysing combination movements provides a more comprehensive understanding of spasticity patterns, highlighting their importance in future research and clinical assessments. In summary, the findings underscore the necessity of movement-specific models for spasticity assessment and the critical role of specific

MMG features. Moreover, the broader range of significant features observed in combination movements emphasizes the potential for providing deeper insights into spasticity dynamics, ultimately paving the way for more refined and effective diagnostic and therapeutic approaches.

4.3.4 Significance Testing Between Healthy and MAS 0 Level Patients

This section provides baseline comparisons between ten healthy individuals and five stroke patients for flexion, and seven for extension, all categorised with no muscle tone (MAS 0). The main aim of this investigation was to determine if notable differences in muscle behaviour could be detected between these two groups, despite both being classified as MAS 0, indicating comparable muscle tone characteristics. The baseline analysis was crucial for comprehending the comparison between stroke patients with MAS 0, who first experienced flaccidity before progressing to spasticity or recovery stages, and healthy persons. Recognising that flaccidity, a condition frequently observed in the early phases of stroke recovery, may lead to subtle changes in muscle activation is essential, even in the absence of explicit spasticity. In this context, multivariate analysis of variance (MANOVA) was utilised to concurrently assess different features derived from the MMG signals of the biceps and triceps between flexion and extension movements.

Table 4.6 shows the results of the MANOVA analysis, emphasizing the statistically significant differences between the healthy group and stroke patients during flexion and extension movement. A significance level of $p < 0.05$ was employed to reject the null hypothesis, which predicted that there were no variations in the mean values within the groups. In both movements, the null hypothesis rejection signifies substantial changes in the MMG signal features, contrary to the anticipation that both groups would demonstrate analogous muscle tone characteristics, especially since the stroke patients were categorised

as MAS 0. For flexion movement, all the *p*-values for features such as RMSy_t, RMSz_t, PTPx_b, PTPy_b, PTPx_t, Maxx_b, Maxz_b, Maxy_t, Maxz_t, Minx_b, Miny_b, Miny_t, Minz_t, MAVx_b, MAVy_b, MAVz_b, MAVy_t, MAVz_t, SDx_t, Sz_t and Ky_b, were below 0.05, effectively rejecting the null hypothesis and indicating significant differences between the groups. Similarly, for extension movement, features such as RMSy_b, RMSz_b, RMSy_t, RMSz_t, PTPy_t, Maxx_b, Maxy_b, Maxx_t, Maxy_t, Maxz_t, Minx_b, Minz_b, Minx_t, Miny_t, Minz_t, MAVx_b, MAVz_b, MAVx_t, MAVy_t, MAVz_t, SDx_b, Sy_t, Kx_t and Ky_t also exhibited *p*-values below 0.05, signifying significant variations. The differences emphasise the consistency of the results across various movement types, reinforcing the reliability of MMG in identifying changes in muscle tone during both flexion and extension.

Table 4.6 One-Way Manova Test Result During Flexion and Extension Movement Between Healthy Individuals and Stroke Patients

Model	Features	P Values						Significant Features Based on Axes
		Biceps			Triceps			
		x_b	y_b	z_b	x_t	y_t	z_t	
Flexion	RMS	0.108	0.208	0.022	0.159	<0.001	<0.001	y_t, z_t
	PTP	0.033	0.045	0.067	0.006	0.200	0.195	x_b, y_b, x_t
	Max	<0.001	0.110	0.002	0.083	<0.001	0.041	x_b, z_b, y_t, z_t
	Min	<0.001	<0.001	0.568	0.959	<0.001	0.020	x_b, y_b, y_t, z_t
	MAV	<0.001	<0.001	0.023	0.298	<0.001	0.022	x_b, y_b, z_b, y_t, z_t
	SD	0.123	0.390	0.249	0.019	0.162	0.072	x_t
	S	0.498	0.137	0.097	0.740	0.109	0.018	z_t
	K	0.069	0.022	0.061	0.146	0.422	0.873	y_b

Table 4.6 One-Way Manova Test Result During Flexion and Extension Movement Between Healthy Individuals and Stroke Patients (cont.)

Model	Features	P Values						Significant Features Based on Axes
		Biceps			Triceps			
		x_b	y_b	z_b	x_t	y_t	z_t	
Extension	RMS	0.094	0.001	0.009	0.673	<0.001	<0.001	y_b, z_b, y_t, z_t
	PTP	0.193	0.125	0.519	0.310	0.007	0.809	y_t
	Max	0.001	0.011	0.072	<0.001	<0.001	<0.001	x_b, y_b, x_t, y_t, z_t
	Min	0.006	0.162	0.004	0.012	<0.001	0.005	x_b, z_b, x_t, y_t, z_t
	MAV	0.006	0.063	0.009	<0.001	<0.001	<0.001	x_b, z_b, x_t, y_t, z_t
	SD	0.203	0.694	0.280	0.039	0.511	0.840	x_t
	S	0.148	0.056	0.091	0.804	0.002	0.105	y_t
	K	0.298	0.051	0.522	0.029	0.017	0.556	x_t, y_t

Contrary to the initial assumption that both groups (healthy individuals and stroke patients with MAS 0 would have similar muscle tone characteristics, the pronounced differences in the MMG features indicate that stroke patients categorised as having no muscle tone may nonetheless demonstrate subtle neuromuscular distinctions. This discovery holds significant importance, as MMG may serve as an effective instrument for identifying early alterations in muscle characteristics before the onset of spasticity. Detecting these changes at an early stage could provide therapists with valuable insights into the progression of neuromuscular disorders in stroke patients, potentially enabling earlier intervention and improving rehabilitation outcomes.

4.4 DEVELOPMENT OF PREDICTIVE MACHINE LEARNING MODELS

4.4.1 Selection of Machine Learning Algorithms

Multiple machine learning techniques were utilised to ascertain the appropriate boundary conditions for recognising each target class. Considering that the MAS level comprises multiple categories—MAS 0, 1, 1+, 2, and 3—a multi-class classification methodology was employed. The models frequently employed in pertinent research were chosen and assessed, as outlined in Table 4.7. Utilising the algorithms, the research can ascertain the most effective methods for differentiating spasticity levels based on MMG signal features. This thorough assessment guarantees the reliability of the results while offering insights into the computational and predictive efficacy of each classifier.

Table 4.7 List of Algorithms Employed in the Analysis

Type	Algorithm
Eager	DT
Linear	LDA
Function	SVM
Lazy	KNN

As shown in Figures 4.1 and 4.2, the distribution of MAS levels varied, with certain levels such as MAS 1+ and MAS 3 represented by fewer samples compared to MAS 1 or MAS 0. To avert overfitting and guarantee the model's robustness, the cross-validation technique was employed during the training procedure. Cross-validation partitions the dataset into several subgroups, utilizing some for-model training and others for validation. The strategy is crucial in the research, as cross-validation ensures the model does not merely memorize the training data but also effectively classifies novel, unknown data. This stratification helps prevent class imbalance from skewing the evaluation metrics, particularly for underrepresented MAS level. The analysis concentrated on two movements: flexion and extension. Each movement was evaluated separately to ascertain their distinct contributions to the features of the MMG signal. The analysis employed two datasets: the first encompassed all available features, whilst the second contained only the significant features determined by a one-way MANOVA test. Each dataset was further partitioned into training and testing subsets, with ratios of 90/10, 80/20, and 70/30. In the 90/10 split, 90% of the data was designated for model training, and the remaining 10% was given for testing. The same partitioning approach was applied to the 80/20 and 70/30 splits, facilitating an assessment of model robustness and generalization capabilities. The selection of training and testing splits significantly influenced algorithm performance in predicting spasticity during flexion, extension, and combined movements. Table 4.8

presents a comparative analysis of accuracy achieved based on selected features for training and testing, highlighting notable variations in classification outcomes.

Table 4.8 Accuracy of Machine Learning Algorithms Based on Training and Testing Splits for All and Significant Features During Flexion, Extension and Combined Movements

Model	Algorithm	Training and Testing Split Percentage of Accuracy					
		All Features			Significant Features		
		90-10	80-20	70-30	90-10	80-20	70-30
Flexion	DT	64.20	65.28	55.56	65.43	63.89	65.08
	LDA	69.14	59.72	46.03	76.54	70.83	66.67
	SVM	65.43	69.44	60.32	72.84	68.06	69.84
	KNN	**83.95**	80.56	66.67	**90.12**	86.11	84.13
Extension	DT	72.84	59.72	66.67	60.49	59.72	71.43
	LDA	64.20	50.00	47.62	53.09	59.72	55.56
	SVM	65.43	61.11	53.97	64.20	59.72	71.43
	KNN	**90.12**	86.11	82.54	**83.95**	83.33	74.60
Combined	DT	54.94	72.22	46.53	52.78	60.32	40.74
	LDA	51.23	50.00	56.25	58.33	50.00	55.56
	SVM	58.02	50.00	61.11	66.67	57.14	61.11
	KNN	**80.86**	66.67	76.39	**82.72**	73.81	79.63

For the flexion movement, the dataset incorporating all features, along with the dataset containing significant features under the 90/10 split, achieved the highest accuracy among various data ratios. Within the comprehensive dataset, the K-Nearest Neighbors (KNN) algorithm demonstrated superior performance with an accuracy of 83.95%, surpassing other techniques. Notably, using only significant features further improved the KNN algorithm's accuracy to 90.12%. This enhancement highlights the pivotal role of feature selection in boosting model efficacy, underscoring its contribution to achieving optimal machine learning performance. The confusion matrix findings, as shown in Figures 4.12 and 4.13, illustrate the accuracy of the KNN algorithm for both all-feature and significant-feature datasets. The True Positive Rate (TPR) and False Negative Rate (FNR) reveal that the KNN algorithm achieves high accuracy across the MAS levels 0, 1, 1.5 (1+), 2, and 3. Specifically, with all features, the algorithm achieves strong accuracy in detecting extreme classes (MAS levels 0 and 3) while maintaining high TPRs across most classes. However, with significant features, the KNN algorithm not only retains its accuracy for extreme classes but also demonstrates an improvement in identifying intermediate classes, particularly MAS level 1 and 1.5. The improvement highlights the effectiveness of significant features in enhancing classification accuracy and suggests that reducing the dataset to its most relevant attributes optimises the model's performance.

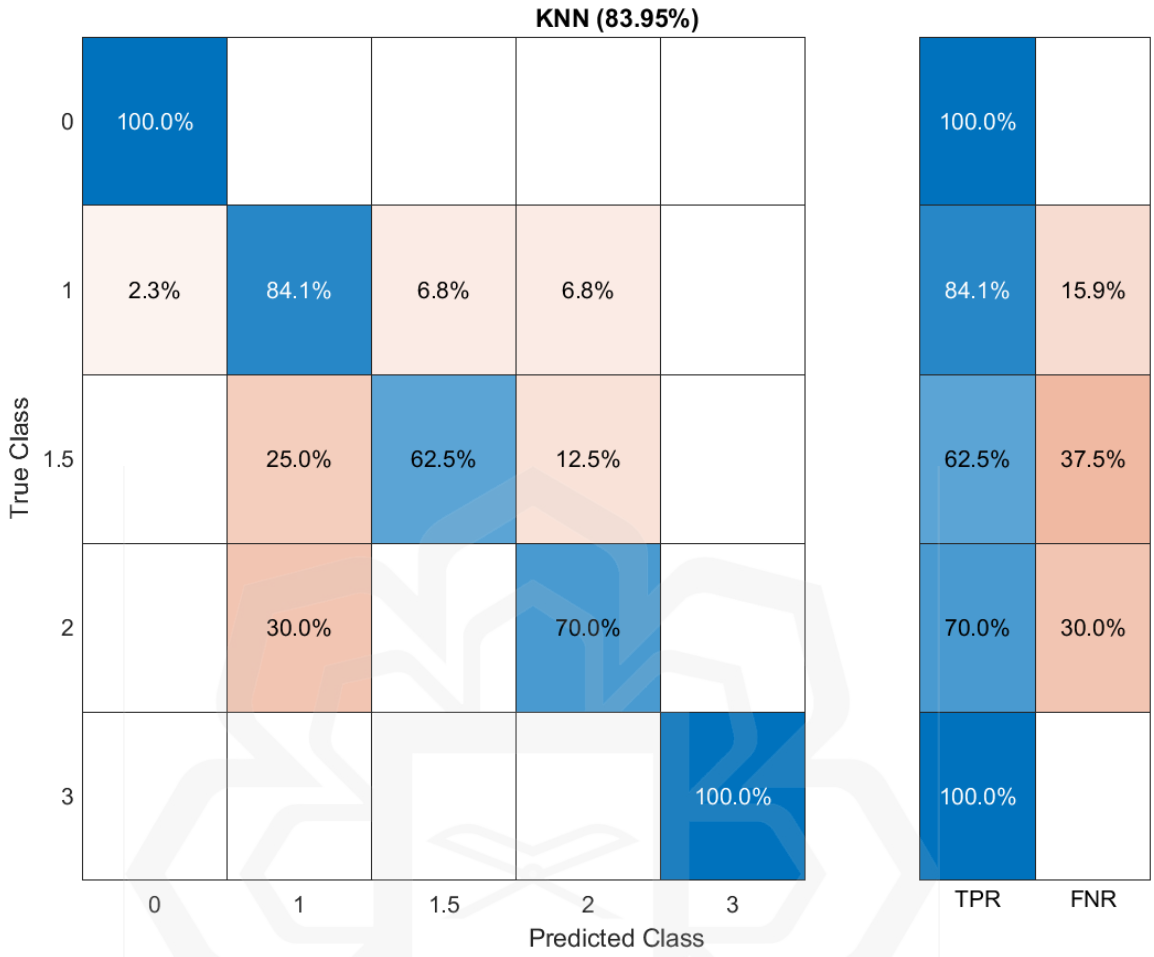

Figure 4.12 Confusion matrix for KNN using all features with 90/10 split for Flexion Movement

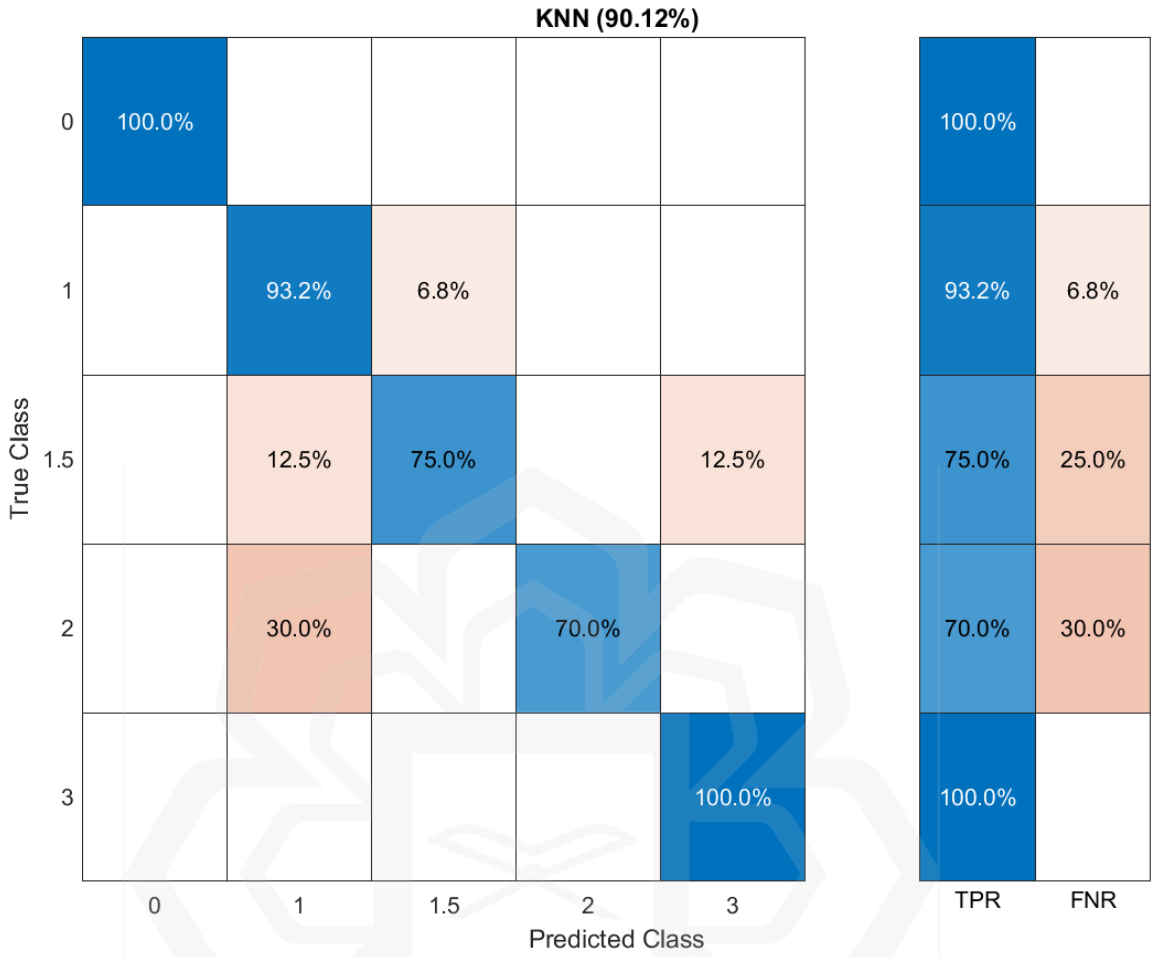

Figure 4.13 Confusion matrix for KNN using significant features 90/10 split for Flexion Movement

Similarly, for the extension movement, the dataset encompassing all features, as well as the dataset with significant features under the 90/10 split, achieved the highest accuracy among the various data ratios. The KNN algorithm attained an accuracy of 90.12% using all features, outperforming other techniques. However, the algorithm's accuracy slightly declined to 86.42% when only significant features were utilised. This reduction suggests that, while the selected features are crucial, omitting additional features may result in the loss of valuable information. The excluded features, though individually less significant, might contribute to improving model performance through interactions

with other attributes. The confusion matrix findings, presented in Figures 4.14 and 4.15, provide additional insights. When utilising all features, the KNN algorithm achieves exceptional performance in accurately detecting severe classes, such as MAS level 3, while maintaining high TPRs for intermediate levels (MAS levels 1 and 2). However, when using significant features, the classifier shows a slight reduction in accuracy, particularly in identifying intermediate classes like MAS level 1.5. The observation emphasizes the trade-off between computational efficiency and predictive performance when reducing the feature set.

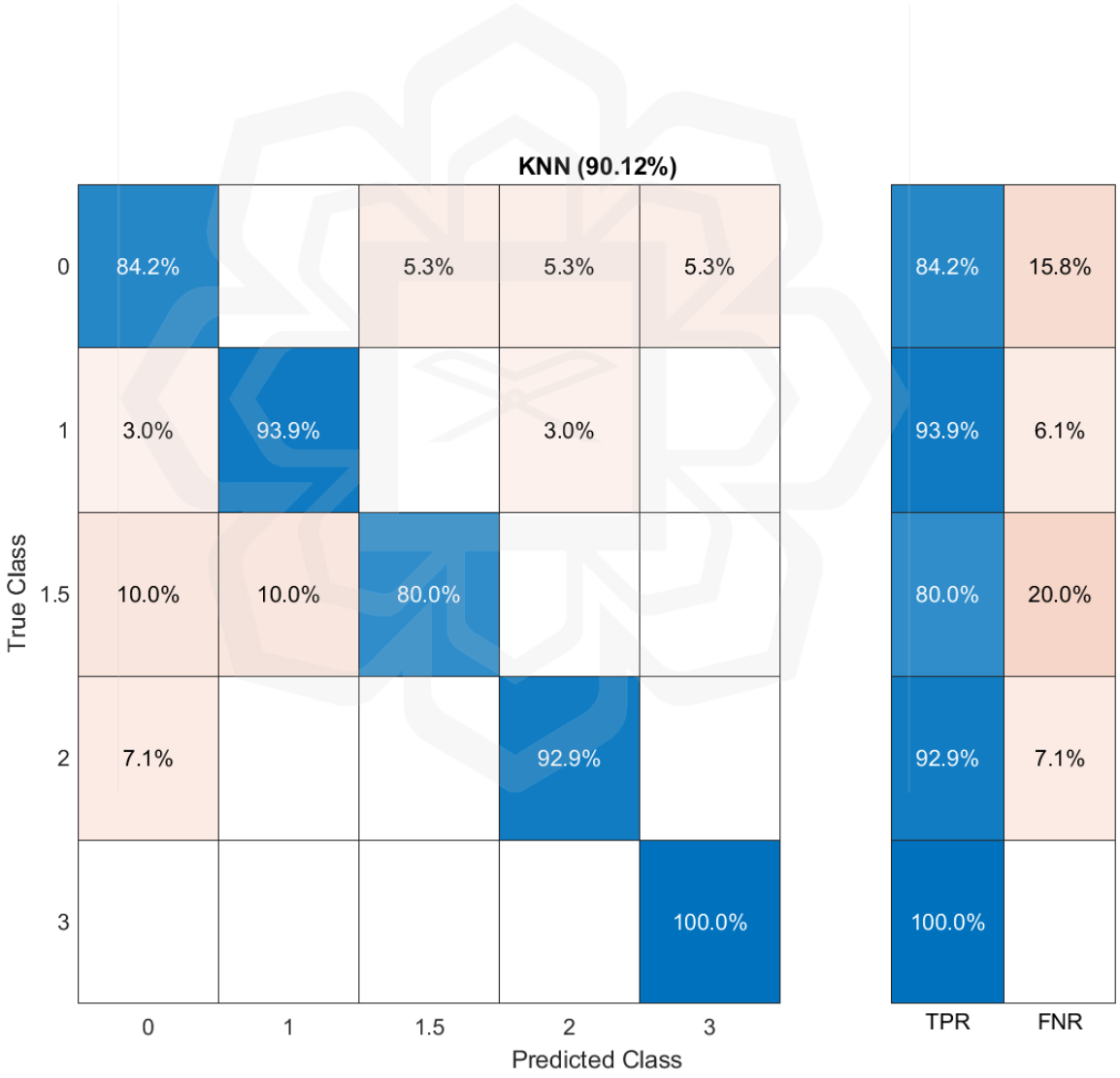

Figure 4.14 Confusion matrix for KNN using all features with 90/10 split for Extension Movement

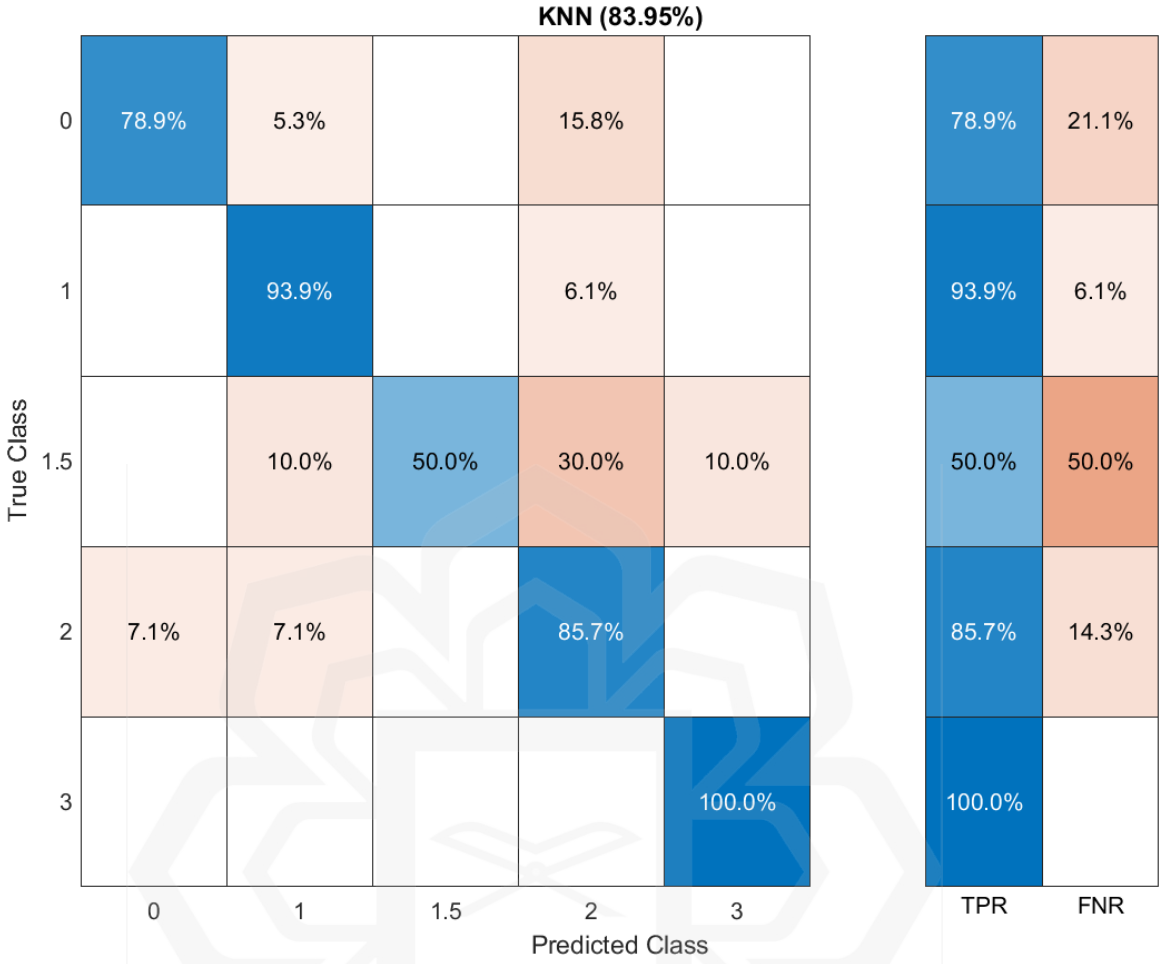

Figure 4.15 Confusion matrix for KNN using significant features with 90/10 split for Extension Movement

For combined movements, the dataset incorporating all features and the dataset with significant features for the 90/10 split demonstrated the highest accuracy. Using the full dataset, the KNN algorithm achieved an accuracy of 80.86%, outperforming other methods. Interestingly, the accuracy improved slightly to 82.72% when only significant features were considered. This improvement underscores the value of feature selection in refining model performance by focusing on the most pertinent attributes. However, a comparison of predictive accuracy between individual flexion and extension movements versus combined movements reveals lower performance for the combined dataset. This outcome suggests

that flexion and extension movements exhibit distinct characteristics that, when combined, may dilute the model's ability to differentiate spasticity levels effectively. These findings highlight the importance of developing movement-specific models to achieve more precise spasticity assessments. The confusion matrix findings, shown in Figures 4.16 and 4.17, further support this observation. With all features, the KNN algorithm achieves an overall accuracy of 80.86%, maintaining relatively high TPRs for intermediate and severe classes such as MAS levels 1, 1.5, and 3. When the dataset is reduced to significant features, the accuracy slightly improves to 82.72%. However, this refinement comes with trade-offs, as the TPR for certain classes, such as MAS levels 1.5 and 3, declines slightly. This outcome suggests that while feature selection enhances overall accuracy, modifications to the dataset may also impact classification performance for specific categories, highlighting the nuanced effects of feature reduction on classification outcomes.

When comparing the confusion matrices for flexion and extension movements, the classifier's performance for combination movements deviates significantly. The deviation likely stems from the increased complexity and variability introduced when combining flexion and extension actions. The variability in muscle activation patterns and signal characteristics during combined movements contributes to the larger discrepancies observed in the confusion matrices.

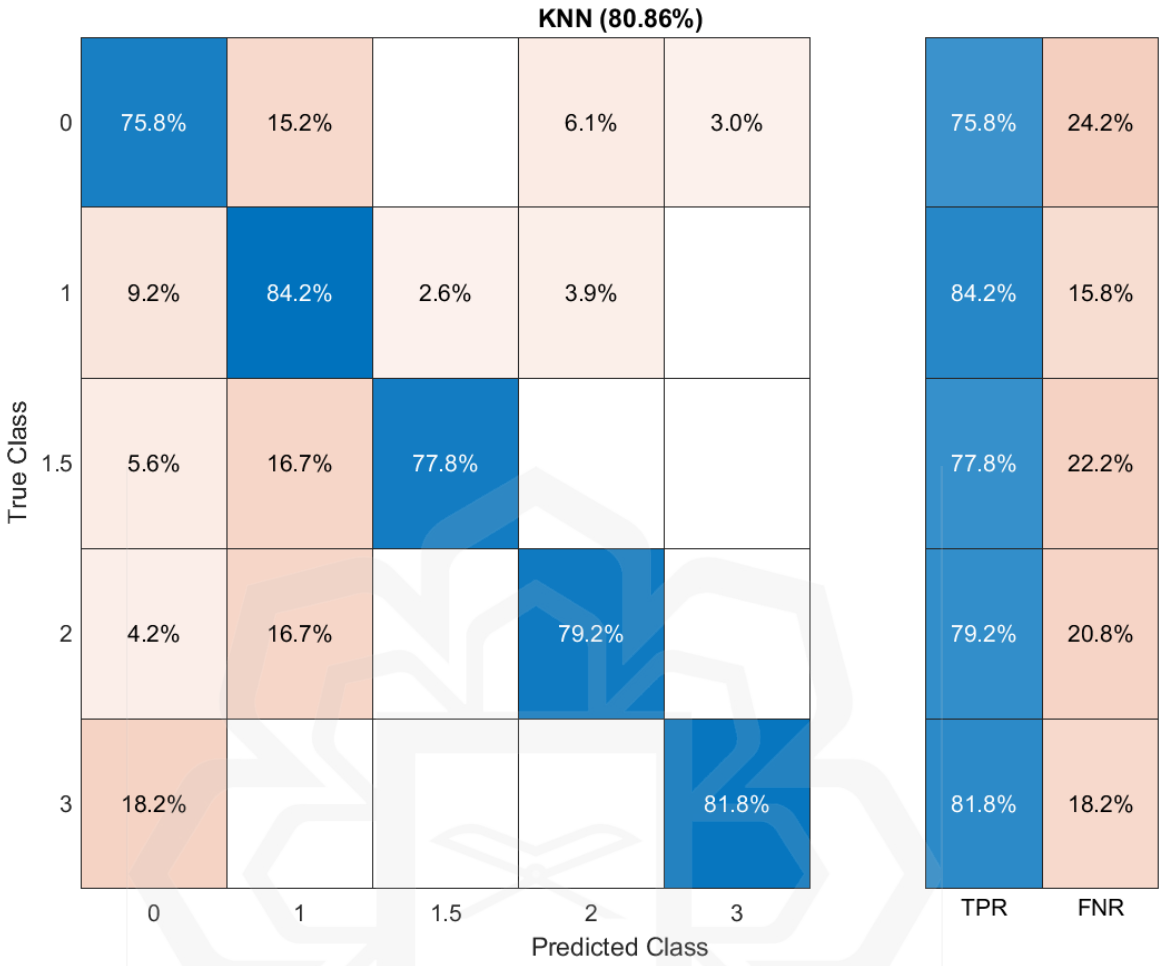

Figure 4.16 Confusion matrix for KNN using all features with 90/10 split for Combined Movement

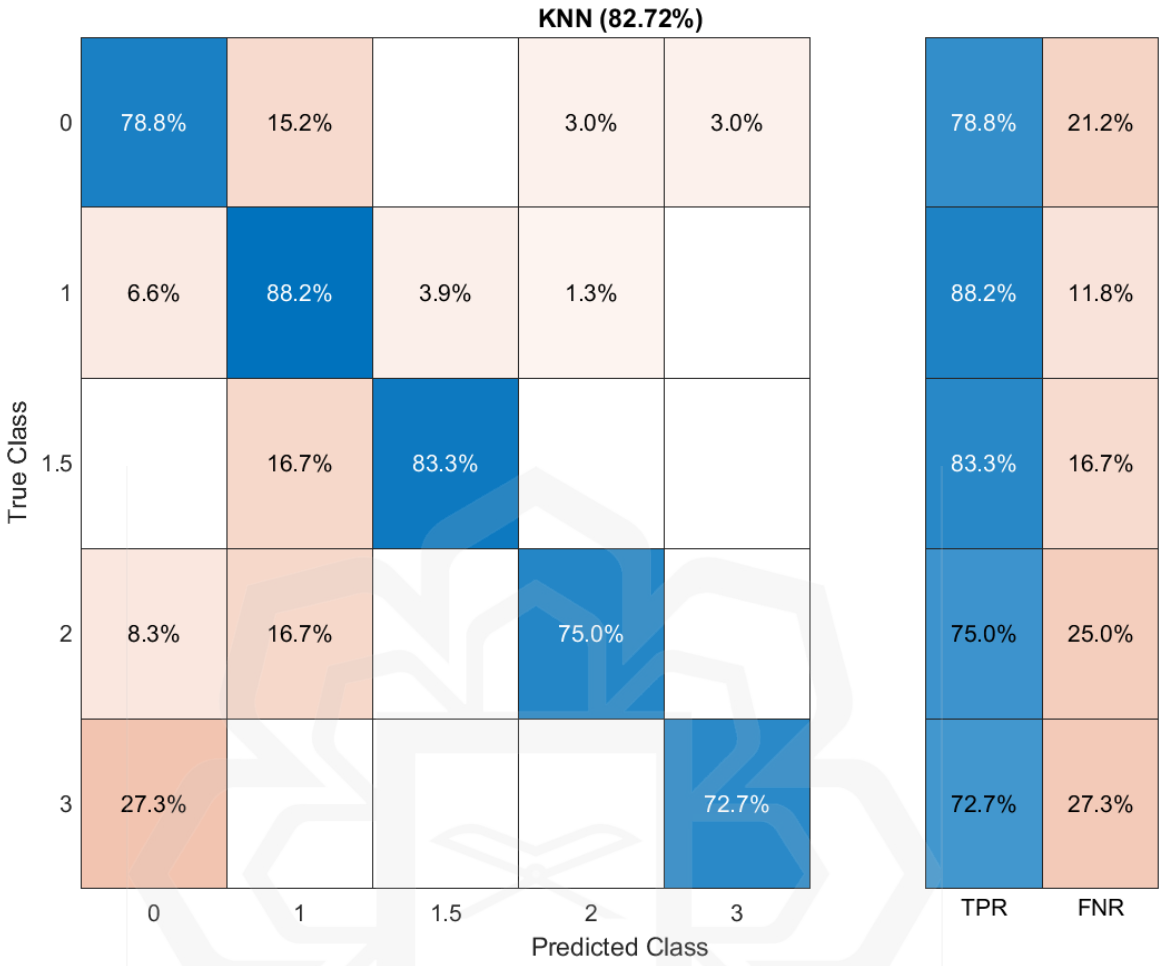

Figure 4.17 Confusion matrix for KNN using significant features with 90/10 split for Combined Movement

Different feature sets can have a significant impact on the computational complexity of machine learning algorithms, particularly influencing the duration required for model training. Table 4.9 presents the training durations for several machine learning algorithms used in the research, comparing the use of all features with the use of significant features for flexion, extension, and combined movements under a 90/10 split. For flexion movement, the training times for all algorithms showed a noticeable reduction when significant features were used. Specifically, the Decision Tree (DT) algorithm's training time decreased from 4.27 seconds to 3.24 seconds. Similarly, the Linear Discriminant

Analysis (LDA) algorithm's training time was reduced from 1.13 seconds to 0.91 seconds, while the Support Vector Machine (SVM) algorithm demonstrated a reduction from 4.35 seconds to 3.75 seconds. The K-Nearest Neighbors (KNN) algorithm also experienced a decrease, with training time reduced from 3.03 seconds to 2.46 seconds. Among the algorithms evaluated, the DT algorithm exhibited the most significant percentage reduction in training time, with a 24.12% decrease. This notable improvement highlights the impact of algorithm structure on computational efficiency. Moreover, utilising crucial features simplifies the training process by decreasing the complexity and size of the dataset, enabling machine learning algorithms to function more effectively and attain quicker convergence (Sarker, 2021).

For extension movement, a similar trend of reduced training times was observed across most algorithms. The DT algorithm achieved a dramatic decrease, with training time reduced from 10.24 seconds to 3.31 seconds. Likewise, the LDA algorithm's training time dropped from 6.82 seconds to 1.15 seconds, and the SVM algorithm demonstrated a reduction from 10.95 seconds to 3.39 seconds. The KNN algorithm also benefited, with training time decreasing from 9.22 seconds to 1.35 seconds. Among the evaluated algorithms, the KNN algorithm exhibited the most significant percentage reduction, achieving an 85.36% decrease due to its algorithmic characteristics. These findings underscore the consistent benefits of feature selection in reducing computational demands across different algorithms and movement types.

For combined movement, the impact of feature selection was mixed, with reductions observed in some algorithms and increases in others. The DT algorithm achieved a substantial reduction, with training time dropping from 15.82 seconds to 7.22 seconds, representing a 37.33% decrease. Similarly, the SVM algorithm's training time was reduced from 15.99 seconds to 9.40 seconds. However, not all algorithms exhibited improvements. The KNN algorithm experienced an increase in training time, rising from 12.68 seconds to 14.55 seconds, likely due to the heightened computational demands of distance calculations in a reduced feature space. Similarly, the LDA algorithm showed a significant increase in

training time, from 6.56 seconds to 10.71 seconds, potentially reflecting its sensitivity to feature transformations. Despite these anomalies, the DT algorithm remained the most efficient, achieving the largest training time reduction among the algorithms evaluated. Overall, these results highlight the importance of selecting the most relevant features to enhance computational efficiency and optimize model performance. Nevertheless, the findings also reveal that the impact of feature selection may vary depending on the structure and computational requirements of the algorithm, emphasizing the need to consider algorithm-specific behaviors when implementing feature selection strategies.

Table 4.9 Training Time of All Algorithm with All Features and Significant Features for Flexion, Extension and Combined Movement

Model	Algorithm	Training Time (seconds)		Percentage Difference (%)
		All Features	Significant Features	
Flexion	DT	4.27	3.24	24.12
	LDA	1.13	0.91	19.47
	SVM	4.35	3.75	13.79
	KNN	3.03	2.46	18.81
Extension	DT	10.24	3.31	67.68
	LDA	6.82	1.15	83.14
	SVM	10.95	3.39	69.04
	KNN	9.22	1.35	85.36

Table 4.9 Training Time of All Algorithm with All Features and Significant Features for Flexion, Extension and Combined Movement (cont.)

Model	Algorithm	Training Time (seconds)		Percentage Difference (%)
		All Features	Significant Features	
Combined	DT	15.82	7.22	37.33
	LDA	6.56	10.71	24.03
	SVM	15.99	9.40	25.96
	KNN	12.68	14.55	21.58

Based on the results for all movements, machine learning models trained on datasets with significant features identified through a one-way MANOVA test consistently showed higher accuracy across all data split tests compared to those using all available features except for extension movement. The improved performance underscores the impact of feature selection on model effectiveness, as statistically significant features often enhance accuracy by reducing dimensionality and isolating the most relevant characteristics (Maiwan Bahjat Abdulrazzaq & Jwan Najeeb Saeed, 2019; Padmaja & Vishnuvardhan, 2016). The selection of meaningful attributes plays a crucial role in improving both accuracy and computational efficiency. Furthermore, the efficacy and efficiency of a machine learning solution are contingent upon the inherent qualities and attributes of the data, as well as the proficiency of the learning algorithms (Sarker, 2021). Among the algorithms, KNN exhibited the highest accuracy across all datasets. The KNN classifier proves to be the optimal method for classifying biomechanical parameter features, particularly in scenarios with limited datasets and low dimensionality (Seth et al., 2015; Sharma & Sharma, 2016). For flexion movements, selecting a model trained on significant

features would be the preferred approach, as a refined feature set enables a more efficient and accurate spasticity assessment. However, an analysis of extension movement models indicates that more complex dynamics are involved, as higher accuracy was achieved when all available features were included. For extension movement, the comparison of two models with varying feature sets indicates that the movements exhibit more complex dynamics, as demonstrated by the enhanced accuracy achieved by the inclusion of all features. The necessity of a broader set of characteristics for extension movements suggests that additional parameters are essential to accurately capture intricate patterns and interactions, ultimately enhancing predictive capabilities for spasticity levels. When evaluating combined movements, models trained on significant features demonstrated improved accuracy, confirming that the refined feature set effectively characterizes spasticity across different movement types. The integration of relevant attributes into classification models enhances both accuracy and efficiency, particularly when assessing spasticity across multiple movement patterns. However, omitting essential attributes during feature selection for extension movements risks excluding critical information, potentially reducing predictive performance (Zebari et al., 2020). Incorporating a comprehensive range of biomechanical characteristics strengthens the model's ability to capture meaningful interactions, ensuring reliable and holistic predictions of spasticity levels.

4.5 EVALUATION OF MACHINE LEARNING MODELS

This subchapter presents the results of the k-fold cross-validation conducted for the flexion and extension movements, which were selected based on their superior accuracy performance compared to the combination movement. Only flexion and extension underwent training and evaluation using k values of 5, 10, and 15 to ensure a thorough assessment of the models' reliability and generalisability. The combination movement was excluded from this analysis due to its comparatively lower accuracy, which did not meet the criteria for effective cross-validation. By focusing on flexion and extension, the

research highlights the robustness of these movements in supporting machine learning model development and evaluation.

The KNN algorithm was evaluated using significant features with a 90/10 split and k-fold cross-validation testing k values of 5, 10, and 15 with different measure distance such as Euclidean, Cosine and Correlation. This methodology enabled a thorough evaluation of the performance of KNN algorithm by dividing the dataset into k subsets, or folds, in a systematic manner. The algorithm underwent k-fold cross-validation, where it was trained and tested k times. In each iteration, a different fold was used as the validation set, while the remaining k-1 folds were utilised for training. Varying the value of k allowed for an examination of the models' stability and robustness across different partitioning schemes, providing a thorough evaluation of their predictive capabilities and overall performance in diverse scenarios. Table 4.10 presents a comparison of the KNN algorithm's accuracy in classifying spasticity levels based on MAS output for both flexion and extension movements.

Table 4.10 Performance of KNN Algorithm with Different Value of K-Folds for Flexion and Extension Movements

Model	k-folds	Measure Distance	Accuracy (%)	Precision (%)	Recall (%)	F1-Score (%)
Flexion	5	Euclidean	90.12	90.85	90.12	90.08
		Cosine	88.89	90.53	88.89	89.39
		Correlation	88.89	90.06	88.89	89.21

Table 4.10 Performance of KNN Algorithm with Different Value of K-Folds for Flexion and Extension Movements (cont.)

Model	k-folds	Measure Distance	Accuracy (%)	Precision (%)	Recall (%)	F1-Score (%)
Flexion	10	Euclidean	88.89	90.74	88.89	89.53
		Cosine	87.65	89.33	87.65	88.07
		Correlation	85.19	87.59	85.19	85.80
	15	Euclidean	91.29	91.94	91.25	91.47
		Cosine	87.50	89.22	87.50	87.80
		Correlation	88.75	91.06	88.75	89.32
Extension	5	Euclidean	90.12	90.32	90.12	90.12
		Cosine	88.89	89.11	88.89	88.81
		Correlation	92.59	92.81	92.59	92.55
	10	Euclidean	88.89	89.44	88.89	89.00
		Cosine	91.36	91.36	91.36	91.36
		Correlation	91.36	91.38	91.36	91.27
	15	Euclidean	96.30	96.53	96.30	96.33
		Cosine	95.06	95.23	95.06	95.09
		Correlation	95.06	95.23	95.06	95.09

For flexion movement, the accuracy of the KNN algorithm decreased as the number of folds increased from 5 to 10 when using Euclidean and Correlation distance measures. However, accuracy improved significantly when the number of folds reached 15. In contrast, accuracy declined with the increasing value of k when using Cosine distance. The optimal accuracy of 91.29% was achieved with k = 15 and Euclidean distance. Similarly, for extension movements, the KNN algorithm showed comparable results. The accuracy also decreased as the number of folds increased from 5 to 10 with Euclidean and Correlation distance metrics but improved with k = 15. For Cosine distance, accuracy improved as k increased. The highest accuracy of 96.30% was achieved with k = 15 and Euclidean distance. To further illustrate the evaluation of the KNN classifier, bar charts were constructed to visualize the classification performance across different values of k and distance metrics. Figures 4.18 and 4.19 show the classification accuracy of the KNN model for flexion and extension movements, respectively. Each bar represents the classification accuracy corresponding to a specific combination of k and distance metric.

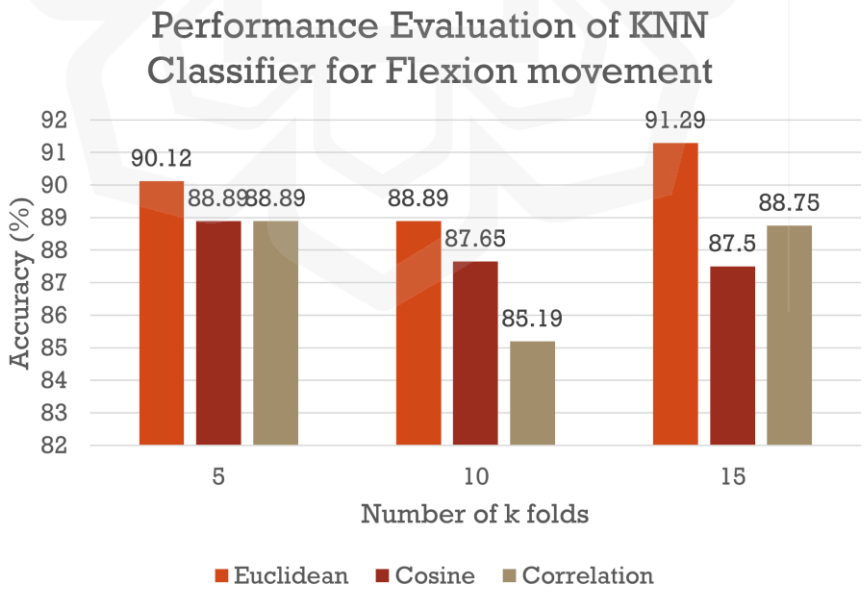

Figure 4.18 Classification accuracy of KNN model for flexion movement using different values of k and distance metrics.

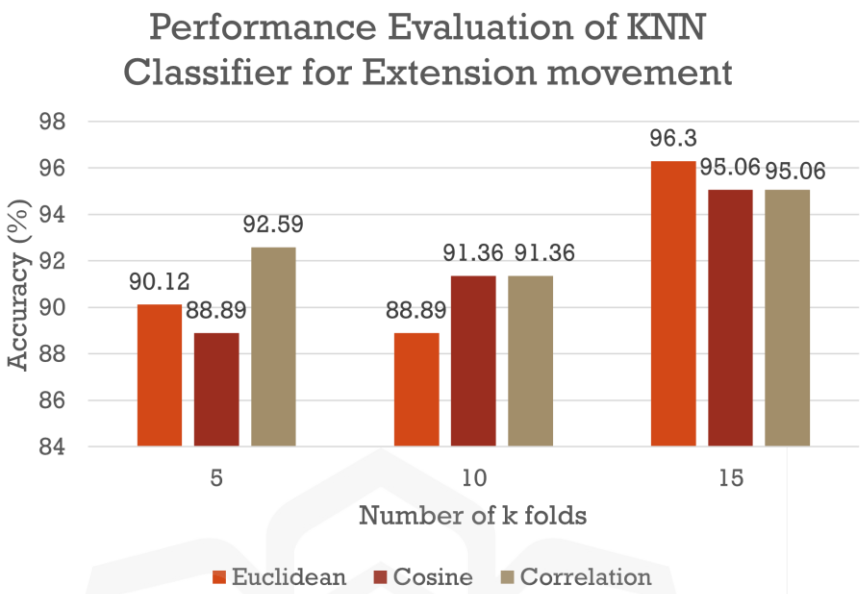

Figure 4.19 Classification accuracy of KNN model for extension movement using different values of k and distance metrics.

In addition to accuracy, precision, recall, and F1-score were also computed to provide a more detailed understanding of the classifier's performance. For flexion movement, precision values remained consistently high across all configurations, with the highest precision of 91.94% recorded using Euclidean distance at k = 15. This indicates that the classifier was highly effective in minimizing false positives in spasticity classification. Recall, which measures the model's ability to detect true positive cases, followed a similar trend. The highest recall of 91.25% was also observed with Euclidean distance at k = 15, suggesting that the classifier was effective in correctly identifying subjects across MAS level. The F1-score, which combines both precision and recall into a single metric, reached a peak value of 91.47% for the same configuration. For extension movement, the KNN classifier exhibited even higher performance levels. The best results were observed at k = 15 using Euclidean distance, yielding the highest accuracy of 96.30%. Precision and recall also peaked at 96.53% and 96.30% respectively, resulting in a maximum F1-score of 96.33%. Cosine and Correlation distances also produced competitive

metrics at this fold count, both reaching accuracy scores of 95.06% and identical precision, recall, and F1-scores of 95.23%, 95.06%, and 95.09%, respectively. However, Euclidean distance consistently outperformed the other measures across all metrics. These findings suggest that the classifier performed more effectively in extension movements than in flexion movements, particularly when optimized with Euclidean distance and higher k-fold values. While Cosine and Correlation distances offered reliable alternatives, Euclidean distance demonstrated the most stable and superior results in both movement categories. The inclusion of precision, recall, and F1-score alongside accuracy confirms the robustness and consistency of the KNN classifier under optimal configurations, especially in its ability to balance false positives and false negatives across different types of joint movement.

In both flexion and extension movements, no direct correlation was observed between adjusting the value of k in k-fold cross-validation and the accuracy of the machine learning algorithms (Nti et al., 2021). Choosing the value of k requires careful consideration: a lower k value reduces computing costs and variance but increases bias, whereas a larger k value increases computational demand while reducing bias and increasing variability. Thus, the selection of k must strike a balance, ensuring that the validation set size is sufficient for reliable model performance assessment. In terms of distance metrics, Euclidean distance consistently yielded superior accuracy compared to Cosine and Correlation metrics. Euclidean distance is particularly well-suited for datasets like muscle vibration data, which often exhibit linear relationships. This metric remains effective in low-dimensional spaces, mitigating the "curse of dimensionality" and providing resilience to noise. These advantages establish Euclidean distance as an optimal choice for spasticity assessment based on muscle vibration data, facilitating accurate machine learning classification of spasticity levels during both flexion and extension movements.

4.5.1 Inter- and Intra-Rater Reliability Results of the QSAT Platform in Comparison with the Modified Ashworth Scale (MAS)

This subsection presents a comparison between the computational model developed in this study and the conventional MAS used in clinical settings. Performance analysis using the KNN algorithm demonstrated high classification accuracy for both flexion (91.29%) and extension (96.30%) movements when configured with 15-fold cross-validation and Euclidean distance. To further evaluate the robustness of the QSAT system, a dedicated inter and intra rater reliability study was conducted. Moreover, precision, recall, and F1-scores exceeded 91% in both movements, demonstrating high reliability in detecting spasticity across MAS grades.

To further evaluate the robustness of the QSAT system, a dedicated inter- and intra-rater reliability study was conducted involving two experienced physiotherapists and the QSAT model across 30 patients. Figures 4.20 and 4.21 illustrate the distribution of MAS level for 30 patients as recorded by two experienced physiotherapists and predicted by the QSAT model for both flexion and extension movements, respectively. As the second trial produced identical results to the first across all raters and the QSAT model, only the first trial results are presented in Figures 4.18 and 4.19 to avoid redundancy and maintain clarity. In both figures, the absence of coloured bars for a given patient indicates that a MAS level of 0 was assigned by the corresponding therapist, signifying no abnormal increase in muscle tone.

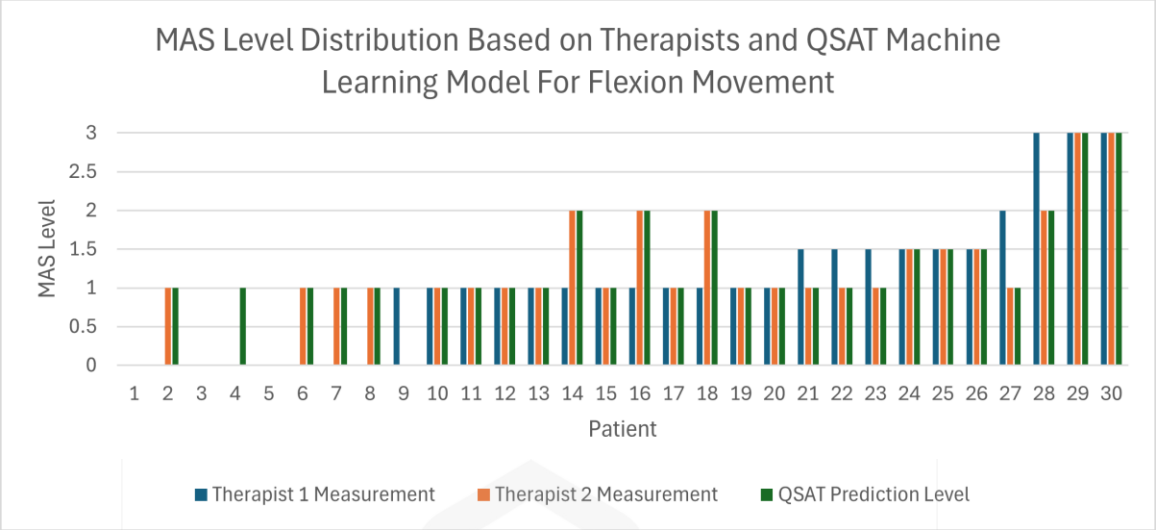

Figure 4.20 MAS Level Distribution Based on Therapists and QSAT Machine Learning Model for Flexion Movement (First Trial)

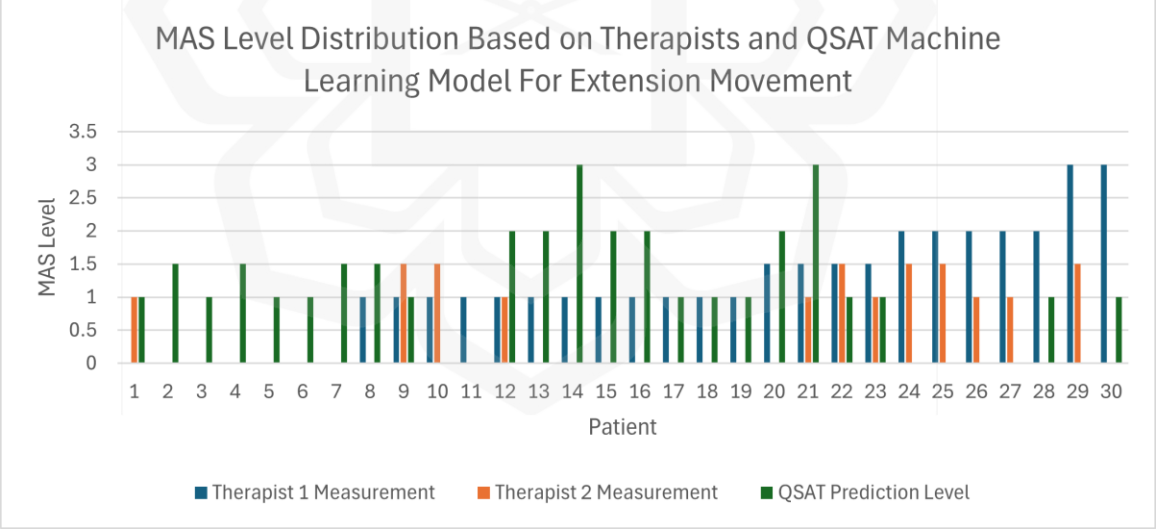

Figure 4.21 MAS Level Distribution Based on Therapists and QSAT Machine Learning Model for Extension Movement (First Trial)

As shown in Figure 4.18, the QSAT model's predictions (green bars) closely aligned with those of both therapists (blue and orange bars) across most patients, particularly for MAS levels 0 and 1. Notable variation between therapist assessments is observed in higher MAS levels (Patients 14–16 and 28–30), where one therapist assigned different scores than the other. In contrast, the QSAT model provided consistent classifications across all cases, highlighting its stability and objectivity. Figure 4.19 presents the distribution for extension movement. Compared to flexion, greater variability is evident between therapist ratings, particularly in patients 20 to 30. Therapist 1 recorded MAS levels of 2 or 3 in several cases, while Therapist 2 assigned lower or zero values. Despite these inconsistencies, the QSAT model predictions remained stable across all patients, reinforcing its measurement consistency. These findings are further substantiated in Table 4.11, which summarises the inter- and intra-rater reliability results for both clinical MAS assessments and the QSAT model. For flexion movement, the clinical MAS assessment yielded a moderate inter-rater agreement with a Cohen's Kappa (k) value of 0.391, while for extension, the inter-rater agreement was poor, with a Kappa of only 0.057. In contrast, the QSAT model achieved a perfect inter-rater agreement (k = 1.000) in both flexion and extension evaluations. Similarly, intra-rater reliability for the QSAT model was also perfect (k = 1.000), whereas the clinical MAS assessments showed variability depending on the rater and session. These results underscore the superior consistency and reliability of the QSAT platform in comparison to traditional MAS assessments. The quantitative nature of the system eliminates subjectivity, standardizes data interpretation, and reduces the risk of assessor bias.

Table 4.11 Inter- and Intra-Rater Reliability Comparison between MAS and QSAT Model for Flexion and Extension Movements

Model	Reliability Types	Rater	Kappa (K)	Standard Error	T Value	P Value
Flexion	Inter Rater	Therapist 1 vs. Therapist 2	0.391	0.073	6.894	< 0.01
		QSAT Machine Learning Model	1.000	0.000	16.426	< 0.01
	Intra Rater	Therapist 1 (Trial 1 vs. Trial 2)	1.000	0.000	16.146	< 0.01
		Therapist 2 (Trial 1 vs. Trial 2)	1.000	0.000	16.441	< 0.01
		QSAT Machine Learning Model (Trial 1 vs. Trial 2)	1.000	0.000	16.426	< 0.01
Extension	Inter Rater	Therapist 1 vs. Therapist 2	0.057	0.054	1.038	0.299
		QSAT Machine Learning Model	1.000	0.000	17.091	< 0.01

Table 4.11 Inter- and Intra-Rater Reliability Comparison between MAS and QSAT Model for Flexion and Extension Movements (cont.)

Model	Reliability Types	Rater	Kappa (K)	Standard Error	T Value	P Value
Extension	Intra Rater	Therapist 1 (Trial 1 vs. Trial 2)	1.000	0.000	17.108	< 0.01
		Therapist 2 (Trial 1 vs. Trial 2)	1.000	0.000	12.996	< 0.01
		QSAT Machine Learning Model (Trial 1 vs. Trial 2)	1.000	0.000	17.091	< 0.01

Although the QSAT platform demonstrated strong classification accuracy and perfect inter- and intra-rater agreement, certain discrepancies between its predictions and the therapists' MAS scores were observed in a few cases. These inconsistencies can be attributed to multiple factors. Firstly, the MAS inherently involves a degree of subjectivity, particularly at intermediate spasticity levels such as MAS 1+ and 2, where therapists may interpret muscle resistance differently based on experience, technique, or patient cooperation. Secondly, the MAS is based on qualitative criteria that lack precise biomechanical thresholds, increasing variability in human scoring. In contrast, the QSAT system relies on quantitative MMG signal features, which may capture muscular activity not readily perceived through manual assessment. Conversely, in some cases, the MMG sensors might not detect nuanced variations that therapists feel during passive movement, such as sudden muscle catches or subtleties in velocity-dependent resistance. Furthermore, slight physiological fluctuations in patients—such as fatigue, anxiety, or reflex sensitivity—can influence both therapist perception and sensor readings, leading to

potential mismatches. Lastly, as with all machine learning-based models, even high-performing algorithms may occasionally misclassify due to feature overlaps or insufficient representation of rare patterns in the training data. Nonetheless, the consistency and objectivity demonstrated by QSAT reinforces its utility as a reliable and reproducible tool to complement traditional therapist-based evaluations.

In conclusion, while the MAS remains the prevailing tool for clinical spasticity assessment, the results of this study highlight its limitations, particularly in terms of inter-rater consistency. The QSAT platform addresses these issues by providing a repeatable, quantitative, and reliable approach to spasticity classification. The high agreement observed across trials, combined with strong classification performance, supports the QSAT model's role as a complementary tool to enhance the objectivity of clinical assessments and improve the accuracy of rehabilitation planning.

4.6 SUMMARY

Chapter 4 highlights the findings and analysis of the research, concentrating on the data gathering methodologies, and the developing of predictive models for the assessment of muscular spasticity, and the evaluation of high-performing models with superior accuracy. The chapter begins with an overview of the frequency of patient participation in the research, followed by an introduction to the clinical data gathering method, which encompasses pre-processing procedures and the selection of movements for analysis. The chapter then delves into the statistical analysis and feature selection process, highlighting the critical biomechanical features associated with flexion and extension movements. The distinctions between flexion and extension are highlighted, along with their relevance to spasticity, while findings are generalized across various muscle movements by integrating datasets. This approach accounts for the unique biomechanical and physiological

characteristics of flexion and extension, which can significantly influence MMG signal patterns. Descriptive statistics for both healthy individuals and stroke patients with MAS 0 are presented, followed by comparative research of MMG signals at varying MAS levels during flexion and extension movements of the biceps and triceps muscles. The machine learning model was developed to systematically map the intricate characteristics of spasticity in the musculature under examination, encompassing both flexion and extension movements. Additionally, a combined movement analysis was incorporated to leverage their complementary features, further enhancing the model's ability to accurately capture and predict spasticity patterns. The chapter then examines the evolution of predictive machine learning models, detailing the selection of suitable algorithms for flexion and extension movements, as well as for the combined analysis of both. This comprehensive evaluation highlights the distinct and complementary features of each movement type and demonstrates how integrating them can enhance the overall predictive accuracy and robustness of the models. The chapter concludes by assessing the efficacy of these models in categorising spasticity severity, emphasising their generalisability across various MAS levels throughout both types of movement. Following this, inter- and intra-rater reliability assessments were conducted to evaluate the clinical reliability of the QSAT system. These assessments involved comparing the consistency of spasticity ratings generated by the QSAT platform with those obtained through conventional MAS evaluations. This step was essential in demonstrating the repeatability and objectivity of the QSAT system across different raters and repeated assessment sessions, thereby strengthening the clinical validity and potential for real-world implementation.

CHAPTER FIVE

CONCLUSION AND RECOMMENDATION

5.1 CONCLUSION

The integration of the Modified Ashworth Scale (MAS) using computational method into the Quantitative Spasticity Assessment Technology (QSAT) represents a substantial advancement in the objective evaluation of muscle spasticity levels within the affected upper limb. This significant advancement highlights QSAT's aim to establish a standardised system for the thorough evaluation of spasticity, therefore improving objectivity and accuracy in the measurement process. Through a systematic and standardised approach, QSAT facilitates the discernment of subtle variations in muscle characteristics, further contributing to the refinement and accuracy of the spasticity evaluation.

A comprehensive literature review was conducted to identify the most reliable, widely used neurological assessment techniques employed by therapists. Among the available tools, the MAS emerged as the most effective due to its high reliability in evaluating upper extremities and its ease of use. However, MAS is solely offering a subjective evaluation of spasticity, reliant on the therapist's interpretation of resistance to passive stretching which makes the measurement not consistent and accurate. The research aims to address the gap by providing an objective assessment of spasticity levels based on the MAS framework utilising the Mechanomyography (MMG) signal. Machine learning techniques offer a robust solution for categorising spasticity severity by analysing biomechanical features in alignment with the MAS criteria. The integration of this data-driven approach enhances existing subjective assessment methods, ensuring a more precise and reliable evaluation of spasticity.

The primary aim of this research is to develop a novel muscle spasticity model using the QSAT platform for more accurate assessments. Data was gathered from neurological disorder patients through the platform, and these data signals were utilised to model spasticity severity using the MAS tool. This process led to the development of two distinct models, one designed for flexion and another for extension movements. The biomechanical data collected throughout the research played a crucial role in constructing a machine learning model capable of predicting the severity of spasticity in limbs affected by neurological disorders. Ultimately, the developed model offers a more reliable and objective method for assessing spasticity, providing significant improvements over existing subjective evaluation techniques.

5.2 MAJOR OUTCOMES AND CONTRIBUTION

5.2.1 Innovative Perspectives in Research

This research contributes significantly to quantitative spasticity assessment, which is a critical area in the field of computing. By employing machine learning techniques on Mechanomyography signals, the research proposes a quantitative and unbiased framework for assessing muscle spasticity. The proposed methodology is particularly relevant for computing applications, where accurate and automated evaluations play a vital role in facilitating effective interaction with the physical environment.

The research establishes a muscle spasticity model that bridges the gap between biomechanical signals and computational analysis. Significant features extracted from MMG signals, such as root mean square (RMS), mean average value (MAV), peak-to-peak amplitude (PTP), mean power frequency (MPF), median frequency (MF), Standard Deviation (SD), Skewness (S) and Kurtosis (K) are aligned with key principles of

movement analysis. The integration of these features enhances the predictive capabilities of the model, facilitating application in clinical contexts, even though evaluation occurs offline rather than in real-time.

The development of systems for healthcare and rehabilitation depends on the integration of sensors and data processing techniques. The research contributes to that goal by employing tri-axial accelerometer mechanomyography (ACC-MMG) sensors and potentiometer to collect detailed muscle movement data during the assessment. Although the platform does not involve actuators, the proposed Quantitative Spasticity Assessment Technology (QSAT) platform exemplifies a well-designed system for offline data analysis, enabling accurate spasticity assessments based on pre-recorded data.

Moreover, the spasticity assessment tool integrated within the QSAT platform emphasizes the relationship between physical muscle movement and its computational analysis in a standardised and objective manner. Although the developed model operates offline, the approach offers a thorough understanding of muscle spasticity through data-driven methods, contributing to improved spasticity assessment in clinical environments. The insights gained from this work will inform the development of future tools aimed at providing more precise and consistent evaluations of spasticity in patients with neurological disorders.

5.2.2 Impact on Society and Economy

The data obtained from the QSAT platform serves as the foundation for developing a robust muscle spasticity model using machine learning techniques. By analysing the MMG signals and biomechanical data captured during assessments, machine learning algorithms can identify patterns and relationships between these features and the severity of spasticity, as

measured by the Modified Ashworth Scale (MAS). This approach facilitates the creation of an accurate and predictive model that systematically maps spasticity levels, enabling therapists to classify and quantify muscle spasticity objectively. The integration of machine learning into the QSAT platform not only enhances the precision of spasticity assessments but also provides valuable insights for tailoring treatment strategies, ultimately advancing personalised rehabilitation approaches.

Economically, the implementation of the proposed QSAT platform can lead to cost savings in healthcare. Accurate and automated evaluations of muscle spasticity may reduce the need for prolonged therapy sessions, minimising the overall healthcare costs associated with rehabilitation. Additionally, utilising the platform enhances spasticity assessments, contributing to faster recovery times and enabling patients to return to daily activities more quickly, thereby improving productivity and participation in the workforce. Moreover, the implementation of advanced assessment technology in clinical settings may stimulate innovation within the healthcare sector. With the rising demand for more effective diagnostic instruments, investments in research and development are expected to expand, hence promoting economic growth and job creation in medical technology and rehabilitation services. The implications of this research extend beyond muscular spasticity assessment, potentially transforming social perceptions of neurological illnesses and improving cost efficiencies within the healthcare system. Establishing a comprehensive framework for assessing spasticity facilitates breakthroughs in neurorehabilitation, ultimately enhancing the quality of life for individuals affected by neurological diseases.

5.2.3 Achievement of Research Objectives

To enhance the clarity and alignment between the research objectives and the outcomes, this section provides a structured summary that explicitly references the objectives

established in Chapter 1 (Section 1.3). Each objective is revisited and linked to the respective achievements and key findings derived from the experimental procedures, statistical analyses, and model evaluations. The table below also reflects on the overall contribution of this research to both academic knowledge and practical applications in neurorehabilitation.

Table 5.1 Summary of Research Objectives, Achievements, and Contributions

Objective	Achievement	Contribution to Knowledge and Society
To identify significant features in time domain from the MMG signal of the forearm musculature.	Significant time-domain features such as RMS, MAV, PTP, SD, Skewness, and Kurtosis were extracted from biceps and triceps MMG signals in *x*, *y*, and *z* axes. Statistical validation using one-way MANOVA identified features strongly correlated with MAS levels.	Established a foundation of reliable, biomechanical signal features relevant for spasticity analysis. This supports the advancement of objective, signal-based diagnostic tools in clinical settings.

Table 5.1 Summary of Research Objectives, Achievements, and Contributions (cont.)

Objective	Achievement	Contribution to Knowledge and Society
To develop a muscle spasticity model of neurological disorder patients using machine learning.	A classification model using the KNN algorithm was developed to map MMG signal features to MAS scores. The model was trained and validated for flexion, extension, and combined movements using cross-validation techniques.	Demonstrated the feasibility of integrating computational intelligence with MMG for automated spasticity evaluation, offering a complementary approach to conventional therapist-based assessments.
To evaluate the performance of the muscle spasticity model for neurological disorder patients.	The model was evaluated using metrics such as accuracy, precision, recall, and F1-score under varying k-fold cross-validation settings and distance measures. The highest performance was achieved during extension movement with 96.30% accuracy, 96.53% precision, 96.30% recall, and 96.33% F1-score using Euclidean distance and k = 15.	Validated the robustness, accuracy, and clinical potential of MMG-based assessment models. The high performance suggests the model's suitability for objective decision support in clinical rehabilitation environments.

These outcomes confirm that all research objectives were successfully achieved. The identification of statistically significant MMG features enabled the construction of reliable input variables for spasticity modelling. The development and evaluation of machine learning classifiers demonstrated that spasticity levels, as measured by the Modified Ashworth Scale, can be objectively predicted using MMG signal characteristics. Furthermore, the adoption of stratified k-fold cross-validation, multiple train-test splits, and statistical dimensionality reduction techniques strengthened the model's robustness and generalisability, mitigating overfitting risks. In terms of contribution, this study provides a practical framework for integrating MMG and machine learning into clinical workflows, offering an alternative to subjective evaluation methods. It enhances the objectivity, consistency, and traceability of spasticity assessment, which is vital in stroke rehabilitation and neurorehabilitation practices. Moreover, the findings contribute to the existing body of knowledge by demonstrating the viability of MMG as a quantitative tool for muscle condition evaluation and by laying the groundwork for future expansion into real-time assessment and IoT-based clinical applications.

5.2.4 List of Publication

1. Daud, M. a. I., Puzi, A. A., Sidek, S. N., Zainuddin, A. A., Khairuddin, I. M., & Mutalib, M. a. A. (2025). Quantitative Measurement of Muscle Spasticity for Neurological Disorders Using Mechanomyography: A Statistical Analysis. *Jurnal Kejuruteraan 37(5)* (Accepted and Publish in September 2025).
2. Puzi, A. A., Daud, M. a. I., Sidek, S. N., Zainuddin, A. A., Khairuddin, I. M., & Mutalib, M. a. A. (2025). Evaluating the Reliability of Mechanomyography in Muscle Spasticity: Inter and Intra-Rater Consistency in Flexion and Extension Movements with Machine Learning Model. Journal of Information Systems Engineering & Management, 10(29s), 338–348.
3. Daud, M. a. I., Puzi, A. A., Sidek, S. N., Khairuddin, I. M., & Mutalib, M. a. A. (2025). Performance Analysis of Quantitative Muscle Spasticity Model in Flexion

and Extension Passive Movements, 2025 21st IEEE International Colloquium on Signal Processing & Its Applications (CSPA), Pulau Pinang, Malaysia, pp. 134-139.

4. Daud, M. a. I., Puzi, A. A., Sidek, S. N., Zainuddin, A. A., Khairuddin, I. M., & Mutalib, M. a. A. (2024). Leveraging Mechanomyography Signal for Quantitative Muscle Spasticity Assessment of Upper Limb in Neurological Disorders Using Machine Learning. *International Journal of Advanced Computer Science and Applications*, *15*(8). https://doi.org/10.14569/ijacsa.2024.0150898
5. Daud, M. a. I., Puzi, A. A., Sidek, S. N., Hassan, S. a. A., Zainuddin, A. A., Khairuddin, I. M., & Mutalib, M. a. A. (2024). Mechanomyography in Assessing Muscle Spasticity: A Systematic Literature Review. *journal.ump.edu.my. https://doi.org/10.15282/mekatronika.v6i1.10204*
6. Daud, M. a. I., Puzi, A. A., Sidek, S. N., Hassan, S. a. A., Zainuddin, A. A., Khairuddin, I. M., & Mutalib, M. a. A. (2024a). Recent studies of Human Limbs Rehabilitation Using Mechanomyography Signal: A survey. In *Lecture notes in networks and systems* (pp. 263–273). https://doi.org/10.1007/978-981-99-8819-8_21
7. Daud, M. a. I., Puzi, A. A., Sidek, S. N., Khairuddin, I. M., & Mutalib, M. a. A. (2024). Formulation of Muscle Spasticity Characteristics Model for Quantifying the Clinical Assessment of Neurological Disorder Patients. *Postgraduate Colloquium 2024: Innovating for a Sustainable Future: Interdisciplinary Approaches in the Digital Era* (pp. 9–13).

5.2.5 List of Copyright

1. Quantitative Spasticity Assessment Technology (QSAT) Design and Development
2. Quantitative Spasticity Assessment Technology (QSAT) Data Collection Procedure

5.2.6 List of Award

1. Platinum Award (Special Award) for International Grand Invention, Innovation, and Design Expo (IGIIDeation) 2025
2. Gold Award for International Grand Invention, Innovation, and Design Expo (IGIIDeation) 2025
3. Best Paper Award at the 2025 21st IEEE International Colloquium on Signal Processing & Its Applications (CSPA2025)
4. Gold Award, Johor International Innovation Invention Competition and Symposium (JIIICaS 2024)
5. Best Presenter Award for the category "Master's Programme" of Postgraduate Colloquium 2024 (IIUM Gombak Campus)
6. Gold Award (International Jasin Multimedia & Computer Science Invention and Innovation Exhibition (i-JaMCSIIX) 2023)

5.3 LIMITATION OF RESEARCH

While the research highlights the promise of mechanomyography (MMG) in assessing muscular spasticity, it is essential to recognize several limitations that may affect the findings. First, although MMG is proficient in measuring muscle vibrations within the frequency range of 2 to 100 Hz, enhancing the sampling rate could lead to greater accuracy in data acquisition. Higher sampling rates would allow for a more detailed capture of intricate muscle signal characteristics, ultimately improving the precision of assessments and deepening our understanding of spasticity.

Additionally, the analysis primarily focuses on temporal domain features. While these features provide valuable insights, they may not encompass the full spectrum of

complexities inherent in MMG signals. In contrast, incorporating frequency domain features could uncover additional patterns and behaviors that remain hidden in temporal analyses. By integrating frequency domain analysis, the research could achieve a more comprehensive and accurate representation of muscle vibrations, which would likely enhance model performance and yield more reliable spasticity assessments. Moreover, the current research's scope is limited to a specific patient population, which may affect the generalizability of the results. Although the sample size was determined using G*Power analysis to ensure sufficient statistical power, the number of recruited patients remains a limitation. A larger and more diverse sample, encompassing various demographics and clinical conditions, would strengthen the validation of the findings and improve the robustness of the developed assessment models.

Furthermore, the current version of the QSAT platform operates through Python-based scripts without a dedicated graphical user interface (GUI), which may pose a challenge for immediate clinical adoption. While the data collection and analysis processes are technically functional and yield accurate results under controlled conditions, they require a level of technical proficiency that may not be practical in many clinical settings. The absence of a user-friendly interface could hinder widespread use by therapists unfamiliar with programming environments or command-line tools. This gap limits the platform’s ease of integration into typical clinical workflows. Addressing this limitation by developing a dedicated interface or dashboard in future work would enhance the platform's accessibility, simplify data interpretation, and promote seamless adoption in rehabilitation clinics and hospitals.

Lastly, another key limitation is the absence of formal validation through direct consultation with medical professionals. Although the machine learning predictions aligned with MAS-based classifications and were evaluated using statistical metrics such as accuracy, precision, and recall, the findings were not reviewed or interpreted by clinical experts such as neurologists or physiotherapists. This lack of expert validation limits the ability to confirm whether the model's outputs are clinically meaningful and applicable in

real-world rehabilitation scenarios. Incorporating expert consultation would strengthen the clinical reliability of the system and ensure that model outputs align with the nuanced judgments made by experienced clinicians.

In summary, while the research contributes significantly to the understanding of MMG in evaluating spasticity, overcoming the identified limitations in future studies will be crucial for advancing the field and improving the clinical applicability of MMG.

5.4 RECOMMENDATION

An accurate evaluation of muscle spasticity is crucial for the effective management and therapy of neurological disorders in patients. While MMG holds promise for evaluating spasticity, its current applications predominantly depend on the extraction of time-domain features from MMG data. To fully optimise the potential of MMG and improve its practical applicability in clinical environments, next research should focus on three essential areas of advancement.

First, the exploration of advanced optimization techniques and ensemble learning methods can significantly enhance the accuracy and reliability of predictive models used in spasticity evaluation. Techniques such as hyperparameter tuning, ensemble learning, and deep learning approaches offer promising opportunities to improve the interpretation of MMG data. Specifically, ensemble methods such as bagging, boosting, and stacking can combine the predictions of multiple algorithms to reduce variance, mitigate overfitting, and enhance the overall predictive performance. Implementing these strategies has the potential to improve the model's ability to generalize across different patient populations and clinical environments, thereby increasing the robustness of spasticity assessments.

Second, the integration of deep learning methodologies, such as convolutional neural networks (CNNs) and recurrent neural networks (RNNs), may facilitate the automated extraction of complex and relevant features from MMG signals. The implementation of these models has demonstrated great effectiveness in biomedical signal processing, particularly in identifying intricate patterns and relationships that may be overlooked by traditional feature extraction methods. Incorporating such advanced techniques would allow for a more nuanced and precise analysis of the MMG signals, which could lead to improved predictions of spasticity levels.

Third, the research primarily relied on time-domain features derived from MMG signals. However, there is significant potential to enhance model performance by employing more sophisticated feature engineering methods. Increasing the sampling rate of MMG data would allow for the capture of more detailed signal characteristics, enabling the use of frequency-domain extraction techniques. Implementing frequency-domain analysis could provide a more comprehensive evaluation of MMG signals, potentially uncovering features that remain undetectable through time-domain analysis alone.

Fourth, the current QSAT platform lacks a graphical user interface (GUI), which may limit its ease of use and accessibility in clinical settings. To facilitate broader adoption by healthcare professionals, future development should focus on creating a user-friendly interface that enables therapists to interact with the system without requiring programming knowledge. A GUI would streamline patient data entry, visualize MMG signal activity in real-time, and generate automated assessment reports. By improving usability and integration into clinical workflows, the addition of a GUI would greatly enhance the system's practicality and impact in rehabilitation environments.

Finally, future studies should incorporate formal validation of the model predictions through structured consultation with medical experts, such as neurologists, physiatrists, and certified physiotherapists. These consultations would serve to verify the clinical relevance

of the predicted MAS classifications and offer critical feedback on the interpretability of the extracted features. Expert input would ensure that the model outputs align with real-world diagnostic criteria and clinical observations, thereby reinforcing the reliability and applicability of MMG-based systems in patient care. Incorporating expert review into the evaluation process would also strengthen the overall clinical confidence in the system and support its adoption in multidisciplinary rehabilitation settings.

In conclusion, future research should explore advanced methodologies to augment the clinical utility of MMG in the objective assessment of muscle spasticity. By incorporating optimization techniques, ensemble learning, and deep learning models, the precision and reliability of spasticity evaluations can be significantly improved, paving the way for more accurate and dependable clinical assessments.

REFERENCES

Ahuja, C. S., Wilson, J. R., Nori, S., Kotter, M. R. N., Druschel, C., Curt, A., & Fehlings, M. G. (2017). Traumatic spinal cord injury. In *Nature Reviews Disease Primers* (Vol. 3).

Akkaya, K. U., & Elbasan, B. (2021). Acute effects of intramuscular stretching and passive stretching on spasticity in children with cerebral palsy. *Turkish Journal of Physiotherapy and Rehabilitation*, *32*(1), 60–66.

Akpinar, P., Atici, A., Ozkan, F. U., Aktas, I., Kulcu, D. G., Sarl, A., & Durmus, B. (2017). Reliability of the Modified Ashworth Scale and Modified Tardieu Scale in patients with spinal cord injuries. *Spinal Cord*, *55*(10), 944–949.

Aliff, M., Daud, I., Puzi, A. A., Na'im Sidek, S., Zainuddin, A. A., Khairuddin, I. M., Azri, M., Mutalib, A., Pahang, M., & Abdullah, A.-S. (2024). Leveraging Mechanomyography Signal for Quantitative Muscle Spasticity Assessment of Upper Limb in Neurological Disorders Using Machine Learning. In *IJACSA) International Journal of Advanced Computer Science and Applications* (Vol. 15, Issue 8).

Alvi, M. A., Pedro, K. M., Quddusi, A. I., & Fehlings, M. G. (2024). Advances and Challenges in Spinal Cord Injury Treatments. *Journal of Clinical Medicine*, *13*(14), 4101.

Andelova, M., Vodehnalova, K., Krasensky, J., Hardubejova, E., Hrnciarova, T., Srpova, B., Uher, T., Menkyova, I., Stastna, D., Friedova, L., Motyl, J., Lizrova Preiningerova, J., Kubala Havrdova, E., Maréchal, B., Fartaria, M. J., Kober, T., Horakova, D., & Vaneckova, M. (2022). Brainstem lesions are associated with diffuse spinal cord involvement in early multiple sclerosis. *BMC Neurology*, *22*(1).

Annaswamy, T., Mallempati, S., Allison, S. C., & Abraham, L. D. (2007). Measurement of plantarflexor spasticity in traumatic brain injury: Correlational study of resistance torque compared with the modified Ashworth scale. *American Journal of Physical Medicine and Rehabilitation*, *86*(5), 404–411.

Ansari, N. N., Rahimi, M., Naghdi, S., Barzegar-Ganji, Z., Hasson, S., & Moghimi, E. (2022). Inter- and intra-rater reliability of the modified modified ashworth scale in the assessment of muscle spasticity in cerebral palsy: A preliminary study. *Journal of Pediatric Rehabilitation Medicine*, *15*(1), 151–158.

Ardila, A., Fatima, S., & Rosselli, M. (2019). Dysexecutive Syndromes: Clinical and Experimental Perspectives. In *Springer eBooks.*

Asheghabadi, A. S., Moqadam, S. B., & Xu, J. (2021). Multichannel Finger Pattern Recognition Using Single-Site Mechanomyography. *IEEE Sensors Journal*, *21*(6), 8184–8193.

Axel R, Fugl-Meyer, Lisbeth Jaasko, Ingegerd Leyman, Sigyn Olsson, & Solveig Steglind. (1975). The Post-Stroke Hemiplegic Patient. *Scand J Rehab Med 7*, 13–31.

Ayala, L., Winter, S., Byrne, R., Fehlings, D., Gehred, A., Letzkus, L., Noritz, G., Paton, M. C. B., Pietruszewski, L., Rosenberg, N., Tanner, K., Vargus-Adams, J., Novak, I., & Maitre, N. L. (2021). Assessments and Interventions for Spasticity in Infants with or at High Risk for Cerebral Palsy: A Systematic Review. In *Pediatric Neurology* (Vol. 118, pp. 72–90).

Baak, M., Koopman, R., Snoek, H., & Klous, S. (2020). A new correlation coefficient between categorical, ordinal and interval variables with Pearson characteristics. *Computational Statistics and Data Analysis*, *152*.

Banky, M., Clark, R. A., Mentiplay, B. F., Olver, J. H., & Williams, G. (2021). Clinical spasticity assessment using the modified tardieu scale does not reflect joint angular velocity or range of motion during walking: Assessment tool implications. *Journal of Rehabilitation Medicine*, *53*(1).

Barr, E., Popkin, R., Roodzant, E., Jaworski, B., & Temkin, S. M. (2024). Gender as a social and structural variable: research perspectives from the National Institutes of Health (NIH). In *Translational Behavioral Medicine* (Vol. 14, Issue 1, pp. 13–22).

Baunsgaard, C. B., Nissen, U. V., Christensen, K. B., & Biering-Sørensen, F. (2016). Modified Ashworth scale and spasm frequency score in spinal cord injury: Reliability and correlation. *Spinal Cord*, *54*(9), 702–708.

Bavikatte, G., Subramanian, G., Ashford, S., Allison, R., & Hicklin, D. (2021). Early Identification, Intervention and Management of Post-stroke Spasticity: Expert Consensus Recommendations. In *Journal of Central Nervous System Disease* (Vol. 13).

Bayram, K. B., Şengül, I., Aşkin, A., & Tosun, A. (2022). Inter-rater reliability of the Australian Spasticity Assessment Scale in poststroke spasticity. *International Journal of Rehabilitation Research*, *45*(1), 86–92.

Billington, Z. J., Henke, A. M., & Gater, D. R. (2022). Spasticity Management after Spinal Cord Injury: The Here and Now. *Journal of Personalized Medicine*, *12*(5).

Blackburn, M., van Vliet, P., & Mockett, S. P. (2002). Reliability of measurements obtained with the modified Ashworth scale in the lower extremities of people with stroke. *Physical Therapy*, *82*(1), 25–34.

Bohannon, R. W., & Smith, M. B. (1987). Interrater reliability of a modified Ashworth scale of muscle spasticity. *Physical Therapy*, *67*(2), 206–207.

Brambilla, C., Pirovano, I., Mira, R. M., Rizzo, G., Scano, A., & Mastropietro, A. (2021). Combined use of emg and eeg techniques for neuromotor assessment in rehabilitative applications: A systematic review. In *Sensors* (Vol. 21, Issue 21).

Brandt, T. (2003). *Neurological disorders: course and treatment*. Academic Press.

Calame, A., & Singer, B. J. (2015). Inter- and Intra-Rater Reliability of the Australian Spasticity Assessment Scale in Adults with Acquired Brain Injury. *Open Journal of Therapy and Rehabilitation*, *03*(03), 77–86.

Campbell, B. C. V., & Khatri, P. (2020). Stroke. *The Lancet*, *396*(10244), 129–142.

Castelli, M., Vanneschi, L., & Largo, Á. R. (2018). Supervised learning: Classification. In *Encyclopedia of Bioinformatics and Computational Biology: ABC of Bioinformatics* (Vols. 1–3, pp. 342–349).

Cè, E., Rampichini, S., & Esposito, F. (2015). Novel insights into skeletal muscle function by mechanomyography: from the laboratory to the field. *Sport Sciences for Health*, *11*(1).

Cha, Y., & Arami, A. (2020). Quantitative modeling of spasticity for clinical assessment, treatment and rehabilitation. *Sensors (Switzerland)*, *20*(18), 1–22.

Chakraborty, S., Skolnick, B. E., Alves, W. M., Marshall, L. F., & Narayan, R. K. (2017). Traumatic Brain Injury. *Handbook of Neuroemergency Clinical Trials*, 85–109.

Chen, A., Yin, R., Cao, L., Yuan, C., Ding, H. K., & Zhang, W. J. (2017). Soft robotics: Definition and research issues. *2017 24th International Conference on Mechatronics and Machine Vision in Practice, M2VIP 2017*, *2017-December*, 366–369.

Clayton, J. A., & Tannenbaum, C. (2016). Reporting sex, gender, or both in clinical research? In *JAMA - Journal of the American Medical Association* (Vol. 316, Issue 18, pp. 1863–1864).

Correa, M., Projetti, M., Siegler, I. A., & Vignais, N. (2023). Mechanomyographic Analysis for Muscle Activity Assessment during a Load-Lifting Task. *Sensors*, *23*(18).

Cruz, D. A., Villar-Patiño, C., Guevara, E., & Martinez-Alanis, M. (2020). Cervix Type Classification Using Convolutional Neural Networks. In *IFMBE Proceedings* (Vol. 75).

Cui, W., Sun, Z., Ma, H., & Wu, S. (2020). The Correlation Analysis of Atmospheric Model Accuracy Based on the Pearson Correlation Criterion. *IOP Conference Series: Materials Science and Engineering*, *780*(3).

Cunningham, P., & Delany, S. J. (2021). K-Nearest Neighbour Classifiers-A Tutorial. In *ACM Computing Surveys* (Vol. 54, Issue 6). Association for Computing Machinery.

Currà, A., Gasbarrone, R., Cardillo, A., Fattapposta, F., Missori, P., Marinelli, L., Bonifazi, G., Serranti, S., & Trompetto, C. (2021). In vivo non-invasive near-infrared spectroscopy distinguishes normal, post-stroke, and botulinum toxin treated human muscles. *Scientific Reports*, *11*(1).

De POL, S., Neves, E. B., Lazzaretti, A. E., Smaili, S. M., & Krueger, E. (2021). Punctual mechanical oscillation in modulation of muscular tonus in children with spasticity. *Bioscience Journal*, *37*, 1–11.

Deshmukh, A. A., Krishnaswamy, V., & Deshpande, M. S. (2021). Short Term Effect of Knee-to-Chest Position Plus 90-90 Passive-Hamstring-Stretching Versus 90-90 Passive-Hamstring-Stretching in 5-15 Years of Spastic Cerebral Palsy: Non-Randomized Controlled Study. *International Journal of Scientific Research in Research Paper. Multidisciplinary Studies E*, *7*(8), 31–37.

Doussoulin, A., Rivas, C., Bacco, J., Sepúlveda, P., Carvallo, G., Gajardo, C., Soto, A., & Rivas, R. (2020a). Prevalence of Spasticity and Postural Patterns in the Upper Extremity Post Stroke. *Journal of Stroke and Cerebrovascular Diseases*, *29*(11).

Doussoulin, A., Rivas, C., Bacco, J., Sepúlveda, P., Carvallo, G., Gajardo, C., Soto, A., & Rivas, R. (2020b). Prevalence of Spasticity and Postural Patterns in the Upper Extremity Post Stroke. *Journal of Stroke and Cerebrovascular Diseases*, *29*(11).

Dressler, D., Bhidayasiri, R., Bohlega, S., Chana, P., Chien, H. F., Chung, T. M., Colosimo, C., Ebke, M., Fedoroff, K., Frank, B., Kaji, R., Kanovsky, P., Koçer, S., Micheli, F., Orlova, O., Paus, S., Pirtosek, Z., Relja, M., Rosales, R. L., … Saberi, F. A. (2018). Defining spasticity: a new approach considering current movement disorders terminology and botulinum toxin therapy. *Journal of Neurology*, *265*(4), 856–862.

Ellerbusch, C. L., Chapple, K. M., & Seibert, J. B. (2023). A case series in individuals with multiple sclerosis using direct current electrical stimulation to inhibit spasticity and improve functional outcomes. *Multiple Sclerosis Journal - Experimental, Translational and Clinical*, *9*(3).

El-Tallawy, S. N., Nalamasu, R., Salem, G. I., LeQuang, J. A. K., Pergolizzi, J. V., & Christo, P. J. (2021). Management of Musculoskeletal Pain: An Update with Emphasis on Chronic Musculoskeletal Pain. In *Pain and Therapy* (Vol. 10, Issue 1, pp. 181–209).

Enslin, J. M. N., Rohlwink, U. K., & Figaji, A. (2020). Management of Spasticity After Traumatic Brain Injury in Children. In *Frontiers in Neurology* (Vol. 11).

Erden, M. S., McColl, W., Abassebay, D., & Haldane, S. (2020). Hand exoskeleton to assess hand spasticity. *2022 9th IEEE RAS/EMBS International Conference for Biomedical Robotics and Biomechatronics (BioRob)*, 1004–1009.

Esposito, D., Andreozzi, E., Fratini, A., Gargiulo, G. D., Savino, S., Niola, V., & Bifulco, P. (2018). A piezoresistive sensor to measure muscle contraction and mechanomyography. *Sensors (Switzerland)*, *18*(8), 1–12.

Esquenazi, A., Alfaro, A., Ayyoub, Z., Charles, D., Dashtipour, K., Graham, G. D., McGuire, J. R., Odderson, I. R., Patel, A. T., & Simpson, D. M. (2017). OnabotulinumtoxinA for lower limb spasticity: Guidance from a Delphi Panel approach. *PM&R*, *9*(10), 960–968.

Etana, B. B., Malengier, B., Krishnamoorthy, J., & Van Langenhove, L. (2024). Integrating wearable textiles sensors and IoT for continuous SEMG monitoring. *Sensors*, *24*(6), 1834.

Falcone, N., Leo, F., Chisari, C., & Dalise, S. (2024). Long-Term Management of Post-Stroke Spasticity with Botulinum Toxin: A Retrospective Study. *Toxins*, *16*(9), 383.

Fang, Q., Cao, S., Qin, H., Yin, R., Zhang, W., & Zhang, H. (2023). A Novel Mechanomyography (MMG) Sensor Based on Piezo-Resistance Principle and with a Pyramidic Microarray. *Micromachines*, *14*(10).

Feigin, V. L., Brainin, M., Norrving, B., Martins, S., Sacco, R. L., Hacke, W., Fisher, M., Pandian, J., & Lindsay, P. (2022). World Stroke Organization (WSO): Global Stroke Fact Sheet 2022. In *International Journal of Stroke* (Vol. 17, Issue 1, pp. 18–29).

Filippetti, M., Lugoboni, L., Di Censo, R., Degli Esposti, L., Facciorusso, S., Varalta, V., Santamato, A., Calabrese, M., Smania, N., & Picelli, A. (2024). Classification Of Upper Limb Spasticity Patterns in Patients with Multiple Sclerosis: A Pilot Observational Study. *Journal of Rehabilitation Medicine*, *56*, jrm40548.

Forman, C. R., Svane, C., Kruuse, C., Gracies, J. M., Nielsen, J. B., & Lorentzen, J. (2019). Sustained involuntary muscle activity in cerebral palsy and stroke: same symptom, diverse mechanisms. *Brain Communications*, *1*(1).

Fujimura, K., Mukaino, M., Itoh, S., Miwa, H., Itoh, R., Narukawa, D., Tanikawa, H., Kanada, Y., Saitoh, E., & Otaka, Y. (2022). Requirements for Eliciting a Spastic Response with Passive Joint Movements and the Influence of Velocity on Response Patterns: An Experimental Study of Velocity-Response Relationships in Mild Spasticity with Repeated-Measures Analysis. *Frontiers in Neurology*, *13*.

Ganguly, J., Kulshreshtha, D., Almotiri, M., & Jog, M. (2021). Muscle tone physiology and abnormalities. In *Toxins* (Vol. 13, Issue 4).

Gill, R., Banky, M., Yang, Z., Medina Mena, P., Woo, C. C. A., Bryant, A., Olver, J., Moore, E., & Williams, G. (2024). The Effect of Botulinum Neurotoxin-A (BoNT-A) on Muscle Strength in Adult-Onset Neurological Conditions with Focal Muscle Spasticity: A Systematic Review. In *Toxins* (Vol. 16, Issue 8).

Goliwąs, M., Małecka, J., Adamczewska, K., Flis-Masłowska, M., Lewandowski, J., & Kocur, P. (2024). Polish Cultural Adaptation and Reliability of the Fugl-Meyer Assessment of Motor Performance and Sensory Assessment Scale in Stroke Patients. *Journal of Clinical Medicine*, *13*(13).

Gomez-Cuaresma, L., Lucena-Anton, D., Gonzalez-Medina, G., Martin-Vega, F. J., Galan-Mercant, A., & Luque-Moreno, C. (2021). Effectiveness of stretching in post-stroke spasticity and range of motion: Systematic review and meta-analysis. In *Journal of Personalized Medicine* (Vol. 11, Issue 11).

Gracies, J. M., Marosszeky, J. E., Renton, R., Sandanam, J., Gandevia, S. C., & Burke, D. (2000). Short-term effects of dynamic lycra splints on upper limb in hemiplegic patients. *Archives of Physical Medicine and Rehabilitation*, *81*(12), 1547–1555.

Gregson, J. M., Leathley, M., Moore, A. P., Sharma, A. K., Smith, T. L., & Watkins, C. L. (1999). *Reliability of the Tone Assessment Scale and the Modified Ashworth Scale as Clinical Tools for Assessing Poststroke Spasticity*.

Guo, X., Wallace, R., Tan, Y., Oetomo, D., Klaic, M., & Crocher, V. (2022). Technology-assisted assessment of spasticity: a systematic review. *Journal of NeuroEngineering and Rehabilitation*, *19*(1), 1–17.

Gupta, A. D., Visvanathan, R., Cameron, I., Koblar, S. A., Howell, S., & Wilson, D. (2019). Efficacy of botulinum toxin in modifying spasticity to improve walking and quality of life in post-stroke lower limb spasticity - a randomized double-blind placebo controlled study. *BMC Neurology*, *19*(1).

Haas, B. M., Bergström, E., Jamous, A., & Bennie, A. (1996). The inter rater reliability of the original and of the modified Ashworth scale for the assessment of spasticity in patients with spinal cord injury. *Spinal Cord*, *34*(9), 560–564.

Hachem, L. D., Ahuja, C. S., & Fehlings, M. G. (2017). Assessment and management of acute spinal cord injury: From point of injury to rehabilitation. *Journal of Spinal Cord Medicine*, *40*(6), 665–675.

Hägglund, G., Hollung, S. J., Ahonen, M., Andersen, G. L., Eggertsdóttir, G., Gaston, M. S., Jahnsen, R., Jeglinsky-Kankainen, I., Nordbye-Nielsen, K., Tresoldi, I., & Alriksson-Schmidt, A. I. (2021). Treatment of spasticity in children and adolescents with cerebral palsy in Northern Europe: a CP-North registry study. *BMC Neurology*, *21*(1).

Harvey, L. A., Katalinic, O. M., Herbert, R. D., Moseley, A. M., Lannin, N. A., & Schurr, K. (2017). Stretch for the treatment and prevention of contractures. In *Cochrane Database of Systematic Reviews* (Vol. 2017, Issue 1).

Hashimoto, S., Nagoshi, N., Nakamura, M., & Okano, H. (2024). Regenerative medicine strategies for chronic complete spinal cord injury. *Neural Regeneration Research*, *19*(4), 818–824.

Haugh, A., Pandyan, A., & Johnson, G. (2006). A systematic review of the Tardieu Scale for the measurement of spasticity. In *Disability and Rehabilitation* (Vol. 28, Issue 15, pp. 899–907).

Hazem, T., Soubra, H., & Othman, H. (2023). MMG Signal Analysis for Muscle Performance Assessment. *Procedia Computer Science*, *219*, 1412–1419.

He, J., Luo, A., Yu, J., Qian, C., Liu, D., Hou, M., & Ma, Y. (2023). Quantitative assessment of spasticity: a narrative review of novel approaches and technologies. In *Frontiers in Neurology* (Vol. 14).

Hernández, E. D., Galeano, C. P., Barbosa, N. E., Forero, S. M., Nordin, Å., Sunnerhagen, K. S. M. P. D., & Alt Murphy, M. (2019). Intra- And inter-rater reliability of Fugl-Meyer assessment of upper extremity in stroke. *Journal of Rehabilitation Medicine*, *51*(9), 652–659.

Hoffman, B. (2015). The biopsychology of motivation. In *Motivation for Learning and Performance* (pp. 47–78).

Hong, M. J., Park, J. B., Lee, Y. J., Kim, H. T., Lee, W. C., Hwang, C. M., Lim, H. K., & Lee, D. H. (2018). Quantitative evaluation of post-stroke spasticity using neurophysiological and radiological tools: A pilot study. *Annals of Rehabilitation Medicine*, *42*(3), 384–395.

Houtchens, M. K., & Khoury, S. J. (2013). Multiple Sclerosis. *Women and Health*, 785–801.

Hugos, C. L., & Cameron, M. H. (2019). Assessment and Measurement of Spasticity in MS: State of the Evidence. *Current Neurology and Neuroscience Reports*, *19*(10).

Ibitoye, M. O., Hamzaid, N. A., Zuniga, J. M., Hasnan, N., & Wahab, A. K. A. (2014). Mechanomyographic parameter extraction methods: An appraisal for clinical applications. *Sensors (Switzerland)*, *14*(12), 22940–22970.

Islam, M. A., Sundaraj, K., Ahmad, R. B., Ahamed, N. U., & Ali, M. A. (2013). Mechanomyography sensor development, related signal processing, and applications: A systematic review. *IEEE Sensors Journal*, *13*(7), 2499–2516.

Jakob, M. O., Kofoed-Branzk, M., Deshpande, D., Murugan, S., & Klose, C. S. N. (2021). An Integrated View on Neuronal Subsets in the Peripheral Nervous System and Their Role in Immunoregulation. In *Frontiers in Immunology* (Vol. 12). Frontiers Media S.A.

Jun, S. W., Yong, S. J., Jo, M., Kim, Y. H., & Kim, S. H. (2018). Brief report: Preliminary study on evaluation of spasticity in patients with brain lesions using mechanomyography. *Clinical Biomechanics*, *54*, 16–21.

Katz, R. T., Rovai, G. P., Brait, C., & Zev Rymer, W. (1992). *Objective Quantification of Spastic Hypertonia: Correlation with Clinical Findings*.

Kaya Keles, C. S., & Ates, F. (2022). Botulinum Toxin Intervention in Cerebral Palsy-Induced Spasticity Management: Projected and Contradictory Effects on Skeletal Muscles. In *Toxins* (Vol. 14, Issue 11).

Khairuddin, I. M., Sidek, S. N., Majeed, A. P. P. A., Razman, M. A. M., Puzi, A. A., & Yusof, H. M. (2021). The classification of movement intention through machine learning models:

the identification of significant time-domain EMG features. *PeerJ Computer Science*, *7*, 1–15.

Kim, J. H., Kim, S. Y., Kim, B., Lee, S. R., Cha, S. H., Lee, D. S., & Lee, H. J. (2021). Prospects of therapeutic target and directions for ischemic stroke. *Pharmaceuticals*, *14*(4).

Kim, J. Y., Park, G., Lee, S. A., & Nam, Y. (2020). Analysis of machine learning-based assessment for elbow spasticity using inertial sensors. *Sensors (Switzerland)*, *20*(6), 1–15.

Kristinsdóttir, K. Ó., Ruipérez-Campillo, S., & Helgason, Þ. (2023). *Quantifying Spasticity: A review. IntechOpen eBooks.*

Krueger, E., Popović-Maneski, L., & Nohama, P. (2018). Mechanomyography-Based Wearable Monitor of Quasi-Isometric Muscle Fatigue for Motor Neural Prostheses. *Artificial Organs*, *42*(2), 208–218.

Krueger, E., Scheeren, E. M., Nogueira-Neto, G. N., Button, V. L. D. S. N., & Nohama, P. (2014). Advances and perspectives of mechanomyography. *Revista Brasileira de Engenharia Biomedica*, *30*(4), 384–401.

Kuo, C. L., & Hu, G. C. (2018). Post-stroke Spasticity: A Review of Epidemiology, Pathophysiology, and Treatments. In *International Journal of Gerontology* (Vol. 12, Issue 4, pp. 280–284).

Lackritz, H., Parmet, Y., Frenkel-Toledo, S., Baniña, M. C., Soroker, N., Solomon, J. M., Liebermann, D. G., Levin, M. F., & Berman, S. (2021). Effect of post-stroke spasticity on voluntary movement of the upper limb. *Journal of NeuroEngineering and Rehabilitation*, *18*(1).

Lance, J. W. (1980). The control of muscle tone, reflexes, and movernent: Robert Wartenbeg lecture. *Neurology*, *30*(12), 1303–1313.

Lee, K., Carson, L., Kinnin, E., & Patterson, V. (1989). The Ashworth Scale: a reliable and reproducible method of measuring spasticity. *Neurorehabilitation and Neural Repair, 3(4), 205–209.*

Lee, S., Lee, Y. S., & Kim, J. (2018). Automated Evaluation of Upper-Limb Motor Function Impairment Using Fugl-Meyer Assessment. *IEEE Transactions on Neural Systems and Rehabilitation Engineering*, *26*(1), 125–134.

Lewandowska-Sroka, P., Stabrawa, R., Kozak, D., Poświata, A., Łysoń-Uklańska, B., Bienias, K., Roksela, A., Kliś, M., & Mikulski, M. (2021). The influence of emg-triggered robotic movement on walking, muscle force and spasticity after an ischemic stroke. *Medicina (Lithuania)*, *57*(3), 1–11.

Li, N., Zhou, R., Krishna, B., Pradhan, A., Lee, H., He, J., & Jiang, N. (2024). Non-invasive Techniques for Muscle Fatigue Monitoring: A Comprehensive Survey. *ACM Computing Surveys*, *56*(9).

Liu, M. K., Lin, Y. T., Qiu, Z. W., Kuo, C. K., & Wu, C. K. (2020). Hand Gesture Recognition by a MMG-Based Wearable Device. *IEEE Sensors Journal*, *20*(24), 14703–14712.

Lonnemann, E., Olson, K. A., Deyle, G. D., Silvernail, J. L., Plock, H., Puentedura, E., Mintken, P., Rhon, D. I., Hutting, N., & Paris, S. (2021). What is in a Name? Perhaps your Professional Identity and Practice–A Call to Maintain IFOMPT as the International Federation of Orthopedic Manipulative Physical Therapists. *Journal of Manual & Manipulative Therapy*, *29*(4), 201–202.

Lorentzen, J., Pradines, M., Gracies, J. M., & Bo Nielsen, J. (2018). On Denny-Brown's 'spastic dystonia' – What is it and what causes it? In *Clinical Neurophysiology* (Vol. 129, Issue 1, pp. 89–94).

Love, S., Gibson, N., Smith, N., Bear, N., & Blair, E. (2016). Interobserver reliability of the Australian Spasticity Assessment Scale (ASAS). *Developmental Medicine and Child Neurology*, *58*, 18–24.

Luo, Z., Lo, W. L. A., Bian, R., Wong, S., & Li, L. (2019). Advanced quantitative estimation methods for spasticity: a literature review. In *Journal of International Medical Research* (Vol. 48, Issue 3).

Maiwan Bahjat Abdulrazzaq, & Jwan Najeeb Saeed. (2019). *A Comparison of Three Classification Algorithms for Handwritten Digit Recognition*. 58–63.

Man Lau, B. W., Yau, S. Y., Po, K. T., & So, K. F. (2016). Neurological Disorders. In *Adult Neurogenesis in the Hippocampus: Health, Psychopathology, and Brain Disease* (pp. 249–275).

Martins, L. M., Ribeiro, N. F., Soares, F., & Santos, C. P. (2022). Inertial Data-Based AI Approaches for ADL and Fall Recognition. *Sensors*, *22*(11).

Maulud, D., & Abdulazeez, A. M. (2020). A Review on Linear Regression Comprehensive in Machine Learning. *Journal of Applied Science and Technology Trends*, *1*(2), 140–147.

Meagher, C., Franco, E., Turk, R., Wilson, S., Steadman, N., McNicholas, L., Vaidyanathan, R., Burridge, J., & Stokes, M. (2020). New advances in mechanomyography sensor technology and signal processing: Validity and intrarater reliability of recordings from muscle. *Journal of Rehabilitation and Assistive Technologies Engineering*, *7*, 205566832091611.

Mendiola, J. M. F. P. de, Arboix, A., García-Eroles, L., & Sánchez-López, M. J. (2023). Acute Spontaneous Lobar Cerebral Hemorrhages Present a Different Clinical Profile and a More Severe Early Prognosis than Deep Subcortical Intracerebral Hemorrhages—A Hospital-Based Stroke Registry Study. *Biomedicines*, *11*(1).

Milinis, K., Tennant, A., & Young, C. A. (2016). Spasticity in multiple sclerosis: Associations with impairments and overall quality of life. *Multiple Sclerosis and Related Disorders*, *5*, 34–39.

Mohamad, N. Z. (2019). *Muscle Performance Using Mc-Sensor During Fes-Evoked Contractions in Individuals with Spinal Cord Injury* (Master Dissertation). University of Malaya.

Mohamad, N. Z., Hamzaid, N. A., Davis, G. M., Abdul Wahab, A. K., & Hasnan, N. (2017). Mechanomyography and torque during FES-evoked muscle contractions to fatigue in individuals with spinal cord injury. *Sensors (Switzerland)*, *17*(7), 1–15.

Mokri, C., Bamdad, M., & Abolghasemi, V. (2022). Muscle force estimation from lower limb EMG signals using novel optimised machine learning techniques. *Medical and Biological Engineering and Computing*, *60*(3), 683–699.

Moreta, M. C., Fleet, A., Reebye, R., McKernan, G., Berger, M., Farag, J., & Munin, M. C. (2020). Reliability and Validity of the Modified Heckmatt Scale in Evaluating Muscle Changes with Ultrasound in Spasticity. *Archives of Rehabilitation Research and Clinical Translation*, *2*(4), 100071.

Morris, S. L., & Williams, G. (2018). A historical review of the evolution of the Tardieu Scale. *Brain Injury*, *32*(5), 665–669.

Naghdi, S., Ansari, N. N., Ghorbani-rad, S., Senobari, M., & Sahraian, M. A. (2017). Intra-rater reliability of the Modified Tardieu Scale in patients with multiple sclerosis. *Neurological Sciences*, *38*(1), 93–99.

Nair, K. P. S., & Marsden, J. (2014). The management of spasticity in adults. In *BMJ (Online)* (Vol. 349).

Noor Ayuni Che Zakaria, Takashi Komeda, Cheng Vee Low, Fazah Akhtar Hanapiah, & Kaoru Inoue. (2015). *ICCAS 2015: 2015 15th International Conference on Control, Automation and Systems: proceedings: October 13-16, 2015, BEXCO, Busan, Korea.* IEEE Xplore.

None Felix Siaw-Debrah, Kusah, M., Ayenyimah, G., & None Emmanuel Adjei-Osei. (2024). Spasticity: A general outlook of pathogenesis and current management. *International Journal of Science and Research Archive*, *13*(1), 457–469.

Norbye, A. D., Midgard, R., & Thrane, G. (2020). Spasticity, gait, and balance in patients with multiple sclerosis: A cross-sectional study. *Physiotherapy Research International*, *25*(1).

Nourizadeh, M., Shadgan, B., Abbasidezfouli, S., Juricic, M., & Mulpuri, K. (2024). Methods of muscle spasticity assessment in children with cerebral palsy: a scoping review. In *Journal of Orthopaedic Surgery and Research* (Vol. 19, Issue 1).

Nti, I. K., Nyarko-Boateng, O., & Aning, J. (2021). Performance of Machine Learning Algorithms with Different K Values in K-fold CrossValidation. *International Journal of Information Technology and Computer Science*, *13*(6), 61–71.

Nurul Atiqah Othman, F. I., Noor Ayuni Che Zakaria, Fazah Akhtar Hanapiah, & Cheng Yee Low. (2016). Supporting Clinical Evaluation of Upper Limb Spasticity with Quantitative

Data Measurement in Accordance to the Modified Ashworth Scale. *2016 IEEE EMBS Conference on Biomedical Engineering and Sciences (IECBES)*, 731–736.

Padmaja, D. L., & Vishnuvardhan, B. (2016). Comparative Study of Feature Subset Selection Methods for Dimensionality Reduction on Scientific Data. *Proceedings - 6th International Advanced Computing Conference, IACC 2016*, 31–34.

Pan, C. T., Chang, C. C., Yang, Y. S., Yen, C. K., Kao, Y. H., & Shiue, Y. L. (2020). Development of MMG sensors using PVDF piezoelectric electrospinning for lower limb rehabilitation exoskeleton. *Sensors and Actuators, A: Physical*, *301*, 111708.

Park, J. H., Kim, Y., Lee, K. J., Yoon, Y. S., Kang, S. H., Kim, H., & Park, H. S. (2019). Artificial Neural Network Learns Clinical Assessment of Spasticity in Modified Ashworth Scale. *Archives of Physical Medicine and Rehabilitation*, *100*(10), 1907–1915.

Patel, D. R., Neelakantan, M., Pandher, K., & Merrick, J. (2020). Cerebral palsy in children: A clinical overview. In *Translational Pediatrics* (Vol. 9, pp. S125–S135).

Paterson, R. W., Brown, R. L., Benjamin, L., Nortley, R., Wiethoff, S., Bharucha, T., Jayaseelan, D. L., Kumar, G., Raftopoulos, R. E., Zambreanu, L., Vivekanandam, V., Khoo, A., Geraldes, R., Chinthapalli, K., Boyd, E., Tuzlali, H., Price, G., Christofi, G., Morrow, J., … Zandi, M. S. (2020). The emerging spectrum of COVID-19 neurology: clinical, radiological and laboratory findings.

Petek Balci, B. (2018). Spasticity Measurement. *Archives of Meuropychiatry*, *55*(Supplement 1), S49–S53.

Powers, R. K., Marder-Meyer, J., & Rymer, W. 2. (1988). Quantitative Relations Between Hypertonia and Stretch Reflex Threshold in Spastic Hemiparesis.

Pradines, M., Baude, M., Marciniak, C., Francisco, G., Gracies, J. M., Hutin, E., & Bayle, N. (2018). Effect on Passive Range of Motion and Functional Correlates After a Long-Term Lower Limb Self-Stretch Program in Patients with Chronic Spastic Paresis. *PM and R*, *10*(10), 1020–1031.

Prajapati, B., Dunne, M., & Armstrong, R. (2010). Sample size estimation and statistical power analyses.

Puig, J., Shankar, J., Liebeskind, D., Terceño, M., Nael, K., Demchuk, A. M., Menon, B., Dowlatshahi, D., Leiva-Salinas, C., Wintermark, M., Thomalla, G., Silva, Y., Serena, J., Pedraza, S., & Essig, M. (2020). From “Time is Brain” to “Imaging is Brain”: A Paradigm Shift in the Management of Acute Ischemic Stroke. In *Journal of Neuroimaging* (Vol. 30, Issue 5, pp. 562–571).

Puzi, A. A., Sidek, S. N., Khairuddin, I. M., & Yusof, H. M. (2020). Objective assessment for classification of muscle spasticity level. *ACM International Conference Proceeding Series*, 4–9.

Puzi, A. A., Sidek, S. N., Yusof, H. M., & Khairuddin, I. (2019). Objective analysis of muscle spasticity level in rehabilitation assessment. *International Journal of Integrated Engineering*, *11*(3), 223–231.

Quadri, S. A., Farooqui, M., Ikram, A., Zafar, A., Khan, M. A., Suriya, S. S., Claus, C. F., Fiani, B., Rahman, M., Ramachandran, A., Armstrong, I. I. T., Taqi, M. A., & Mortazavi, M. M. (2020). Recent update on basic mechanisms of spinal cord injury. In *Neurosurgical Review* (Vol. 43, Issue 2, pp. 425–441).

Rech, K. D., Salazar, A. P., Marchese, R. R., Schifino, G., Cimolin, V., & Pagnussat, A. S. (2020). Fugl-Meyer Assessment Scores Are Related with Kinematic Measures in People with Chronic Hemiparesis after Stroke. *Journal of Stroke and Cerebrovascular Diseases*, *29*(1).

Rezaei, S., Morshedi, K., Shafabakhsh, R., & Mahjoubin-Tehran, M. (2023). Current therapies for neurological disorders and their limitations. In *Phytonutrients and Neurological Disorders: Therapeutic and Toxicological Aspects* (pp. 107–130).

Roldan, A., Henríquez, M., Iturricastillo, A., Castillo, D., Yanci, J., & Reina, R. (2022). To What Degree Does Limb Spasticity Affect Motor Performance in Para-Footballers with Cerebral Palsy? *Frontiers in Physiology*, *12*.

Roth, G. A., Mensah, G. A., Johnson, C. O., Addolorato, G., Ammirati, E., Baddour, L. M., Barengo, N. C., Beaton, A., Benjamin, E. J., Benziger, C. P., Bonny, A., Brauer, M., Brodmann, M., Cahill, T. J., Carapetis, J. R., Catapano, A. L., Chugh, S., Cooper, L. T.,

Coresh, J., … Fuster, V. (2020). Global Burden of Cardiovascular Diseases and Risk Factors, 1990-2019: Update from the GBD 2019 Study. In *Journal of the American College of Cardiology* (Vol. 76, Issue 25, pp. 2982–3021).

Rupsha Mukhopadhyay, M. M. (2015). *IFESS: 2014 IEEE 19th International Functional Electrical Stimulation Society Annual Conference: conference proceedings: 17th-19th September 2014, Impiana Hotel KLCC, Kuala Lumpur, Malaysia*. IEEE.

Salazar, A. P., Pinto, C., Ruschel Mossi, J. V., Figueiro, B., Lukrafka, J. L., & Pagnussat, A. S. (2019). Effectiveness of static stretching positioning on post-stroke upper-limb spasticity and mobility: Systematic review with meta-analysis. In *Annals of Physical and Rehabilitation Medicine* (Vol. 62, Issue 4, pp. 274–282).

Santos, E. L. D., Scheeren, E. M., Nogueira-Neto, G. N., Krueger, E., Peixoto, N., & Nohama, P. (2024). Mechanomyography-Based Metric Scale for Spasticity: A Pilot Descriptive Observational study. *Sensors*, *24*(16), 5276.

Santos, E., Krueger, E., Nogueira-Neto, G. N., & Nohama, P. (2017). Comparison of Modified Ashworth Scale with Systems and Techniques for Quantitative Assessment of Spasticity-Literature Review. *Journal of Neurological Disorders & Stroke*, *5*(2), 1–9.

Santos, E. L., Santos, M. C., Krueger, E., Nogueira-Neto, G. N., & Nohama, P. (2016). Mechanomyography signals in spastic muscle and the correlation with the modified Ashworth scale. *Proceedings of the Annual International Conference of the IEEE Engineering in Medicine and Biology Society, EMBS*, *2016-Octob* (Ll), 3789–3792.

Sarathy, K., Doshi, C., & Aroojis, A. (2019). Clinical examination of children with cerebral palsy. *Indian Journal of Orthopaedics*, *53*(1), 35–44.

Sarkar, A., Hossain, S. K. S., & Sarkar, R. (2023). Human activity recognition from sensor data using spatial attention-aided CNN with genetic algorithm. *Neural Computing and Applications*, *35*(7), 5165–5191.

Sarker, I. H. (2021). Machine Learning: Algorithms, Real-World Applications and Research Directions. In *SN Computer Science* (Vol. 2, Issue 3).

Set Foong, N., Yee Ming, C., Pei Eng, C., & Kok Shien, N. (n.d.). *An Insight of Linear Regression Analysis*.

Seth, N., Johnson, D., Taylor, G. W., Allen, O. B., & Abdullah, H. A. (2015). Robotic pilot study for analysing spasticity: Clinical data versus healthy controls. *Journal of NeuroEngineering and Rehabilitation*, *12*(1).

Shaikh, S., Bhatnagar, G., Bhilwade, A., & Deshmukh, A. (2024). Comparison of the Effectiveness between Tendinous Pressure and Maintained Stretch in Roods Inhibitory Techniques on Reduction of Upper Limb Spasticity in Patients with Stroke. *African Journal of Biological Sciences (South Africa)*, *6*(9), 1429–1438.

Sharma, S., & Sharma, V. (2016). Performance of Various Machine Learning Classifiers on Small Datasets with Varying Dimensionalities: A Study. *Circulation in Computer Science*, *1*(1), 30–35.

Sheng, B., Lei, X., Cheng, J., Xie, Q., Tao, J., & Chen, Y. (2024). Novel Digital Assessment System for Upper-Limb Movement in Stroke Patients Using Markless-Sensing Technology and Deep Learning Algorithms. *Journal of Shanghai Jiaotong University (Science)*.

Shu, X., McConaghy, C., & Knight, A. (2021). Validity and reliability of the Modified Tardieu Scale as a spasticity outcome measure of the upper limbs in adults with neurological conditions: A systematic review and narrative analysis. *BMJ Open*, *11*(12), 1–10.

Spieker, E. L., Dvorani, A., Salchow-Hömmen, C., Otto, C., Ruprecht, K., Wenger, N., & Schauer, T. (2024). Targeting Transcutaneous Spinal Cord Stimulation Using a Supervised Machine Learning Approach Based on Mechanomyography. *Sensors*, *24*(2).

Starosta, M., Marek, K., Redlicka, J., & Miller, E. (2024). Extracorporeal Shockwave Treatment as Additional Therapy in Patients with Post-Stroke Spasticity of Upper Limb—A Narrative Review. In *Journal of Clinical Medicine* (Vol. 13, Issue 7).

Stokic, D. S., Bohanec, M., Priebe, M. M., & Sherwood, A. M. (1998). Relating clinical and neurophysiological assessment of spasticity by machine learning. In *International Journal of Medical Informatics* (Vol. 49).

Su, X., Yuan, H., Bai, Y., Chen, J., Sui, M., Zhang, X., Liang, Y., Feng, W., Dou, Z., & Zhu, H. (2020). Clobetasol Attenuates White Matter Injury by Promoting Oligodendrocyte Precursor Cell Differentiation. *Pediatric Neurosurgery*, *55*(4), 188–196.

Swaiman, K. F., & Phillips, J. (2018). 5 - Muscular Tone and Gait Disturbances. *Swaiman's Pediatric Neurology*, 27–32.

Szumilas, M., Władziński, M., & Wildner, K. (2021). A coupled piezoelectric sensor for mmg-based human-machine interfaces. *Sensors*, *21*(24).

Takeuchi, K., Takebayashi, T., Hanioka, D., Okita, Y., & Shimada, S. (2024). Comparison of tendon and muscle belly vibratory stimulation in the treatment of post-stroke upper extremity spasticity: a retrospective observational pilot study. *Scientific Reports*, *14*(1).

Talib, I., Sundaraj, K., & Lam, C. K. (2018). Choice of mechanomyography sensors for diverse types of muscle activities. *Journal of Telecommunication, Electronic and Computer Engineering*, *10*(1–13), 79–82.

Tony, A., Rasouli, A., Farahinia, A., Wells, G., Zhang, H., Achenbach, S., Yang, S. M., Sun, W., & Zhang, W. (2021). Toward a Soft Microfluidic System: Concept and Preliminary Developments. *2021 27th International Conference on Mechatronics and Machine Vision in Practice, M2VIP 2021*, 755–759.

Trompetto, C., Marinelli, L., Mori, L., Bragazzi, N., Maggi, G., Cotellessa, F., Puce, L., Vestito, L., Molteni, F., Gasperini, G., Farina, N., Bissolotti, L., Sciarrini, F., Millevolte, M., Balestrieri, F., Restivo, D. A., Chisari, C., Santamato, A., Del Felice, A., … Currà, A. (2023). Increasing the Passive Range of Joint Motion in Stroke Patients Using Botulinum Toxin: The Role of Pain Relief. *Toxins*, *15*(5).

Tsuji, H., Misawa, H., Takigawa, T., Tetsunaga, T., Yamane, K., Oda, Y., & Ozaki, T. (2021). Quantification of patellar tendon reflex using portable mechanomyography and electromyography devices. *Scientific Reports*, *11*(1), 1–15.

Turnsek, G., & Paravlic, A. H. (2024). Electromechanical efficiency index of skeletal muscle and its applicability: a systematic review. In *Frontiers in Bioengineering and Biotechnology* (Vol. 12).

Uwamahoro, R., Sundaraj, K., & Subramaniam, I. D. (2021). Assessment of muscle activity using electrical stimulation and mechanomyography: a systematic review. In *BioMedical Engineering Online* (Vol. 20, Issue 1).

van den Noort, J. C., Scholtes, V. A., Becher, J. G., & Harlaar, J. (2010). Evaluation of the Catch in Spasticity Assessment in Children with Cerebral Palsy. *Archives of Physical Medicine and Rehabilitation*, *91*(4), 615–623.

Vapnik, V. N. (1999). An Overview of Statistical Learning Theory. In *IEEE TRANSACTIONS ON NEURAL NETWORKS* (Vol. 10, Issue 5).

Vattanasilp, W., Ada, L., & Crosbie, J. (2000). Contribution of thixotropy, spasticity, and contracture to ankle stiVness after stroke. In *J Neurol Neurosurg Psychiatry* (Vol. 69).

Wang, C., Sivan, M., Wang, D., Zhang, Z., Li, G., Bao, T., & Xie, S. Q. (2022). Quantitative elbow spasticity measurement based on muscle activation estimation using maximal voluntary contraction. *IEEE Transactions on Instrumentation and Measurement*, *71*, 1–11.

Wang, H., Wang, L., Xiang, Y., Zhao, N., Li, X., Chen, S., Lin, C., & Li, G. (2017). Assessment of elbow spasticity with surface electromyography and mechanomyography based on support vector machine. *Proceedings of the Annual International Conference of the IEEE Engineering in Medicine and Biology Society, EMBS*, *Table 1*, 3860–3863.

Wang, Y., Zhang, L., Yin, R., Zhang, Y., Dai, Z., Wang, M., Song, J., Fan, X., Zhang, Y., Yang, S., Shen, Y., Yang, C., Song, Q., Sun, S., & Liu, J. (2025). Transcutaneous electrical acupoint stimulation for upper limb spasticity after stroke: effect andd feasibility—a randomised pilot study. *BMJ Supportive & Palliative Care*, spcare-005174.

Wen, J., Fang, X., Cui, J., Fei, L., Yan, K., Chen, Y., & Xu, Y. (2019). Robust Sparse Linear Discriminant Analysis. *IEEE Transactions on Circuits and Systems for Video Technology*, *29*(2), 390–403.

Whitten, T. A., Sanchez, A. L., Gyawali, B., Papathanassoglou, E. D. E., Bakal, J. A., & Krysa, J. A. (2024). Predicting inpatient rehabilitation length of stay for adults with traumatic spinal cord injury. *Journal of Spinal Cord Medicine*, 1–11.

Williams, G., Singer, B. J., Ashford, S., Hoare, B., Hastings-Ison, T., Fheodoroff, K., Berwick, S., Sutherland, E., & Hill, B. (2022). A synthesis and appraisal of clinical practice guidelines, consensus statements and Cochrane systematic reviews for the management of focal spasticity in adults and children. In *Disability and Rehabilitation* (Vol. 44, Issue 4, pp. 509–519).

Wissel, J., & Hernandez Franco, J. (2024). Changing the view on spastic movement disorder management to improve active movement competence in the upper motor neuron syndrome: a clinical perspective. *Frontiers in Neurology*, *15*.

Wołczowski, A., & Zdunek, R. (2017). Electromyography and mechanomyography signal recognition: Experimental analysis using multi-way array decomposition methods. *Biocybernetics and Biomedical Engineering*, *37*(1), 103–113.

Woodward, R. B., Stokes, M. J., Shefelbine, S. J., & Vaidyanathan, R. (2019). Segmenting Mechanomyography Measures of Muscle Activity Phases Using Inertial Data. *Scientific Reports*, *9*(1).

Woytowicz, E. J., Rietschel, J. C., Goodman, R. N., Conroy, S. S., Sorkin, J. D., Whitall, J., & McCombe Waller, S. (2017). Determining Levels of Upper Extremity Movement Impairment by Applying a Cluster Analysis to the Fugl-Meyer Assessment of the Upper Extremity in Chronic Stroke. *Archives of Physical Medicine and Rehabilitation*, *98*(3), 456–462.

Wu, H., Huang, Q., Wang, D., & Gao, L. (2018). A CNN-SVM combined model for pattern recognition of knee motion using mechanomyography signals. *Journal of Electromyography and Kinesiology*, *42*, 136–142.

Wu, Z., Wang, H., Yang, W., Li, G., & Xu, W. (2021). Study on The Likelihood Ratio Used to Evaluate the Muscle Tension of Upper Limb Spasm in Hemiplegia Patients. *Journal of Clinical and Nursing Research*, *5*(4).

Wulf, M. J., & Tom, V. J. (2023). Consequences of spinal cord injury on the sympathetic nervous system. In *Frontiers in Cellular Neuroscience* (Vol. 17).

Xie, T., Leng, Y., Zhi, Y., Jiang, C., Tian, N., Luo, Z., Yu, H., & Song, R. (2020). Increased Muscle Activity Accompanying with Decreased Complexity as Spasticity Appears: High-Density EMG-Based Case Studies on Stroke Patients. *Frontiers in Bioengineering and Biotechnology*, *8*.

Yamaguchi, T., Hvass Petersen, T., Kirk, H., Forman, C., Svane, C., Kofoed-Hansen, M., Boesen, F., & Lorentzen, J. (2018). Spasticity in adults with cerebral palsy and multiple sclerosis measured by objective clinically applicable technique. *Clinical Neurophysiology*, *129*(9), 2010–2021.

Yoo, M., Ahn, J. H., Rha, D. W., & Park, E. S. (2022). Reliability of the Modified Ashworth and Modified Tardieu Scales with Standardized Movement Speeds in Children with Spastic Cerebral Palsy. *Children*, *9*(6).

Yu, S., Chen, Y., Cai, Q., Ma, K., Zheng, H., & Xie, L. (2020). A Novel Quantitative Spasticity Evaluation Method Based on Surface Electromyogram Signals and Adaptive Neuro Fuzzy Inference System. *Frontiers in Neuroscience*, *14*.

Zakaria, N. A. C., Low, C. Y., Hanapiah, F. A., Komeda, T., Inoue, K., Shazidi, M. S., & Hamsan, H. M. (2014). Evaluation of Upper Limb Spasticity towards the Development of a High Fidelity Part-task Trainer. *Procedia Technology*, *15*, 817–826.

Zebari, R., Abdulazeez, A., Zeebaree, D., Zebari, D., & Saeed, J. (2020). A Comprehensive Review of Dimensionality Reduction Techniques for Feature Selection and Feature Extraction. *Journal of Applied Science and Technology Trends*, *1*(1), 56–70.

Zeng, H., Chen, J., Guo, Y., & Tan, S. (2021). Prevalence and Risk Factors for Spasticity After Stroke: A Systematic Review and Meta-Analysis. *Frontiers in Neurology*, *11*(January).

Zhang, X., Tang, X., Zhu, X., Gao, X., Chen, X., & Chen, X. (2019). A regression-based framework for quantitative assessment of muscle spasticity using combined emg and inertial data from wearable sensors. *Frontiers in Neuroscience*, *13*(MAY), 1–12.

Zhang, Y., & Ma, Y. (2019). Application of supervised machine learning algorithms in the classification of sagittal gait patterns of cerebral palsy children with spastic diplegia. *Computers in Biology and Medicine*, *106*, 33–39.

Zhang, Z. (2016). Introduction to machine learning: K-nearest neighbors. *Annals of Translational Medicine*, *4*(11).

Zurawski, E., Behm, K., Dunlap, C., Koo, J., Ismail, F., Boulias, C., Reid, S., & Phadke, C. P. (2019). Interrater reliability of the modified ashworth scale with standardized movement speeds: A pilot study. *Physiotherapy Canada*, *71*(4), 348–354.

APPENDIX A

ETHICS APPLICATION DOCUMENTS

Our Ref. : IIUM/504/14/11/2/ IREC 2023-025
Date : 21 February 2023

Asst. Prof. Dr. Asmarani Binti Ahmad Puzi (Principal Investigator)
Kulliyyah of Information and Communication Technology
IIUM Gombak Campus
53100 Gombak

Dear Asst. Prof. Dr.,

The IIUM Research Ethics Committee (IREC) has reviewed your study protocol as mentioned below:-

ID NO.	:	**IREC 2023-025**
RESEARCH TITLE	:	**Formulation of Transfer Learning to Muscle Spasticity Characteristics Model for Quantifying the Clinical Assessment of Neurological Disorder Patients**
REGISTRATION DATE	:	**04 Feb 2023**
CO-INVESTIGATOR	:	**Assoc. Prof. Dr. Shahrul Na'im** **Dr. Salmah Anim Binti Abu Hassan** **Muhamad Aliff Imran Bin Daud**
STUDY SITE	:	**BioMechatronics Research Lab., Dept of Mechatronics Engineering, Kulliyyah of Engineering, IIUM** **Rehabilitation unit, Sultan Ahmad Shah Medical Centre**
SAMPLE SIZE	:	**30**
ETHICAL EXPIRY DATE	:	**20 February 2024**

The IIUM Research Ethics Committee (IREC) operates in accordance to the Declaration of Helsinki, International Conference of Harmonization Good Clinical Practice Guidelines (ICH-GCP), Malaysia Good Clinical Practice Guidelines and Council for International Organizations of Medical Sciences (CIOMS) International Ethical Guidelines

The following documents have been received and reviewed to the above study:-

1. Study Proposal/Protocol: Version 1, dated 09 Feb 2023
2. Informed Consent Form (ICF) –
   i. Information Sheet (English) – Version 1, dated 09 Feb 2023
   ii. Consent Form (English) - Version 1, dated 09 Feb 2023
3. Questionnaire - Version 1, dated 10 Jan 2023
4. Approval Letter from Research Management Centre, IIUM
5. Principal Investigator's CV

[Informed Consent Form for Patients with neurological disorder]

This informed consent form is for patient with neurological disorder participating in the research titled.

"Formulation of Transfer Learning to Muscle Spasticity Characteristics Model for Quantifying the Clinical Assessment of Neurological Disorder Patients."

Researcher: Dr. Asmarani Binti Ahmad Puzi

Address: Department of Computer Science, International Islamic University Malaysia, PO Box 10, 50728 Kuala Lumpur

This Informed Consent Form has two parts:

Part I	Information Sheet (to share information about the study with you)
Part II	Certificate of Consent (for signatures if you agree to participate in the study)

You will be given a copy of the full Informed Consent Form

PART I: INFORMATION SHEET

Introduction

I'm Dr. Asmarani Binti Ahmad Puzi, a lecturer at International Islamic University Malaysia (IIUM). This research is conducted to develop the spasticity muscle characteristics model based on Modified Ashworth Scale (MAS) scores from forearm musculature by transfer learning using Mechanomyography (MMG) signals. The goal of the research work is to develop the spasticity muscle characteristics model that contains dynamics parameters useful in the mapping of the level of spasticity in the muscle to the assessment tool. Basically, in the research study, the subject will be selected based on their previous treatment background (neurology condition) for forearm musculature and have undergone assessment and rehabilitation with the experienced therapist. They will be assist to be in supine position and the Mechanomyography equipment/machine will placed on the forearm musculature muscle and therapist will move the arm until there is a catch or jerk (resistance) feedback from the patient's arm. The Mechanomyography equipment/machine will analyse the force through mathematical representation and given the results based on the time domain parameter modelling and Modified Ashworth Scale mapping. It is to be noted that before any experiment is conducted the therapist will explain the experiment in detail so to get your permission before we proceed. You do not have to decide immediately whether or not to agree to participate in the research study. Before the decision is made, you could consult anyone preferable to seek alternate opinion.

There may be some words/phrases in the document, that you could not understand hence, please ask the researcher to clarify as both parties should go through the document and understand it clearly. At any time during the experiment, if you have any question, please feel free to ask the therapist.

Purpose

In this research study, the goal is to model mathematically the muscle recovery parameters of neurological disorder. Thus, it can serve significantly in the development of better and standardized assessment tool to measure muscle spasticity. The tool can be used by different therapists to assess the muscle spasticity more consistently and this can increase the efficacy and the efficiency of the choice of rehabilitation regime/task deployed by the therapist. Moreover, it was also gives benefits to patient where their recovery progress can be monitored quantitatively.

Participant selection

You are being invited to take part in this research because you fulfill criteria as described. The subjects under study are patient with neurological disorder condition aged over 18 years old. Furthermore, focus of our research is only for forearm musculature of the patients. The subject are selected from hospital that have undergone assessment and rehabilitation with the experienced therapist.

Voluntary Participation

You do not have to agree to be a subject in this study. You can choose to say no and any services that you and your family receive at this centre will not change. You can ask as many questions as you like and we will take the time to answer them. You don't have to decide today. You can think about it and tell us your decision later.

Procedure

A. We are asking you to help us to mathematically model the muscle recovery parameters of neurological disorder. We are inviting you to take part in this research project. If you accept, you will be asked to be in supine position where Mechanomyography equipment/machine will be place on your hand. After that, therapist will move the arm until there is a catch or jerk (resistance) feedback from your arm. The Mechanomyography equipment/machine will analyse the force through mathematical representation and given the results based on the time-frequency domain modelling and Modified Ashworth Scale mapping. The same procedure will be applied for three times to analyze the reliability of the equipment/machine. Before that, therapist will graded your arm manually based on Modified Ashworth Scale (MAS) sheet.

B. Fill out a questionnaire which will be provided by Muhamad Aliff Imran Bin Daud and collected by Muhamad Aliff Imran Bin Daud. OR You may answer the questionnaire yourself, or it can be read to you and you can say out loud the answer you want me to write down.

If you do not wish to answer any of the questions included in the survey, you may skip them and move on to the next question. The information recorded is confidential, your name is not being included on the forms, only a number will identify you, and no one else except Dr. Asmarani Binti Ahmad Puzi and Muhamad Aliff Imran Bin Daud will have access to your survey.

Duration
Time for a session to complete will take about 20 minutes per participant. Each session may be done at different times depending on the participant willingness and readiness. However, we may need to repeat the procedure in the future to improve the results.

Risks and Discomforts
Mild discomfort might be experienced by you when the equipment/machine try to extend/flex the arm muscle.

Benefits
Your participation is likely generating data that will help us to model mathematically the muscle recovery parameters of neurological disorder. Thus, it can serve significantly in the development of better and standardized assessment tool to measure muscle spasticity. The equipment/machine can be used by different therapists to assess the muscle spasticity more consistently and this can increase the efficacy and the efficiency of the choice of rehabilitation regime/task deployed by the therapist. This will also serve as direct benefit to the patient where their progress of recovery can be monitored quantitatively.

Reimbursements
You will not be provided with any financial incentive to take part in the research study. However, she/he will be given a token of appreciation for the time and effort spent.

Confidentiality:
We will not be sharing information about you outside of the research team. The personal information that we collect from this research project will be kept confidential.

Sharing of Research Findings
At the end of the study, we will share what we have found and learnt with the participants and the community. We will also disseminate the results in order to share the information and reach out to other researchers of the same interest.

Right to refuse or withdraw
You do not have to take part in this research if you do not wish to do so, and choosing to participate will not affect your job or job-related evaluations in any way. You may stop participating in the experiment at any time that you wish without your job being affected. I will give you an opportunity at the end of the experiment to review your remarks, and you can ask to modify or remove portions of those, if you do not agree with my notes or if I did not understand you correctly.

Who to Contact

If you have any questions you may ask them now or later, even after the study has started. If you wish to ask questions later, you may contact any of the followings:

Dr. Asmarani Binti Ahmad Puzi
0182461386
asmarani@iium.edu.my

Assoc. Prof. Dr. Shahrul Na'im
0192614030
snaim@iium.edu.my

Dr. Salmah Anim Binti Abu Hassan
0125797406
anim@iium.edu.my

Muhamad Aliff Imran Bin Daud
0139134523
aliffmohd16@gmail.com

This proposal has been reviewed and approved by IIUM Research Ethics committee (IREC), which is a committee whose task it is to make sure that research participants are protected from harm. If you wish to find about more about the IREC, you may visit to this web http:iium.edu.my/irec

PART II: Certificate of Consent

I have been invited to participate in this research study which will involve my forearm musculature muscle recovery parameters to validate the equipment/machine during the assessment. I have read the foregoing information, or it has been read to me. I have had the opportunity to ask questions about it and any questions that I have been asked have been answered to my satisfaction. I consent voluntarily to be a participant in this study.

Name of Participant: _____

Identity Card (IC): _____

Signature of Participant: _____

Date: _____
Day/month/year

I have witnessed the accurate reading of the consent form the potential participant, and the individual has had the opportunity to ask questions. I confirm that the individual has given consent freely.

Print name of witness_____

I/C of witness _____

Signature of witness _____

Date _____
Day/month/year

Statement by the researcher/person taking consent

I have accurately read out the information sheet to the parent of the potential participant, and to the best of my ability made sure that the person understands the research procedures.
I confirm that the participant was given an opportunity to ask questions about the study, and all the questions asked by participant have been answered correctly and to the best of my ability. I confirm that the individual has not been coerced into giving consent, and the consent has been given freely and voluntarily.
A copy of this Informed Consent Form has been provided to the participant.

Researcher(s)

1. Name: Asmarani Binti Ahmad Puzi
   I/C No.: 870408-02-5172
   Signature:
   Date:

2. Name: Assoc. Prof Dr. Shahrul Na'im Sidek
   I/C No.: 760620-08-5343
   Signature:
   Date:

3. Name: Salmah Anim Binti Abu Hassan
   I/C No.: 850813-07-5722
   Signature:
   Date:

4. Name: Muhamad Aliff Imran Bin Daud
   I/C No.: 990319-03-5199
   Signature:
   Date:

APPENDIX B

PATIENTS INFORMATION

Table B.1 Patient's Information

No.	ID	Age	Gender	Date	Venue	Cause of Symptom	Arm Affected	MAS Level	
								Left (Flexion / Extension)	Right (Flexion / Extension)
1	S1	57	Male	22/04/2024	SASMEC	Stroke	Left	0 / 1	-
2	S2	53	Female	22/04/2024	SASMEC	Stroke	Right	-	1 / 1+
3	S3	67	Male	22/04/2024	SASMEC	Stroke	Right	-	0 / 1
4	S4	64	Male	23/04/2024	SASMEC	Stroke	Right	-	1+ / 1+
5	S5	68	Male	23/04/2024	SASMEC	Stroke	Left	1+ / 1	-
6	S6	53	Female	24/04/2024	SASMEC	Stroke	Right	-	0 / 1
7	S7	57	Male	24/04/2024	SASMEC	Stroke	Right	-	1+ / 1+
8	S8	70	Male	25/04/2024	SASMEC	Stroke	Right	-	1 / 1+
9	S9	70	Female	26/04/2024	SASMEC	Stroke	Left	1 / 1	-
10	S10	64	Male	29/04/2024	SASMEC	Stroke	Right	0 / 0	-
11	S11	67	Male	29/04/2024	SASMEC	Stroke	Right	-	1 / 0
12	S12	63	Male	29/04/2024	SASMEC	Stroke	Left	1 / 2	-
13	S13	57	Male	29/04/2024	SASMEC	Stroke	Right	-	1+ / 2
14	S14	48	Male	29/04/2024	SASMEC	Stroke	Left	3 / 3	-

Table B.1 Patient's Information (cont.)

No.	ID	Age	Gender	Date	Venue	Cause of Symptom	Arm Affected	MAS Level	
								Left (Flexion / Extension)	Right (Flexion / Extension)
15	S15	16	Female	29/04/2024	SASMEC	Cerebral Palsy	Left	2 / 2	-
16	S16	42	Female	30/04/2024	SASMEC	Stroke	Right	-	0 / 2
17	S17	48	Male	01/05/2024	NASAM	Stroke	Left	1 / 1	-
18	S18	67	Male	01/05/2024	NASAM	Stroke	Left	0 / 1	-
19	S19	59	Male	01/05/2024	NASAM	Stroke	Right	-	1 / 1
20	S20	78	Male	01/05/2024	NASAM	Stroke	Left	1 / 2	-
21	S21	58	Male	01/05/2024	NASAM	Stroke	Right	-	3 / 3
22	S22	63	Male	01/05/2024	NASAM	Stroke	Right	-	0 / 1
23	S23	55	Female	01/05/2024	NASAM	Stroke	Right	-	1 / 1
24	S24	68	Female	01/05/2024	NASAM	Stroke	Left	2 / 0	-
25	S25	67	Male	01/05/2024	NASAM	Stroke	Right	-	1 / 0
26	S26	70	Male	03/05/2024	NASAM	Stroke	Left	3 / 0	-
27	S27	76	Male	03/05/2024	NASAM	Stroke	Left	1 / 0	-
28	S28	46	Female	03/05/2024	NASAM	Stroke	Left	1 / 1	-
29	S29	43	Male	03/05/2024	NASAM	Stroke	Left	3 / 0	-

Table B.1 Patient's Information (cont.)

No.	ID	Age	Gender	Date	Venue	Cause of Symptom	Arm Affected	MAS Level	
								Left (Flexion / Extension)	Left (Flexion / Extension)
30	S30	66	Male	03/05/2024	NASAM	Stroke	Right	-	1 / 1
31	S31	31	Male	28/11/2023	IIUM Gombak	Healthy	Right	-	0 / 0
32	S32	28	Male	28/11/2023	IIUM Gombak	Healthy	Right	-	0 / 0
33	S33	31	Male	28/11/2023	IIUM Gombak	Healthy	Right	-	0 / 0
34	S34	43	Male	28/11/2023	IIUM Gombak	Healthy	Right	-	0 / 0
35	S35	39	Male	28/11/2023	IIUM Gombak	Healthy	Right	-	0 / 0
36	S36	33	Male	28/11/2023	IIUM Gombak	Healthy	Right	-	0 / 0
37	S37	25	Male	28/11/2023	IIUM Gombak	Healthy	Right	-	0 / 0
38	S38	26	Male	28/11/2023	IIUM Gombak	Healthy	Right	-	0 / 0
39	S39	24	Male	28/11/2023	IIUM Gombak	Healthy	Right	-	0 / 0
40	S40	26	Male	28/11/2023	IIUM Gombak	Healthy	Right	-	0 / 0